SYNTHESIS OF MONO/DI-[1-(2-ANTHRYL)-1-PHENYLETHYLENE] TELECHELIC POLY(METHYL METHACRYLATE), POLYSTYRENE, AND POLYISOBUTYLENE AND RELATED COPOLYMERIZATIONS VIA PHOTOCHEMICAL REVERSIBLE CYCLOADDITION REACTIONS

by
Çimen ÖZGÜÇ ÖNAL
M.S., Chemistry, Boğaziçi University, 2009

Submitted to the Institute for Graduate Studies in
Science and Engineering in partial fulfillment of
the requirements for the degree of
Doctor of Philosophy
Graduate

Graduate Program in Chemistry
Boğaziçi University
2018

To my beloved mother, father and husband

ACKNOWLEDGEMENTS

I would like to express my sincere gratitude to my thesis supervisor Prof. Turgut Nugay for his guidance throughout this PhD project, for sharing all his knowledge and experiences with me. I would like to thank him for his belief in me and for all the enlightenment he granted during our research together.

I would like to thank my thesis committee members Prof. Duygu Avcı Semiz, Prof. Yusuf Yağcı, Prof. Sinan Şen and Assist. Prof. Mehmet Fırat İlker for granting their valuable time in reviewing this thesis and for all their advices and comments. I would also like to thank Prof. Nihan Nugay for her guidance and support throughout this project.

I would like to express very special thanks to my lab partners Elif Kurnaz and Ekmel Helvacıoğlu for their endless support and friendship during my graduate years. I would not have accomplished all this without their help, especially Ekmel's, thank you for always being there for me.

My oldest friends Dr. Merve Erişen and Seda Önalan Gül; I am truly grateful for the friendship and love you have given me through all these years we have known each other. Dr. Hande Erdin; thank you for always keeping me close to your heart and for your friendship. Dr. Sevgi Sarıgül; thank you for always believing in me and for all the good things you have brought into my life. I would also like to thank my old friend Sarper Şenol for all the great moments we have shared in all these years.

My deepest thanks are to my dear mother Feride Feral Özgüç, my dear father Atila Özgüç and my beloved husband Türkay Önal for their endless love, encouragement and support; for all the happiness and joy they have given me. Thank you for all that you have taught me; and for making me the person that I am today. I am truly grateful to have such amazing and wonderful parents; and I am very proud to be able to call such a perfect man "my husband".

This project has been supported by Boğaziçi University research fund (BAP) with project code 13B05D3 and project number 7088.

ABSTRACT

SYNTHESIS OF MONO/DI-[1-(2-ANTHRYL)-1-PHENYLETHYLENE] TELECHELIC POLY(METHYL METHACRYLATE), POLYSTYRENE, AND POLYISOBUTYLENE AND RELATED COPOLYMERIZATIONS VIA PHOTOCHEMICAL REVERSIBLE CYCLOADDITION REACTIONS

The synthesis of novel 1-(2-anthryl)-1-phenylethylene (APE) di-telechelic polyisobutylenes were done by the utilization of a difunctional cationic initiator and the in situ addition of the non-homopolymerizable APE monomer to the chain ends. Mono and di-anthryl telechelic polystyrenes and anthryl telechelic poly(methyl methacrylate)s were also synthesized via living anionic polymerization by the incorporation of APE at initiation or at chain end. Products were characterized by ^1H NMR spectroscopy and Size Exclusion Chromatography (SEC). The polymers were irradiated with 365 nm and 254 nm UV light and the reversible photocycloaddition of anthryl moieties was investigated. Irradiations at 365 nm were conducted to obtain chain extension of anthryl and di-anthryl telechelic polymers; initially for homopolymer solutions and then for polymer mixtures. The chain extension of di-anthryl telechelic PIBs through photocoupling at 365 nm produced higher molecular weight products from low molecular weight precursors. The effect of precursor polymer concentration on the degree of chain extension was investigated, and intermolecular interactions leading to the formation of tetramers was observed. Intramolecular interactions leading to formation of cyclic products was also observed in some extent during the chain extension process, especially in the low concentration conditions. The photocoupled products were UV irradiated at 254 nm, which yielded partial reversal of photocycloaddition of anthryl groups and consequent photoscission of polymers. Products obtained by UV irradiations of mixtures of di-anthryl telechelic polyisobutylenes and polystyrenes at 365 nm were cast into films and their thermal and mechanical properties were investigated.

ÖZET

MONO/Dİ-[1-(2-ANTRİL)-1-FENİLETİLEN TELEKELİK POLİ(METİL METAKRİLAT), POLİSTİREN, VE POLİİSOBÜTİLEN SENTEZİ VE FOTOKİMYASAL TERSİNİR BAĞLANMA TEPKİMELERİ YOLU İLE KOPOLİMERİZASYONLARI

Bu çalışmada katyonik polimerizasyon yöntemiyle1-(2-antril)-1-feniletilen (APE) ile fonksiyonlandırılmış poliisobütilen (PIB) sentezi ilk kez gerçekleştirilmiştir. Söz konusu APE monomerlerinin birbirleriyle tepkimeye girmediği ve homopolimer oluşturmadığı bilinmektedir; dolayısıyla bifonksiyonel katyonik başlatıcı kullanılarak di-antril telekelik poliisobütilenler elde edilmiştir. APE monomerinin reaksiyon başlangıç aşamasında veya zincir ucu fonksiyonlandırmasında kullanılması ile gerçekleşen anyonik polimerizasyon yöntemi yoluyla antril ve di-antril telekelik polistirenler ile di-antril telekelik poli(metil metakrilat)lar da elde edilmiştir. Sentezlerin başarısı Nükleer Manyetik Rezonans (NMR) ve Büyüklükçe Ayırma Kromatografisi (SEC) teknikleriyle doğrulanmıştır. Bu ürünlerin zincir uçlarındaki antril molekülerinin 365 nm ve 254 nm UV ışınlandırılması sonucu sergilediği fotokimyasal tersinir bağlanma ve ayrılma tepkimeleri incelenmiştir. Homopolimer çözeltileri ve polimer karışımları 365 nm ışınlandırmaya tabi tutularak zincir uzaması tepkimeleri gerçekleştirilmiştir. Düşük moleküler ağırlıklı di-antril telekelik PIB'lerin 365 nm ışık altında antril yapılarının fotodimerizasyonu sonucu birleşerek yüksek moleküler ağırlıklara ulaştığı gözlenmiştir. Başlangıç konsantrasyonu değişimine bağlı olarak zincir uzaması tepkimesi incelenmiş ve konsantre koşullarda tetramer oluşumu gözlenmiştir. Seyreltik koşullarda çalışıldığında zincir uzaması tepkimelerinin yanı sıra halka yapıların oluşumu da gözlenmiştir. Fotokimyasal bağlanma ürünleri 254 nm ışınlandırılmasına tabi tutulduğunda, birbirine bağlanmış antril yapılarının kısmi olarak ayrılmasıyla tekrar düşük moleküler ağırlıklı polimerler elde edilmiştir. Di-antril telekelik poliisobütilen ve polistiren karışımlarının 365 nm UV ışınlandırması gerçekleştirilmiş, elde edilen ürünler film haline getirilerek termal ve mekanik özellikleri incelenmiştir.

TABLE OF CONTENTS

LIST OF FIGURES

LIST OF TABLES

LIST OF SYMBOLS

-b-	Block copolymer
g	Gram
h	Hour
kN	Kilonewton
min	Minute
ml	Milliliter
mm	Millimeter
mmHg	Millimeter of Mercury
mg	Milligram
M_n	Number Average Molecular Weight
M_p	Peak Molecular Weight
M_w	Weight Average Molecular Weight
M_w/M_n	Polydispersity Index
MHz	Megahertz
MPa	Megapascal
mW	Milliwatt
nm	Nanometer
Nmm	Newton millimeter
Tg	Glass Transition Temperature
α	Alpha
β	Beta
δ	Chemical shift
ΔE	Activation energy difference
μL	Microliter

LIST OF ACRONYMS/ABBREVIATIONS

A-ANT	2-acetylanthracene
AIBN	2,2′-azobis(2-methylpropionitrile)
$AlCl_3$	Aluminum chloride
APE	1-(2-anthryl)-1-phenylethylene
APE-PIB-APE	di-anthryl telechelic polyisobutylene
APE-PS-APE	di-anthryl telechelic polystyrene
APEOL	1-(anthracen-2-yl)-1-phenylethanol
APHL	1-(2-anthryl)-1-phenylhexyllithium
Ar	Argon
ATRP	Atom Transfer Radical Polymerization
BCl_3	Boron trichloride
BP	Benzophenone
$CaCl_2$	Calcium chloride
CaH_2	Calcium hydride
$CDCl_3$	Deuterated chloroform
CH_3COOH	Acetic acid
CH_3OH	Methanol
DCM	Dichloromethane
DEE	Diethyl ether
DMA	Dynamic mechanical analysis
DPE	1,1-diphenylethylene
DPHL	1,1-diphenylhexyllithium
DP_n	Degree of Polymerization
DSC	Differential scanning calorimetry
DtBP	di-tert-butylpyridine
DTE	1,1-ditolylethylene
EO	Ethylene oxide
Equiv.	Equivalent

HCl	Hydrogen chloride
H_2SO_4	Sulfuric acid
IB	Isobutylene
K	Potassium
LiCl	Lithium chloride
MeMgBr	Methylmagnesium bromide
$MgSO_4$	Magnesium sulfate
MMA	Methyl methacrylate
MWD	Molecular Weight Distribution
N_2	Nitrogen
Na	Sodium
$NaHCO_3$	Sodium bicarbonate
NaCl	Sodium chloride
NaOH	Sodium hydroxide
n-BuLi	*n*-butyllithium
NH_3	Ammonia
NH_4Cl	Ammonium chloride
NMR	Nuclear Magnetic Resonance Spectroscopy
PDI	Polydispersity Index
PDDPE	1,4-bis(1-phenylethenyl) benzene
PIB	Polyisobutylene
PEG	Poly(ethylene glycol)
PET	Poly(ethylene terephthalate)
PhMgBr	Phenylmagnesium bromide
PIB	Polyisobutylene
PI-b-PMMA	Polyisoprene-b-poly(methyl methacrylate)
PI-b-PS	Polyisoprene-b-polystyrene
PMMA	Poly(methyl methacrylate)
PMMA-APE	Anthryl telechelic poly(methyl methacrylate)
PS	Polystyrene
PS-APE	Anthryl telechelic polystyrene
PS-b-PEO	Polystyrene-b-poly(ethylene oxide)
PS-b-PMMA	Polystyrene-b-poly(methyl methacrylate)

PTFE	Polytetrafluoroethylene
PTHF	Poly(tetrahyrdofuran)
SEC	Size Exclusion Chromatography
sec-BuLi	*sec*-butyllithium
SIBS	poly(styrene-b-isobutylene-b-styrene)
t-Bu-m-DiCumCl	5-tert-butyl-1,3-bis(2-chloro-2-propyl)benzene
t-Bu-m-DiCumOH	5-tert-butyl-1,3-dicumyl alcohol
TGA	Thermogravimetric analysis
THF	Tetrahydrofuran
$TiCl_4$	Titanium tetrachloride
UV	Ultraviolet

1. INTRODUCTION

1.1. Photochemistry of Anthracene Derivatives

Anthracene containing materials have drawn noteworthy research interest, because of their attractive features as fluorescent labels, scintillators and organic semiconductors. They have found usage in areas such as wood preservatives, insecticides, coating materials, production of red alizarin dye, optical memory devices, biosensors, and hydrogels Anthracenes are also utilized in Diels-Alder reaction, due to their ability to undergo [4+2] cycloaddition as reactive dienes [1, 2].

Along with these features, anthracene is a photosensitive molecule. The earliest studies concerning this aspect of anthracenes took place in the 19th century. Fritzsche and co-workers reported that when a saturated anthracene solution was subjected to sunlight, a colorless crystalline material precipitated; which was in turn converted to anthracene upon melting [3, 4]. The photoinduced dimerization reaction was widely studied and it was determined that anthracene molecules have the ability to photodimerize by UV irradiation above 300nm via a [4π+4π] cycloaddition through the 9- and 10-positions [4-6]. The resulting photodimers can be reverted back to original state either thermally at an elevated temperature or via UV irradiation with the wavelength below 300 nm (Figure 1.1) [1].

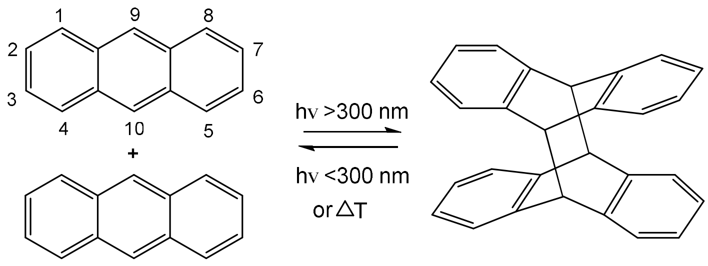

Figure 1.1. Reversible dimerization of anthracene [1].

Many anthracene derivatives with mono and poly substituents undergo the reversible photocycloaddition reaction. Structural aspects and properties of these photodimers have been studied extensively [5, 6]. As the [4π+4π] cycloaddition takes place on the central ring of the anthracene π -system, the conjugation is disrupted by the formation of *ortho*-disubstituted benzene type photodimer. This creates a change in the absorption property of the molecule; the anthracene absorption bands between 350-400 nm decrease, whereas the band at about 200 nm increases as a result of the benzene type product formation [7, 8]. Thus, following the cycloaddition reaction the resulting photodimers no longer absorb light of wavelengths greater than 300 nm. This property is valid for the unsubstituted anthracene molecule as well as various derivatives. The important point is that the substituents should not create an interference with the π- π* transition required for the photodimerization process [6]. It should also be noted that in order to obtain pure photodimerization products, the cycloaddition reaction must be conducted under inert atmosphere. UV irradiation in the presence of oxygen leads to the formation of endoperoxides, by the reaction of anthracene with singlet oxygen (Figure 1.2) [1, 7-10].

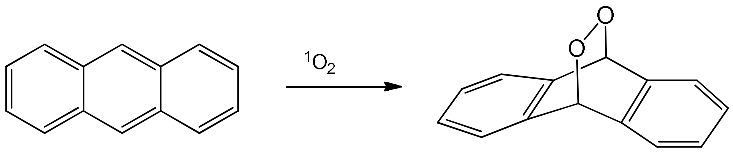

Figure 1.2. Reaction of singlet oxygen with anthracene [7, 10].

Advantageous aspects of the reversible photocycloaddition behavior of anthracene derivatives [5, 6, 11, 12] and anthryl functionalized polymers [13-34] have been widely investigated to be used in different application areas such as the preparation of crosslinked polymers systems [7, 13-17], hydrogels [18, 19], controlled release studies [20, 21], self-healing materials [22, 23] and pattering of polymer films [8, 24-26]. Anthracene end-functionalized polymers were also utilized to perform chain extension [27, 28], to obtain block copolymers [29] and to form cyclic products [30-34] by the aid of photodimerization. Some of these studies are depicted onwards.

Fox et al. utilized 10-thiodecyl 2-anthryl ether to create a self-assembled monolayer on gold surface (Figure 1.3) in order to examine the potential usage as fluorescence switch [12]. It was stated that photodimerization at 350 nm and following photoscission of the terminal anthryl units at 254 nm did not cause a significant damage in the monolayer structure. However, a loss of intensity in the fluorescence measurements was recorded during the UV treatments; indicating that an ideal full recovery after the irradiations could not be achieved.

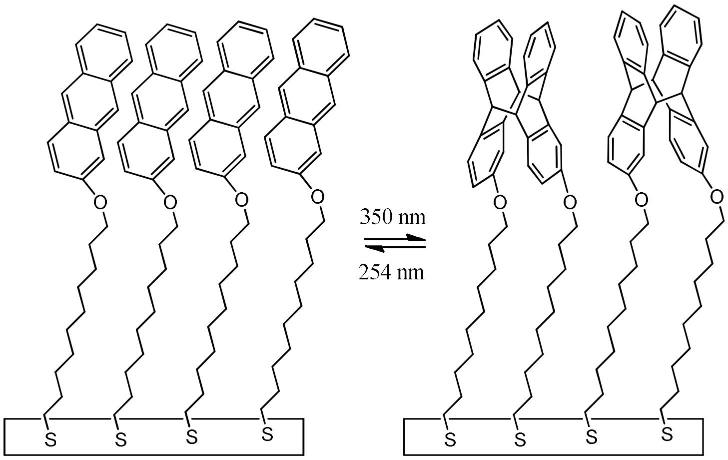

Figure 1.3. Photochemistry of anthryl functionalized self-assembled monolayer on gold surface [12].

Jones et al. synthesized poly(ethylene terephthalate-*co*-2,6-anthracene dicarboxylate) (PET-A) copolymers [13], which were then irradiated at 350 nm as thin films or in solution in order to form crosslinked polymers (Figure 1.4). It was stated that samples irradiated in air showed a greater loss of anthracene absorption with respect to under nitrogen, which was monitored by UV-vis spectroscopy. However, the crosslinking reaction occurring in air was irreversible and the initial polymers could not be obtained upon irradiation at 254 nm. The formation of anthracene-9,10-endoperoxide was considered to be the reason for irreversible behavior as its thermal or photochemical decomposition is stated to lead to crosslinked chains and oxidized products (Figure 1.5).

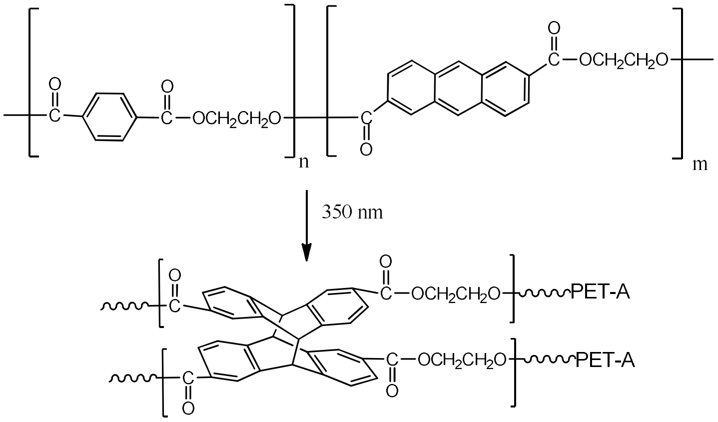

Figure 1.4. Crosslinking of PET-A [13].

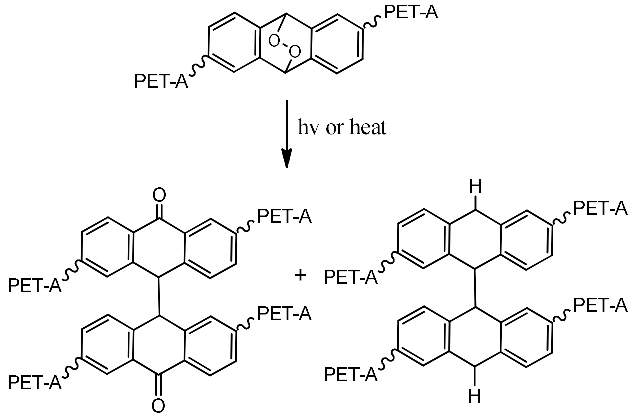

Figure 1.5. Proposed decomposition of anthracene-9,10-endoperoxide [13].

Zheng et al. achieved the synthesis of a poly(ethylene glycol) (PEG) based hydrogel bearing anthracene units [18]. A commercial PEG with eight arms was modified by reaction of the hydroxyl end groups with 9-anthracene carbonyl chloride, obtaining esterification extent of 87.4 % (Figure 1.6).

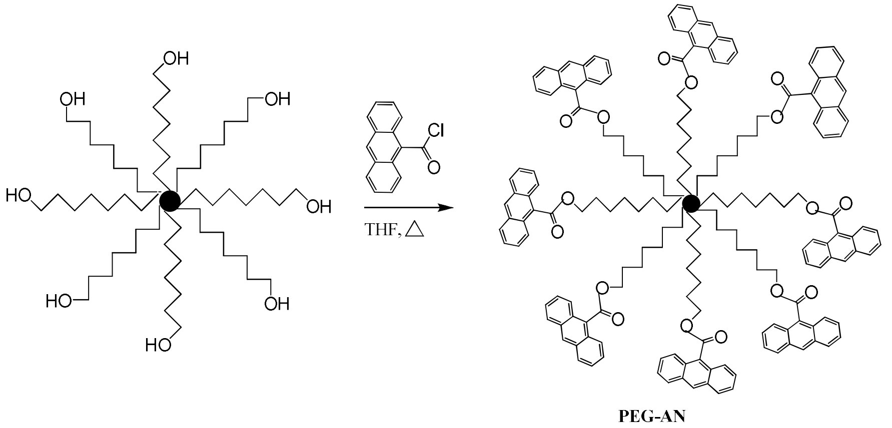

Figure 1.6. Synthesis of PEG-anthracene macromer (PEG-AN) [18].

The anthracene-functionalized PEG macromer (PEG-AN) was subjected to irradiation at 365 nm in order to form a hydrogel network by the dimerization of anthracene units. It was stated that high modification of PEG with anthracene, the flexibility of polymer chains and the hydrophobic nature of anthracene favored the photodimerization reaction in aqueous solution and lead to relatively fast photogelation. The reversibility of the hydrogel was also investigated by exposure to alternated wavelengths of 365 and 254 nm. After an initial absorbance decrease following the 365 nm irradiation, exposure to 254 nm reverted the process only at a degree of 20%, a complete sol-gel-sol process was not obtained. Upon following irradiations, photodimerization and photoscission took place without further losses in the photoreversibility efficiency for more than 10 cycles [18].

Matsui et al. synthesized poly(methacrylic acid) functionalized via esterification reaction with 9-chloromethylanthracene, to be used as a molecularly imprinted polymer and examine the photoinduced crosslinking on binding capacity to an antimalarial drug. After photodimerization of several chains was achieved by irradiation at 365 nm, the reverse reaction at 254 nm did not yield full decrosslinking. The original anthryl peaks were recovered up to 22% of the initial absorbance. However, the reversibility was found to be efficient after the second cycle and the degree of crosslinking in the network was repetitive [17].

Trinh et al. investigated the phase separation of anthracene-labeled polystyrene/poly(vinyl methyl ether) blends resulting from photodimerization with 365 nm irradiation [14]. Homogenization process was induced by irradiation with 295 nm, which caused decrosslinking in the network structure. The kinetics of both processes were followed by light scattering data and investigated as a route to recycle multicomponent polymer blends.

Qiao and co-workers reported the synthesis of anthracene functionalized core crosslinked star poly(methyl acrylate-co- divinyl benzene) as a macromonomer to generate reversibly crosslinkable materials (Figure 1.7). Honeycomb films cast from the product were subjected to repeated crosslinking and decrosslinking for four cycles. It was stated that high reversibility of the photo-crosslinking reaction rendered the material potentially suitable for applications in photolithography [25].

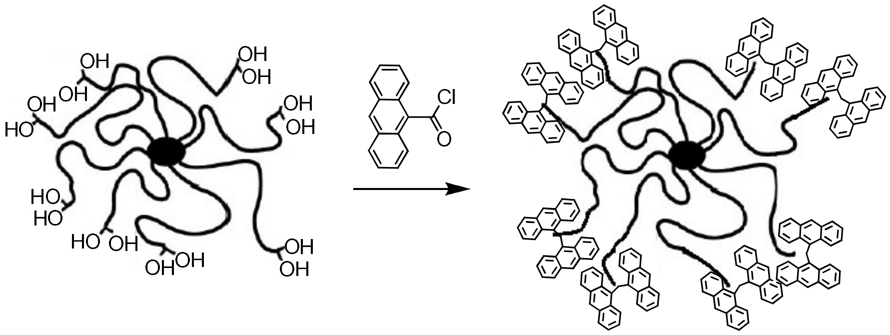

Figure 1.7. Functionalization of core-crosslinked star polymer with anthracene [25].

Wells et al. utilized anthracene functionalized graftable PEG macromolecular crosslinkers to form hydrogels as candidates to be used in drug delivery applications [20]. The macromolecules were obtained by the reaction of 9-anthracene carboxylic acid and diamine terminated PEG. The ability of PEG-anthracene to dimerize reversibly by UV irradiation was found to be less efficient when compared to model compound 9-anthracene carboxylic acid. The lowering of photoreactivity was attributed to steric hindrance imposed by the PEG chains. However, the presence of hydrophilic PEG chains was essential to allow solubilization of hydrophobic anthracene groups and to give them mobility after grafting to backbone of bulk polymers. The amine-terminated PEG-anthracene was then grafted onto the carbonyl group of polysaccharides alginate and hyaluronan. (Figure 1.8).

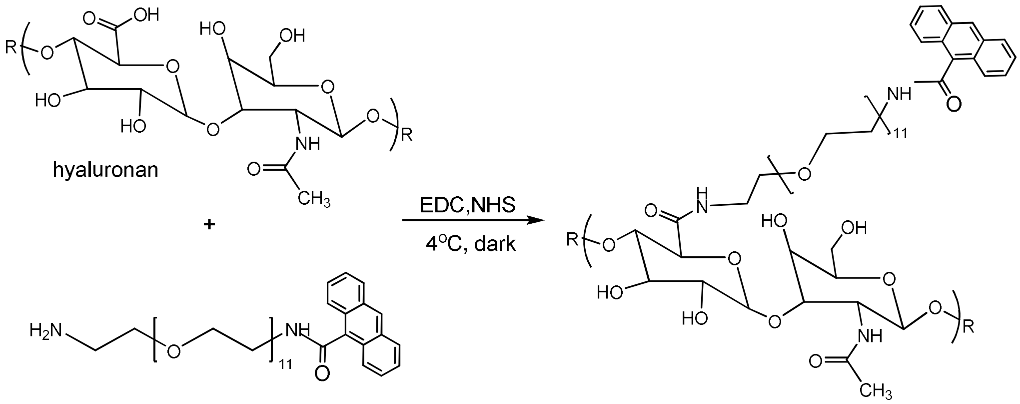

Figure 1.8. Grafting of PEG-anthracene onto hyaluronan [20].

The inclusion of photosensitive anthracene units into the polymer backbone via grafting allowed photoinduced crosslinking with exposure to 365 nm light. Further analysis on these photogels were done including drug loading and release experiments as well as cytocompatibility studies in order to investigate the possibility of usage in drug delivery applications [20].

Froimowicz et al. synthesized anthracene containing hyperbranced polyglycerol macromonomers [22]. Photochemistry of the samples was studied in both solution and cast film forms, in oxygen free conditions. Spectroscopic results confirmed the photo-crosslinking through dimerization of anthracenes by irradiation at 366 nm. It was determined that the crosslinking was faster in solution; the plateau was reached when 62% of the anthracenes dimerized in the aqueous sample whereas in the cast film only 35%

reacted. However, when subjected to irradiation at 254 nm the degree of crosslinking in aqueous system only decreased by 17% the crosslinked network of cast film showed complete backward dimerization to the staring material. The full reversibility of the network was utilized for the generation of self-healing materials [22].

Catalina and coworkers performed low percent modification of ethylene-butyl acrylate copolymer with anthracene moieties by transesterification at molten state. Crosslinking dynamics of the copolymer were examined; by monitoring the change in absorbance the cleavage of the crosslinked material was found to demonstrate 42 % reversibility (Figure 1.9). It was also stated that samples irradiated in air did not revert to the original anthracene moieties due to the formation of endoperoxide type species [15].

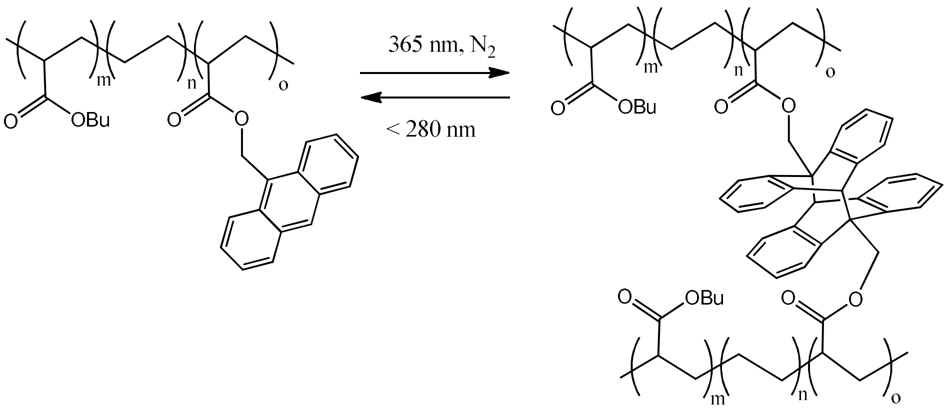

Figure 1.9. Photodimerization and photocleavage of anthracene units in ethylene-butyl acrylate copolymer [15].

Griesser and coworkers reported the synthesis of polynorbornene based polymers containing anthracene molecules in the side chain [8]. A statistical copolymer bearing oligoethyleneglycole groups was obtained, as well as the homopolymer, to provide a higher mobility to the anthracene units and also to lower the glass transition temperature (Figure 1.10). UV irradiation of the polymer films resulted in the crosslinking of the macromolecules and the reverse reaction was accomplished thermally. Due to the higher mobility and flexibility of anthracene units in the copolymer, the photodimerization of these units and the consequent crosslinking in the polymer system occurred at a higher rate with respect to the homopolymer. The conversion of anthracene units into dimers was monitored by UV-Vis spectroscopy and calculated as 45% for the homopolymers and 55% for the copolymer. Thermal dissociation lead to a 62% recovery for both samples, whereas irradiation with 254 nm UV light did not cause significant regeneration of anthracene moieties.

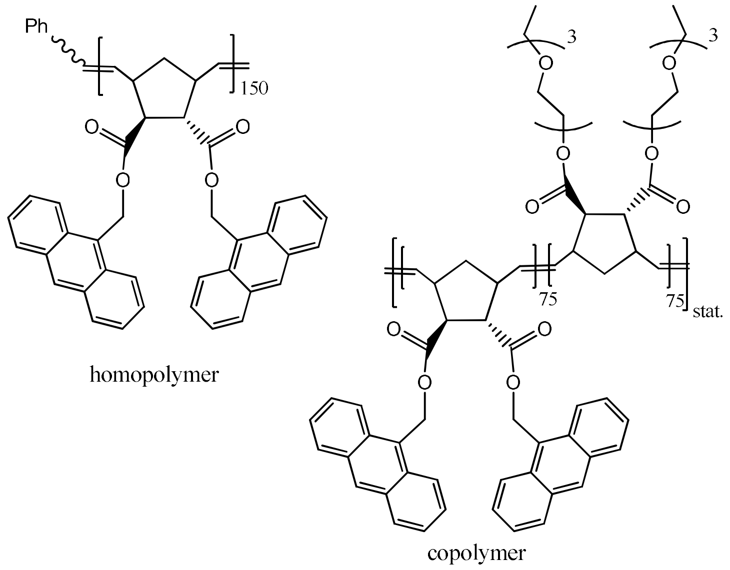

Figure 1.10. Polynorbornene based polymers containing anthracene units [8].

Chain extension of anthryl telechelic polymers was studied by Coursan et al., via preparation of polystyrene end-capped with anthrylmethyl ether group by the reaction of ω-hydroxy-telechelic polystyrene and 9-chloromethylanthracene. Photoreactivity of these polymers were investigated by irradiation under 366 nm light, which lead to the formation of dimerized product via intermolecular photocycloaddition of anthracene units (Figure 1.11). ^{1}H-NMR spectroscopy and size exclusion chromatography (SEC) was utilized to confirm the formation of photodimerized polymers; the former characterization method revealed the new peaks arising from the anthryl photodimer structure, especially the bridgehead protons, while the latter showed a twofold increase in the polymer molecular weight as the original polymer peak diminished. It was stated that the quantum yield of coupling reaction was not high, which was attributed to the large polymer chains restricting the encounter of two anthryl units. Increasing the original polymer concentration did not increase the coupling yield, which suggested that the anthryl units mostly remained embedded within the polymer chains. Irradiation of the photocoupled products with 280 nm light lead to reformation of original polymer chains, which was also confirmed via SEC analysis [27].

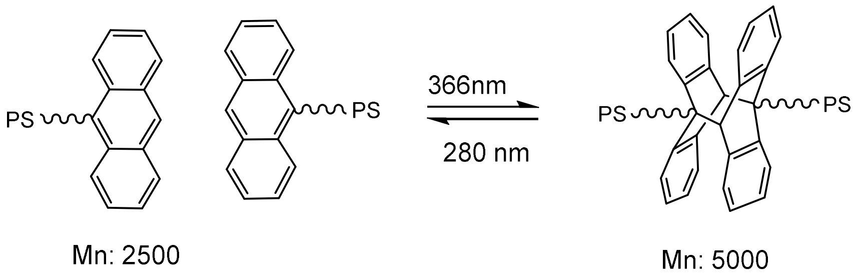

Figure 1.11. Reversible dimerization of ω-anthrylpolystyrene [27].

Kim and coworkers reported the synthesis of di-anthryl telechelic poly(ε-caprolactone)s which were utilized to prepare high molecular weight cyclic polymers (Figure 1.12) [33]. The intermolecular photocycloaddition of anthracene moieties at polymer chain ends by irradiation at 365 nm led to the formation of cyclic poly(ε-caprolactone)s. It was stated that the size of polymer rings could be tuned by adjusting the concentration of precursor solutions; thus combining two to four units of original polymer chains to form cyclic structures. Reversion of the process was performed by heating at 160 °C and afforded to 49.5% dissociation of anthryl units.

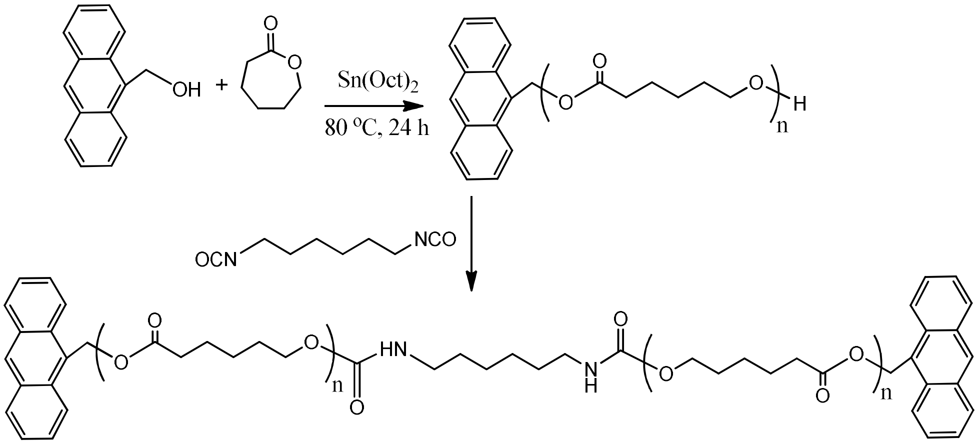

Figure 1.12. Synthesis of di-anthryl telechelic poly(ε-caprolactone) [33].

Yamamoto and coworkers investigated the linear to cyclic transition of di-anthryl telechelic poly(tetrahyrdofuran) (PTHF) and poly(ethylene oxide)s (PEO). It was stated that Ant-O-PEO and Ant-CH_2-PEO (Figure) with electron donating substituents at the 9 position failed in producing a reversible photocycloaddion product. The anthracene units were instead subjected to oxidation which led to formation of anthraquinones. However, 365 nm irradiation of Ant-PTHF and Ant-CO_2-PEO (Figure 1.13) with electron withdrawing substituent at the 9 position resulted in the formation of desired cyclic products. Conversion to initial linear state was said to be accomplished via heating [34].

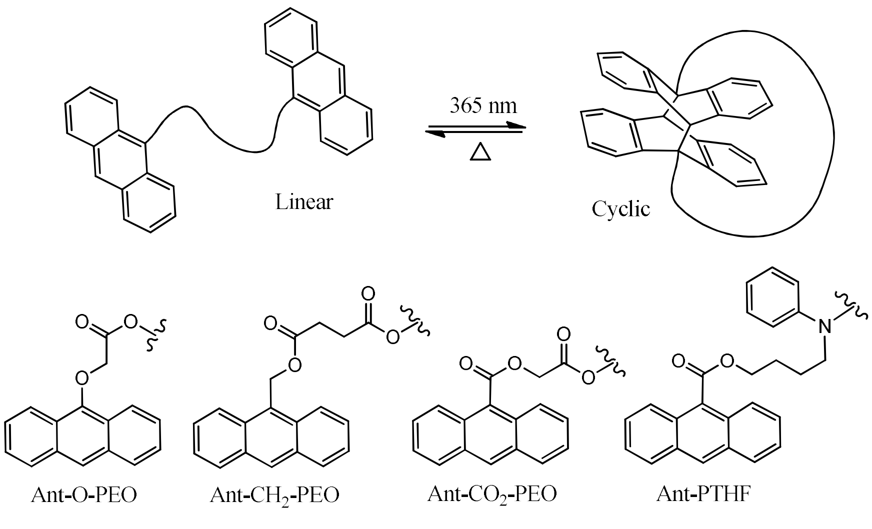

Figure 1.13. Linear to cyclic transition of di-anthryl telechelic PTHF and PEO [34].

1.2. Synthesis of Anthracene Functionalized Polymers

The majority of the mentioned studies utilized 9-substituted anthracenes to be incorporated into different polymer systems. The greater availability of these 9-substituted anthracenes arise from the higher reactivity of the 9 and 10 positions of the molecule, leading to synthesis of derivatives with various functionalities. The reactivity of the 9 and 10 positions, however, may cause problems in some cases if the anthracene derivative interferes with the polymerization process. In the earlier studies Bagdasr'ian and Sinitsina showed that anthracene molecule acts as a strong inhibitor of free radical polymerization of vinyl acetate and acrylonitrile. Methyl acrylate polymerization was also affected, but with a lesser degree, whereas methyl methacrylate polymerization was unaffected. The inhibition ability of anthracene on free radical polymerization followed a trend in the order of 1:10:100 for methyl acrylate, acrylonitrile and vinyl acetate, respectively [35].

In a study for the synthesis of 9-vinyl anthracene polymer, Rembaum and Eisenberg reported the inability to obtain a high molecular weight polymer via free radical method due to the high reactivity of the anthracene group toward free radicals [36]. Stolka also stated that the anthracene group's radical quencher and inhibitor property was the main reason for the failure to synthesize polymers containing anthracene moieties by radical polymerization [37]. It was presumed that during polymerization the propagating macroradicals add directly to the anthracene units and thus get stabilized via the unreactive dibenzylic radicals that form (Figure 1.14).

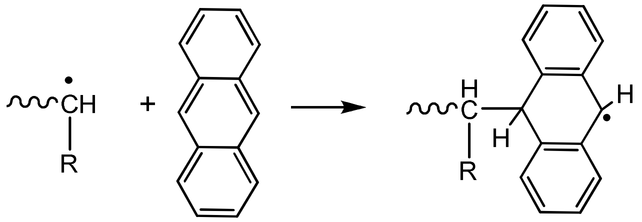

Figure 1.14. Reaction of anthracene with free radicals [37].

Taking into account that anthracene does not interfere in the radical polymerization of methyl methacrylate, an anthracene containing monomer, 1-(2-anthryl)ethyl methacrylate was synthesized to be used in free radical polymerization (Figure 1.15). Homopolymerization of this monomer lead to a high molecular weight polymer; copolymerization with methyl methacrylate and dodecyl methacrylate was also accomplished. The polymerization of N-vinylcarbazole and vinyl acetate was, however, inhibited [37].

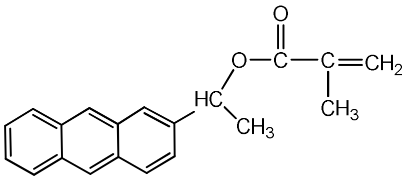

Figure 1.15. 1-(2-anthryl)ethyl methacrylate.

Winnik and coworkers also encountered a similar problem in their non-radiative energy studies to incorporate donor and acceptor chromophores into latex particles [38] The semicontinuous emulsion polymerization of butyl methacrylate worked well with 9-phenanthrylmethyl methacrylate which, selected as the donor chromophore, was distributed along the chains. However, the corresponding acceptor chromophore 9-anthrylmethyl methacrylate lead to the formation of crosslinked particles and acted as inhibitor in the emulsion polymerization reaction of butyl methacrylate. The task was accomplished by the utilization of 9-anthryl methacrylate instead, which lacks the benzylic CH_2 group, since the problem was attributed to the chain transfer reaction from the benzylic position of the chromophore.

In a later study to obtain acrylate-methacrylate copolymer latex, Winnik group faced problems with the utilization of 9-anthryl methacrylate as labelling agent; when butyl acrylate, methyl methacrylate or 2-ethylhexyl acrylate was used [39]. It was stated that this dye molecule was a strong inhibitor for the acrylate polymerization in question. The inability of this anthracene derivative to copolymerize with acrylate monomers was thought to be a result of acrylate radical's competitive addition to the 10 position of anthracene, which led to the formation of a less reactive dibenzylic radical (Figure 1.16). To overcome this problem, of three new anthracene derivatives containing a methyl group at the 10 position were synthesized (Figure 1.17). The blocking of this position enabled these monomers to be utilized as comonomers in the emulsion polymerization of acrylate containing systems [39].

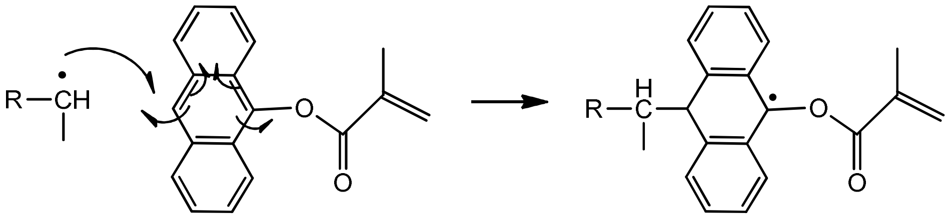

Figure 1.16. Reaction of anthracene with acrylate radical [39].

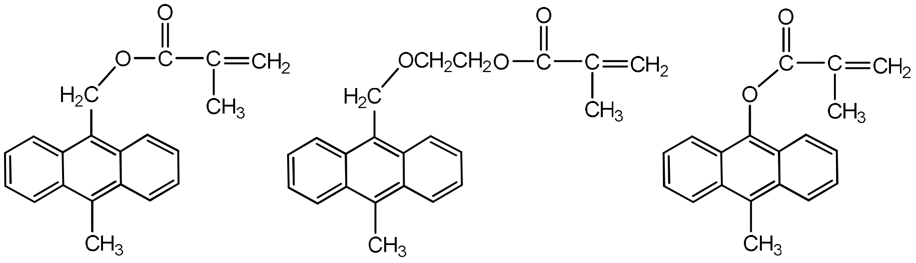

Figure 1.17. Anthracene derivatives with methyl group at the 10 position.

Bratschkov et al. synthesized 6-(9-anthryloxy)-hexylmethacrylate monomer (Figure 1.18) in order to perform copolymerization with n-butyl methacrylate via free radical polymerization [7]. The results showed that copolymerization rate was rather low and the reaction yield was 40% which was attributed to the inhibition property of the anthryl monomer towards radical processes.

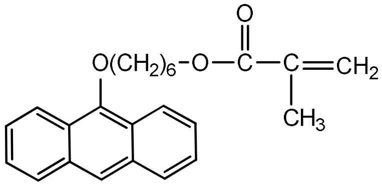

Figure 1.18. 6-(9-anthryloxy)-hexylmethacrylate.

Irradiation of the obtained copolymer at λ >300 nm in the presence of oxygen lead to a rapid formation of endoperoxide type species, as described by others [1, 8, 10], whereas under inert atmosphere photodimerization of anthracene units occurred. The decomposition of the dimers was accomplished via thermal treatment. It was stated that the reversible photodimerization process was improved by the long alkyl spacer and ether bond which linked the anthracene unit to the polymer chains, since it created higher segmental mobility to enable the dimerization of anthracenes [7].

In the next chapter, the synthesis of anthracene functionalized polymers by living anionic polymerization and the characteristics of this polymerization technique will be discussed.

1.3. Living Anionic Polymerization

In 1956, Szwarc introduced and demonstrated the concept of living anionic polymerization through the mechanism of anionic polymerization of styrene initiated by sodium naphthalenide (Figure 1.19) [40, 41]. The initiation step proceeded by the electron transfer from the radical anion sodium napthalenide to the styrene monomer, subsequently formation and dimerization of styryl radical anion to form a dianion, which was monitored via the occurrence of red color of styryl anions. The color of the reaction medium persisted though out the consumption of the present monomer; addition of a second portion of styrene to the system resulted in an increase in viscosity, indicating that the polystyryl chain ends were active and capable of further propagation. These results lead to the formation of the initial definition of living polymerization; characterized by the reactivity of polymer chains that enabled further monomer addition, and the absence of termination and transfer reactions.

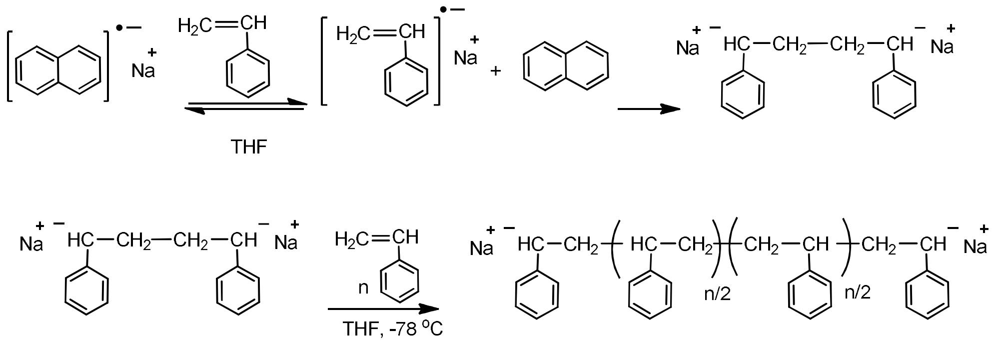

Figure 1.19. Anionic polymerization of styrene via sodium naphthalene initiator [42].

The discovery of Szwarc proved to be a milestone in the research field and pioneered the development of many living polymerization systems. Living anionic polymerization continues to be a powerful and versatile method for synthesizing a wide range of polymer architectures. However, transfer and termination reactions continue to be a challenge through the synthetic pathways and it is crucial to prevent these reactions to obtain the desired well-defined polymeric products. It is possible to accomplish this task provided that the rate of initiation is much greater than that of propagation, and the rate of exchange between the active and dormant species present during the anionic process is fast.

Thus, “living” polymerization is redefined to include the following criteria. First condition is the linearity of the plot of number average degree of polymerization (DP_n) versus conversion, which is a diagnostic tool to demonstrate the absence of transfer reaction, but provides no information regarding terminations. Second criterion is the first order kinetic plot, rate of polymerization versus time. Linearity of this plot indicates that the concentration of active chain end remains constant during the reaction, which proves the absence of termination but does not eliminate the possibility of transfer reactions. Third criterion is a narrow molecular weight distribution of the obtained polymer, characterized by a Poisson distribution, which is highly affected in terms of broadening by transfer and termination reactions.

Therefore, in living anionic polymerization the number average molecular weight (M_n) can be determined by the amount of consumed monomer with respect to initiator:

$$M_n = M/I \tag{1.1}$$

The polymer chains propagate at the same rate and reach the same length after a time period, showing linear growth of chains with respect to consumption of monomer, which leads to the narrow distribution of chain lengths. This Poisson distribution gives the polydispersity index (PDI):

$$\mathrm{PDI} = \frac{\overline{M}_w}{\overline{\overline{M}}_n} \approx 1 + \frac{1}{\overline{\overline{DP}}_n} \tag{1.2}$$

An important factor in anionic polymerization is the presence of different propagating species, as in other types of living polymerizations. Aggregates, ion pairs and free ions are in a state of equilibrium with each other, depending on the reaction conditions. These species are either active and propagate at different rates or inactive (dormant). The rate of exchange between these various chain ends in anionic polymerization should also be fast in order to avoid a broadening in the molecular weight distribution.

Figure 1.20 shows the Winstein spectrum of possible propagating species that exist in equilibrium and contribute to the mechanism of anionic polymerization [43, 44]. The characteristics and reactivities of the carbanions present are dictated by several factors, such as intermolecular ionic interactions, solvent polarity, reaction temperature, size of the metallic counterion. For instance; in polar solvents the Winstein spectrum is shifted to right, towards more ionic and more reactive species, whereas nonpolar media favors the formation of more associated species.

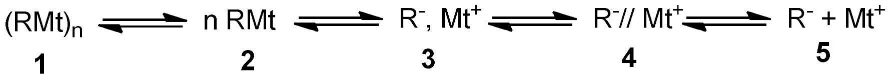

$$\underset{\mathbf{1}}{(RMt)_n} \rightleftharpoons \underset{\mathbf{2}}{n\ RMt} \rightleftharpoons \underset{\mathbf{3}}{R^-, Mt^+} \rightleftharpoons \underset{\mathbf{4}}{R^-//\ Mt^+} \rightleftharpoons \underset{\mathbf{5}}{R^- + Mt^+}$$

1: aggregated species
2: nonaggregated species
3: contact ion pairs
4: solvent separated ion pairs
5: free ions

R^-: carbanionic chain end
Mt^+: metallic counterion

Figure 1.20. Winstein spectrum of possible propagating species in anionic polymerization.

As the anions are stabilized via intermolecular interactions, associated states called aggregates are formed. These aggregated anions exist in a state of equilibrium with the nonaggregated species, depending on factors such as interionic distances, charge density of the anion, solvent properties and dielectric constant [45]. According to Fuoss [46, 47] and Winstein [43] two different forms of ion pairs are present depending on the interionic distance. In solution, the anions may associate themselves tightly or loosely with the counter metal regarding the degree of solvation of this counterion. The tightly associated pair is named as contact ion pair, whereas a solvent-separated ion pair shows loose association due to solvent coordination. The different types of ion pairs are in equilibrium, the polarity of the solvent used and concentration of the ions control the position of this equilibrium. The solvent-separated ion pairs can also dissociate into free ions depending on concentration. The free ions and the solvent-separated ion pairs are highly reactive in comparison to the contact ion pairs. The formation of solvent-separated ion pairs is favored in low reaction temperatures, since solvents have higher dielectric constants at low temperatures. The shift of the equilibrium towards formation of free ions is prominent in case of high solvation and low concentration of ion pairs. In polar solvents, the contact and solvent separated ion pairs dissociate into free ions at a very low extent; but the rate of reaction increases significantly as they partake in propagation [42].

1.3.1. Monomers

Anionic polymerization can be conducted with a variety of α-olefins containing electron withdrawing groups that provide stabilization to the propagating anionic species. Suitable monomers include nonpolar vinyl compounds such as styrenes and dienes. For polar vinyl monomers such as acrylates, methacrylates, vinyl pyridines and acrylonitriles; special reaction conditions and additives must be provided, which will be discussed further on. Cyclic monomers of ethers, esters and siloxanes may also be polymerized anionically via ring opening polymerization. Utilization of monomers that contain acidic protons and other electrophiles must be avoided since they react with the carbanions and terminate the reaction process. However, suitable protection renders the anionic polymerization of labile proton containing monomers possible [42, 48].

1.3.2. Initiators

The initiation process in anionic polymerization takes place by electron transfer or by the utilization of nucleophilic initiators. Electron transfer is conducted by using alkali metals and aromatic hydrocarbons to form radical anions. The direct usage of alkali metals lead to a heterogeneous initiation process, which occurs on the metal surface through reversible transfer of electron to the adsorbed monomer. The radical anions that form initially dimerize to form dianions rapidly. Monomer addition to the dianions lead to the formation of adsorbed oligomers, which then desorb and continue bifunctional anionic propagation in solution. Alkali metals are also utilized in the presence of aromatic hydrocarbons, as in the case of styrene polymerization with sodium naphthalene described previously [42]. The reaction proceeds by the transfer of an electron from the alkali metal to the aromatic hydrocarbon; sodium and naphthalene in this case. Aromatic radical anions react with monomers such as styrene by reversible electron transfer to form styryl or other corresponding monomer radical anions. The equilibrium between these two radical anion species lies to the left, towards the aromatic radical anion, due to the low electron affinity of the monomer radical anion (Figure 1.19) [44, 48]. However, the initiation process remains efficient since the forming monomer radical anions undergo rapid head-to-head dimerization and then anionic propagation continues at both carbanionic chain ends [49]. Styrenics, dienes and epoxides are among the monomers that can be polymerized via aromatic radical anions.

The second type of anionic initiation follows nucleophilic additions. The nucleophilic initiators are monofuctional organometallic bases which include alcoholates, organolithium compounds, Grignard reagents, alkali salts of aromatic hydrocarbons. The rate of initiation is highly influenced by the solvation of the anion and the intermolecular interactions of the ion pairs forming as the vinyl bond opens and new propagating species form. Since the characteristics of carbanions differ significantly, the type of initiator that is necessary to polymerize a particular monomer should be selected depending on the nucleophilic strength of the initiator and the reactivity of the monomer towards nucleophilic attack. In other words, the nucleophilicity of the initiator should be matched with the electrophilic nature of the monomer to have a fast initiation. The reactivity of the monomer increases as the ability to stabilize the charge of carbanion increases. If the propagating anion is not strongly stabilized, very strong nucleophiles such as alkyllithium compounds are required to polymerize monomers containing relatively weak electron-withdrawing substituents as in styrene and 1,3-butadiene [50]. The nucleophilicity of anionic species could be correlated with the pK_a value of the corresponding hydrogenated compounds. Therefore, the pK_a value of the protonated initiator should be higher than or comparable to that of the propagating anion [48].

Among the variety of organometallic compounds, alkyllithium species are the most widely used anionic initiators. These compounds generally associate into dimers, tetramers or hexamers in hydrocarbon solution, the degree of association increases as the steric hindrance of the alkyl group decreases. The relative reactivities of the alkyllithium compounds also depend on the degree of association, generally less associated species are more reactive as initiators. *n*-Butyllithium (*n*-BuLi) and *sec*-butyllithium (*sec*-BuLi) are examples of commercially utilized alkyllithium initiators for anionic process, which are generally used for polymerization of dienes and styrenes in hydrocarbon medium [48].

1.3.3. Experimental Considerations, Solvent and Temperature

Due to the high nucleophilicity and basicity of the initiators and propagating chain ends, it is necessary to conduct the polymerizations under inert atmosphere; in the absence of moisture and protic impurities. Oxygen must also be removed from the reaction medium since it causes chain coupling via electron transfer with the carbanions [51]. Therefore the reactors to be used, the solvents and the monomers must be prepared accordingly and purged with nitrogen or argon.

In order to avoid chain transfer to solvent, anionic polymerizations are conducted in aprotic solvents. Generally; polar solvents such as tetrahydrofuran (THF) and 1,2-dimethoxyethane or nonpolar solvents such as toluene, cyclohexane and benzene are utilized. The choice of solvent highly affects the propagation step in terms of solvation of the ionic species, as mentioned previously. Electron transfer initiators are known to work efficiently in polar solvents which provide fast generation of bifunctional propagating chains. On the other hand, it is not possible to prepare radical anions in nonpolar medium; electron transfer is not efficient in nonpolar solvents since solvation can not be provided. In the case of alkyllithium initiators, polymerization of hydrocarbon monomers like styrene and 1,3-butadiene may be conducted in nonpolar solvents. Since alkyllithium initiators generally exist in aggregated form as previously described, polymerization in polar solvents cause the initiating and propagating carbanions to be much less aggregated due to solvation. This render alkyllithium compounds highly reactive but also unstable in polar medium. Therefore polymerizations in polar solvents are performed at low temperatures (-78^{o}C) when alkyllithium initiators are utilized, to provide control over the reaction processes [42].

Anionic polymerization acrylate and methacrylate monomers proves to be more complicated than nonpolar monomers due to the ester enolate structure of the active chain end. This functionality renders the monomers more reactive via providing resonance stabilization to the propagating carbanion by forming enolate anion (Figure 1.21). However, such polar substituents induce reactivity towards nucleophilic attacks, which leads to side reactions competing with initiation and propagation in addition to termination reactions. For instance, the reaction of methyl methacrylate (MMA) with *n*-BuLi induces the attack of the initiator to the carbonyl group; which leads to the formation of a vinyl ketone (Figure 1.22). Moreover, the active alkyllithium initiator is converted to the less reactive alkoxide species which can not initiate the polymerization of MMA, thus the process results in termination. Similarly the nucleophilic attack of the propagating chain end to the carbonyl group of another polymer chain results in coupling, to yield branched polymer via intermolecular polymer termination (Figure 1.23) [42].

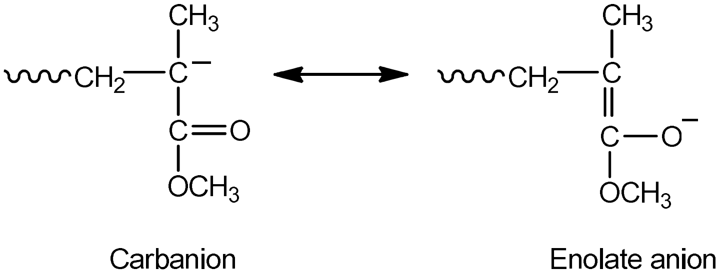

Figure 1.21. Resonance structures of active chain end.

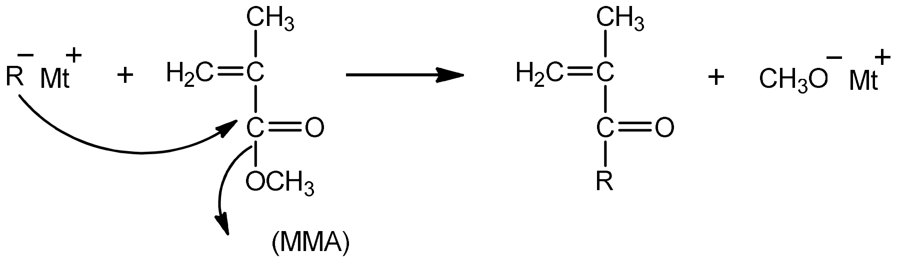

Figure 1.22. Nucleophilic substitution of alkyllithium type initiator to carbonyl group of MMA monomer.

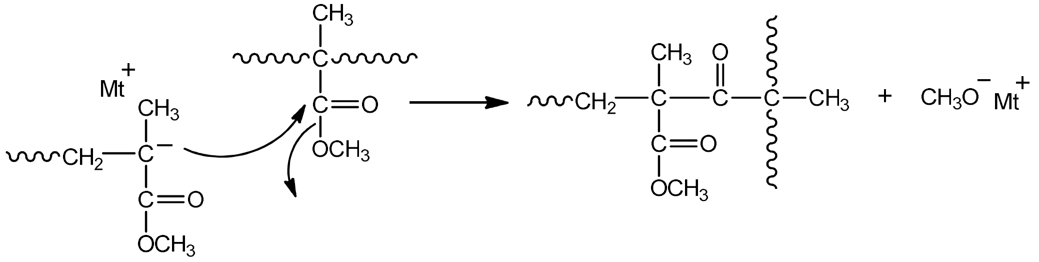

Figure 1.23. Nucleophilic substitution of active chain end to carbonyl group of polymer.

The propagating carbanion may also perform a unimolecular attack on the penultimate ester group, forming a six membered cyclic β-keto ester structure (Figure 1.24). This type of intramolecular termination is called backbiting; the forming methoxide can not initiate the polymerization of MMA [42, 48]. The rate of backbiting is diminished considerably in low temperatures (-78°C), since activation energy of cyclization is higher than that of propagation, and with increasing size of counterion. On the other hand, the above mentioned nucleophilic side reactions can be avoided with the utilization of ligands. Inorganic salts (e.g. LiCl), metal alkoxides (e.g. lithium (2-methoxy)ethoxide), and crown ethers are among the widely used additives in ligated anionic polymerization. These ligands interact with the propagating species by coordinating the anionic center and/or the counterion, enabling the anionic polymerizations to proceed in a controlled manner and sustain "livingness" [52].

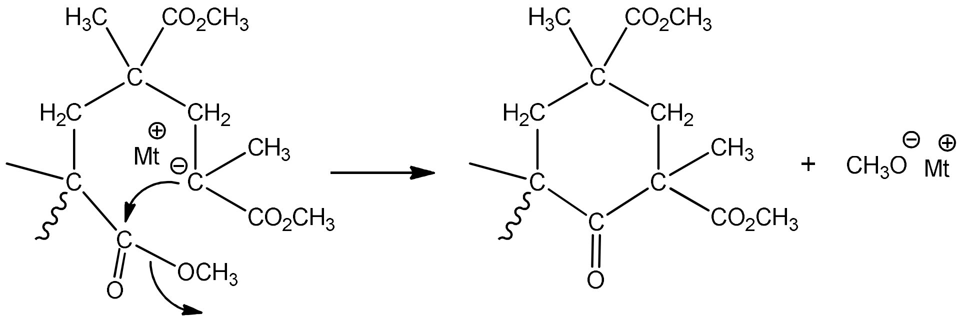

Figure 1.24. Unimolecular back-biting reaction in MMA polymerization.

Another successful methodology to overcome the undesired side reactions is the utilization of a bulky and resonance stabilized initiator, such as 1,1-diphenylhexyllithium (DPHL), which is formed by the reaction of 1,1-diphenylethylene and *n*-BuLi (Figure 1.25) [53]. The usage of this sterically hindered and less nucleophilic initiator prevents the attack on the carbonyl group of the monomer. Thus, the living anionic polymerization of MMA was rendered possible by using DPHL as initiator in THF at -78°C [54].

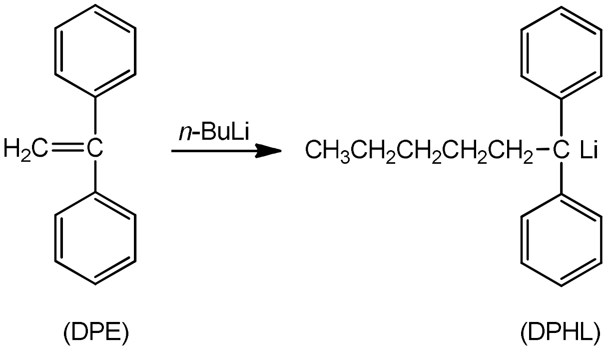

Figure 1.25. Reaction of 1,1-diphenylethylene (DPE) and *n*-BuLi.

1.4. Anthracene Derivatives in Living Anionic Polymerization

The demand for the quantitative labelling of polymers with chromophoric units lead to the usage of anthracene derivatives in anionic polymerization systems. Teyssie and coworkers synthesized (9-anthracenylmethyl) lithium (Figure 1.26), which was employed as a chromophoric initiator for the anionic polymerization of methyl methacrylate [55].

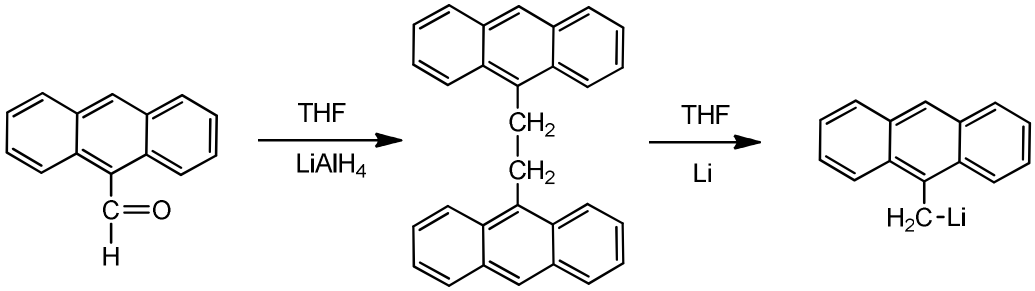

Figure 1.26. Synthesis of (9-anthracenylmethyl) lithium [55].

Müllen group followed this approach and determined that the product contained a fairly large amount of non-functionalized polymers. Therefore they investigated another method for the quantitative labelling of polymers; which involved deprotonation of dihydroanthracene to yield the initiator for the anionic polymerization of methyl methacrylate, styrene and 4-vinylpyridine. The dihydroanthracene was dehydrogenated at the end of the process to regain the chromophoric structure (Figure 1.27) [56].

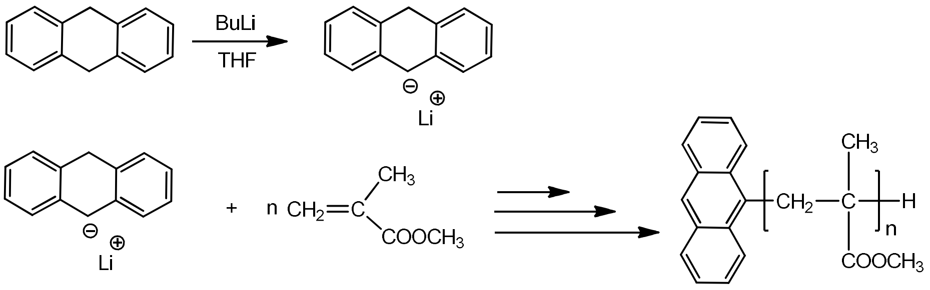

Figure 1.27. Synthesis of anthracene labelled poly(methyl methacrylate) [56].

1,1-diarylethylene type monomers were also utilized for the functionalization of polymers; the labelling methods were based on the addition reactions of carbanionic species to diphenylethylene derivatives. The process gained advantage from the fact that 1,1-diphenylethylene did not homopolymerize and reactions with simple and polymeric organolithium compounds proceeded quantitatively to yield diphenylalkyllithium species. Quirk et al. reported the synthesis of several 1,1-diphenylethylene derivatives for the functionalization of polymers [57-59]. It was stated that the 1,1-diphenylethylene system could be utilized to obtain polymers functionalized at the initiation step (Figure 1.28a), termination step (Figure 1.28b), or within the polymer chain (Figure 1.28c) [58]. Moreover, the addition reactions could be monitored by UV-visible spectroscopy, owing to the chromophoric nature of these diphenylethylene derivatives.

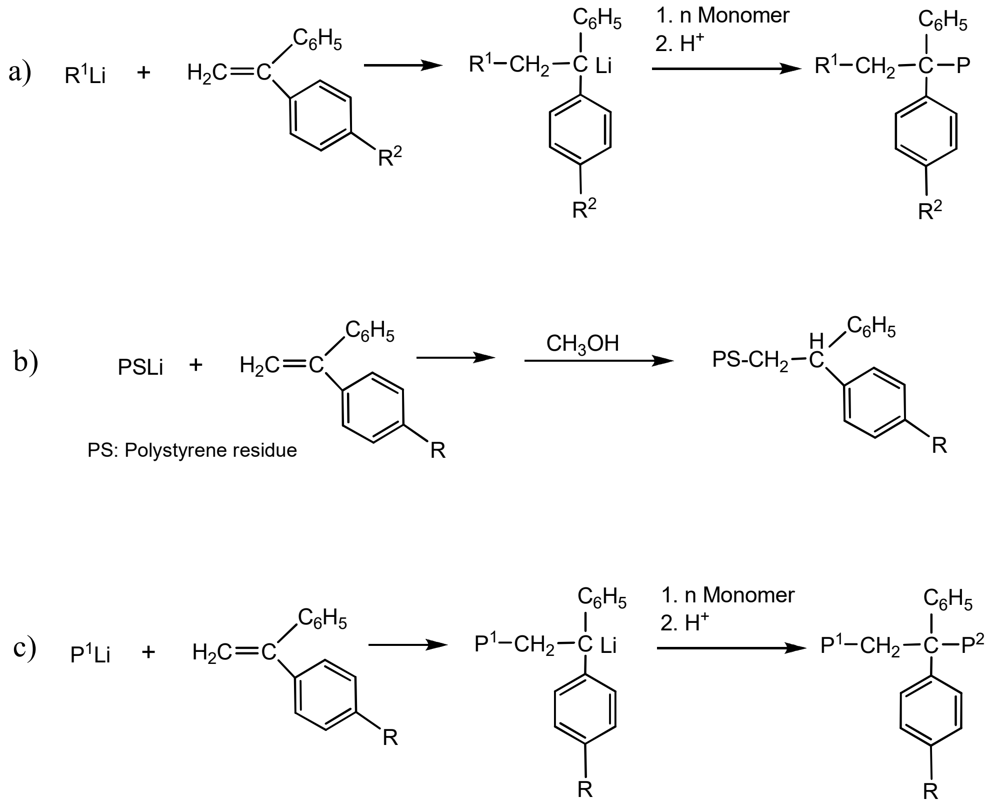

Figure 1.28. Preparation of 1,1-diarylethylene functionalized polymers [57-59].

1.4.1. 1-(2-anthryl)-1-phenylethylene Functionalized Polymers

Following the strategy discussed above, two fluorescent monomers 1-(2-anthryl)-l-phenylethylene and 1-(9-phenanthryl)-l-phenylethylene were synthesized and utilized in anionic polymerization systems [60-62]. Figure 1.29 shows the structure of 1-(2-anthryl)-1-phenylethylene (APE), which bears the greater interest for the current study due to the anthracene functionality. Various APE functionalized polymers were synthesized over the years [60-62, 66-74], some of which will be discussed onwards.

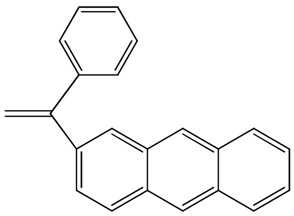

Figure 1.29. 1-(2-anthryl)-1-phenylethylene (APE).

APE was first incorporated in the copolymer structure to determine both molecular weight and critical micelle concentration in two studies by Riess and Nugay [60]. In this work, APE and 1-(9-phenanthryl)-1-phenylethylene were employed as fluorescent monomers at the block junction of polystyrene-b-poly(ethylene oxide) (PS-b-PEO) copolymers (Figure 1.30). The synthesis of block copolymers was achieved via sequential anionic polymerization technique. The fact that these 1,1-diarylethylene compounds did not homopolymerize proved to be an advantage. It was determined that when they are used in slight excess quantity with the polymer anion, it leads to formation of polymers with only one 1,1-diarylethylene unit at the chain end. Thus every polymer chain becomes labeled with one fluorescent unit. This property enables to determine the molecular weight of the synthesized polymer by UV analysis, and correlate it with the obtained number average of molecular weight provided that suitable molar absorption coefficient value for the chromophore at the utilized wavelength is determined.

Initially, anionic polymerization of styrene was conducted and the polymer chains were end-functionalized by either APE or 1-(9-phenanthryl)-1-phenylethylene, with active chain end. This macroinitiator was then used in the polymerization of ethylene oxide (EO), which forms ethoxy chain end that is incapable of reinitiating APE. As a result, well-defined block copolymers were obtained (Figure 1.30). They were utilized for the formation of micellar structures and the investigation of non-radiative energy transfer, owing to the coinciding donor and acceptor properties of the fluorescent dyes phenanthrene and anthracene, respectively [61].

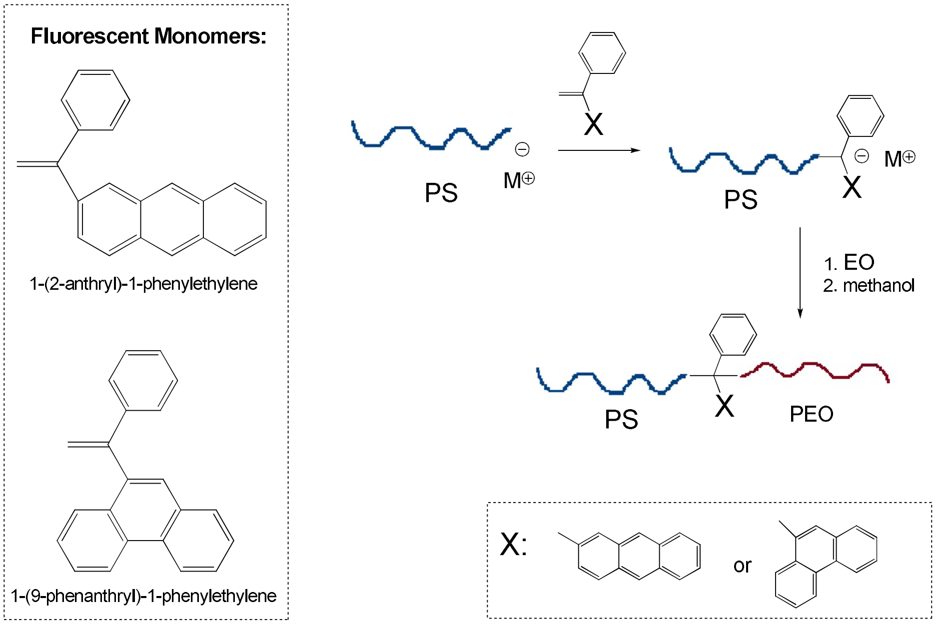

Figure 1.30. Synthesis of block copolymers [60].

Riess et al. reported the synthesis polystyrene-b-poly(tert-butyl acrylate) diblock copolymers containing APE or 1-(9-phenanthryl)-1-phenylethylene at the block junction as well [62]. Sequential anionic polymerization was utilized; to obtain the PS chains initially, then label them with one unit of fluorescent monomer via addition to the living polystyryl chain end, finally initiating the growth of poly(tert-butyl acrylate) chains to obtain the desired block copolymer.

Concerning the choice of fluorescent monomer APE, 2-anthryl derivative was preferred instead of 1- or 9-anthryl derivatives mainly based on the problems regarding the anionic polymerizations of different isomers of vinylanthracenes, previously reported by Stolka et al. [63-65]. It was stated that 9-anthryl derivatives were prone to undergo electron transfer reactions through the 10-position; which could lead to recombination, disproportionation or hydrogen abstraction reactions. In the case of 1-anthryl derivatives, the steric constraint that arise from the H atom at 9-position create a negative effect in terms of resonance stabilization of the molecule.

Winnik and coworkers utilized APE in several studies [66-72]. Polystyrene-b-poly(methyl methacrylate) (PS-b-PMMA) diblock copolymers containing a chromophoric unit at the block junction were synthesized for nonradiative direct energy transfer (DET) experiments and fluorescence decay measurements [66-68]. Anionic polymerization of styrene was performed, followed by the end-functionalization of polystyryl chains with APE or 1-(9-phenanthryl)-1-phenylethylene, which formed an anionic chain end capable of initiating methyl methacrylate polymerization. Similarly, polyisoprene-b-poly(methyl methacrylate) (PI-b-PMMA) diblock copolymers were synthesized sequentially; by the anionic polymerization of isoprene, addition of APE or 1-(9-phenanthryl)-1-phenylethylene to the active chain end and initiating the growth of the methyl methacrylate block [69, 70]. However, this approach could not be followed to obtain polyisoprene-b-polystyrene (PI-b-PS) labelled at the junction; the addition of the anthryl dye molecule failed to produce a carbanionic center reactive enough to initiate the polymerization of isoprene or styrene. Therefore the anionic polymerization process was combined with atom transfer radical polymerization (ATRP) to obtain the desired block copolymers [71]. The synthesis of poly(methyl methacrylate)-b-poly(alkyl acrylate) diblock copolymers with anthracene or phenanthrene units at the junction was also investigated, once again conjoining ATRP with anionic polymerization [72]. Initially, APE labelled poly(methyl methacrylate) macro-initiator was synthesized to carry out the chain extension with acrylates via ATRP. However it was observed that during the latter process, the propagating acrylate radicals add to the 10- position of anthryl unit to and form dibenzylic radicals (Figure 1.31). Therefore an inverse pathway was chosen for the synthesis of anthryl labelled block copolymers. First APE functionalized poly(tert-butyl acrylate) was prepared by anionic polymerization, followed by ATRP of MMA to obtain diblock copolymers; due to the fact that anthracene does not interfere with radical polymerization of methacrylates [35, 37].

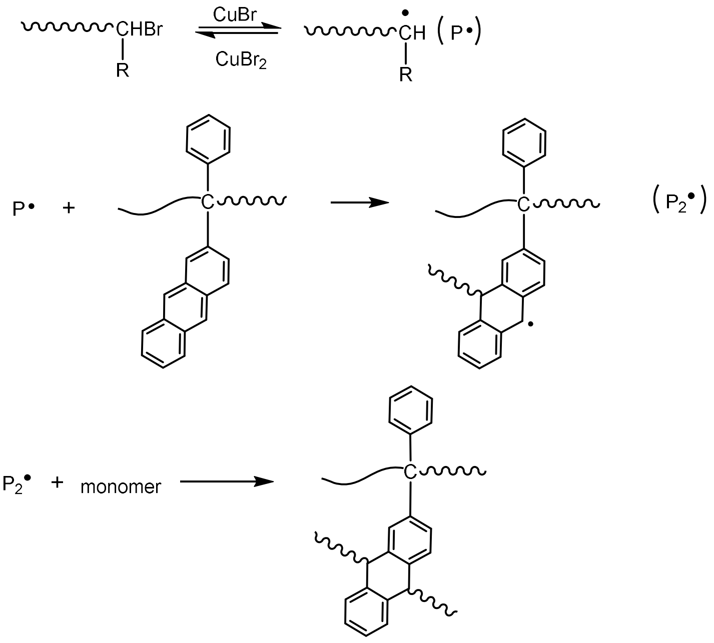

Figure 1.31. Addition of propagating acrylate radicals to 2-anthryl derivative [72].

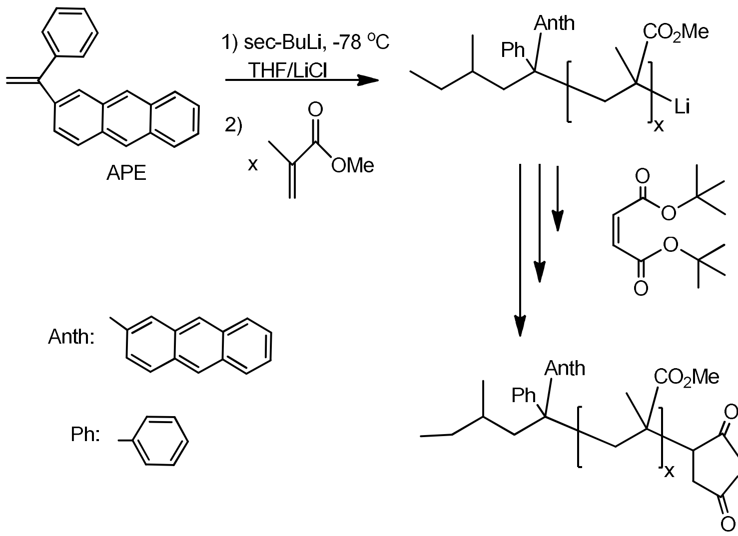

Figure 1.32. Synthesis of anthracene labelled PMMA anhydride [73].

Moon et al. studied the synthesis of anthracene labelled PMMA and PS containing a terminal anhydride unit via anionic polymerization. These polymers were prepared for further reaction with amine terminated counterparts, with anthracene units acting as fluorescent labels for the monitoring of the process. A single unit of APE was incorporated into polymer structure of both PMMA and PS. For the latter, APE monomer was introduced into the prepared polystyryllithium solution, yielding anthryl end-functionalized PS. In the case of PMMA, the reaction of APE with *sec*-BuLi provided the anionic initiator for the polymerization of MMA monomer (Figure 1.32) [73].

Penelle and coworkers also synthesized anthracene functionalized PS and PMMA by the utilization of APE monomer in anionic polymerizations (Figure 1.33) [29]. APE end-functionalized PS was obtained again by introducing the monomer into living polystyryllithium solution; whereas for PMMA the addition of *sec*-BuLi to APE was required to start the initiation of MMA, as described above.

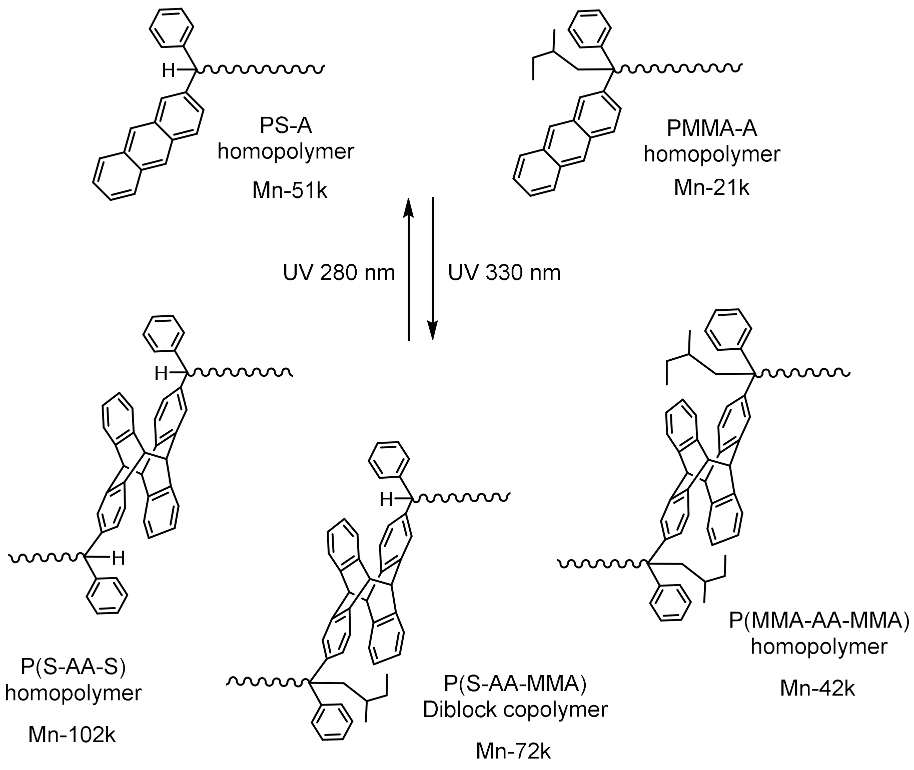

Figure 1.33. Coupling of the APE labelled polymers under UV irradiation [29].

The main object of the study was to obtain PS-b-PMMA diblock copolymers via the coupling of these APE labelled polymers under UV irradiation. This strategy lead to the formation of mixed products, containing coupled PS and PMMA homopolymers alongside the desired diblock copolymers (Figure 1.33). It was stated that the homopolymers could be removed with selective solvents, however this approach provides a very small yield of diblock copolymers, and therefore large quantities of labelled polymers are required for the UV irradiation process to yield utilizable amounts of diblock copolymer product [29].

In the next chapter, the characteristics of another well-known and important polymerization technique, which is cationic polymerization, will be discussed.

1.5. Cationic Polymerization

In general, cationic polymerization may be considered as the propagation of positively charged species via chain-growth polymerization. As discussed in the previous section, the first technique to accomplish the synthesis of well-defined polymers with predictable M_n values and low PDIs was living anionic polymerization. The absence of chain transfer and termination reactions was the key to the successful control over polymerization process. Initially it was thought that this concept of “livingness” could not be applied to cationic polymerization due to the above mentioned side reactions arising from the high reactivity of carbocations. β-proton eliminations, which lead to chain transfer, and carbocationic rearrangements are among the most common side reactions encountered during carbocationic processes. The high reactivity of the carbenium ions also makes the polymerization difficult to control, due to the high rate of propagation even at low temperature, and sensitivity to impurities.

The counteranions in carbocationic polymerization play an important role in modulating the reactivity of carbocations [75]. A reversible combination of the counteranion with the carbenium ion creates a covalently bound species, which is in equilibrium with the carbocationic species. The term “quasi-living” refers to this dynamic equilibrium that is established between the reversibly terminated (dormant) and the carbocationic (active) species (Figure 1.34) [48, 76]. Provided that the rate of exchange reactions is higher than that of propagation, the carbocationic chain ends remain active only for a very short time and do not undergo termination or transfer reactions [77]. Such polymerization mechanism can also be referred to as “living” in the literature [75].

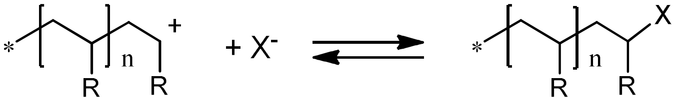

Figure 1.34. The continuous equilibrium between active carbocationic species and dormant covalent species [48].

1.5.1. Monomers

The three major classes of vinyl monomers that can be polymerized by cationic mechanism are vinyl ethers, styrenics and 1,1-disubstituted alkenes. Cationic polymerization of these monomers is possible due to the stabilization of the carbocationic active species by the substituents on the vinyl group [75]. Isobutylene (IB) is one of the most studied monomers for cationic process. Polyisobutylene (PIB) has been in industrial production since 1940s; and has intriguing properties such as low gas and moisture permeability, high thermal stability, low glass transition temperature (Tg) [48, 50]. Copolymers of high molecular weight PIB with small percentage of isoprene units are called butyl rubber, which can be vulcanized due to the presence of double bonds incorporated by isoprene comonomers. Owing to their high stability and low gas permeability butyl rubbers are widely used in tire, engine and automotive industry; as well as for insulation purposes in different fields. [50]. Low molecular weight PIB’s are also utilized in the production sealants, adhesives and lubricating fuels and oils [78]. EPION [79] and Glissopal [80] are examples of commercially available olefin-terminated PIBs. The triblock copolymer of isobutylene and styrene, poly(styrene-b-isobutylene-b-styrene) (SIBS), is stated to be an excellent thermoplastic elastomer in terms of biocompatibility and biostability, thus drawing significant interest for applications in biomaterial science [81].

Cationic polymerization is the sole method for the synthesis of PIB. The monomer IB is a nonpolar hydrocarbon, with two methyl substituents that stabilize the forming tertiary carbocation during the polymerization via inductive effect [75]. The first reported synthesis of PIB by “living” cationic polymerization was by Kennedy group in 1980s [82]. Over the years, numerous studies were done to investigate the kinetics and mechanistic properties of the polymerization technique.

1.5.2. Initiators

The initiation system of IB polymerization includes a carbocation source, which is the initiator, and a Lewis acid that acts as co-initiator. As mentioned previously, choosing a suitable counteranion is very important in maintaining the equilibrium between active carbocationic species and dormant covalent species. Therefore the nucleophilic strength of the Lewis acid and the structure of the initiator should be selected to accord with the reactivity of the monomer. Also, living polymerizations require fast initiation as stated above, which necessitates the use of an initiator that has a faster ionization rate with respect to the dormant chain ends. Provided that termination and chain transfer reactions are absent, or kept to a minimum, the polymer chains can propagate at the same rate and synthesis of monodisperse products can be achieved [83]. In the case of IB polymerization, cumyl and 2,2,4-trimethylpentane derivatives, such as halides, ethers, esters and alcohols are most commonly utilized alongside $TiCl_4$ or BCl_3 Lewis acids for the initiation processes [84].

1.5.3. Experimental Considerations, Solvent and Temperature

The Winstein spectrum and the presence of different ionic species existing in equilibrium in ionic polymerization processes were mentioned in the previous section [85, 86]. The existence of free ions and ion pairs that may both participate in propagation creates complications in the cationic polymerization process. Lewis acids are utilized as catalyst as they induce activation of the carbocation source and maintain the dynamic equilibrium between active ion pairs and the covalently bound dormant species. It is well known that the rate of exchange between active and dormant species should be fast with respect to that of propagation in order to avoid formation of multimodal products. The Lewis acid forms a complex with the leaving group of the initiator, therefore determining the rate of deactivation and inducing control over molecular weight distribution [76, 87].

Salts with common ions could be utilized to shift the equilibrium towards ion pairs and to prevent the propagation of free cations, which are responsible for the formation higher molecular weight fractions in multimodal distributions. Another approach is to use 2,6-di-tert-butylpyridine (DTBP) which, in the presence of $TiCl_4$, is proposed to generate $Ti_2Cl_9^-$ upon reaction with protons and act similarly to salts. Thus, ion pairs may remain the sole propagating species; enabling the synthesis of products with narrow molecular weight distributions [88]. The advantage of 2,6-di-tert-butylpyridine is that it is a widely utilized proton trap with a sterically hindered structure; which reacts with protonic impurities, such as water, and prevents side reactions.

The solvent of choice for IB polymerization is generally a mixture of hexane/dichloromethane (DCM). Solvent polarity affects the ionization and propagation steps differently; while the rate of ionization is increased via the aid of polar DCM component, nonpolar hexane creates a homogeneous medium for the growing PIB chains. Faust et al. also stated that solvent polarity, as well as temperature and Lewis acid strength, had an important effect on overall polymerization rates [89].

In the early stages of cationic polymerization several side reactions rendered the polymerization process difficult to control, as stated above. For instance, the acidic nature of β protons caused vulnerability towards elimination reactions that lead to the formation of terminal unsaturations (Figure 1.35). The presence of a basic species in the reaction medium, including monomers and counterions, may cause the abstraction of β protons [50]. If a β proton is transferred to the monomer, the process is defined as "chain transfer to monomer" and results in the formation of olefinic end groups. The transfer reaction creates a new carbocationic center that also initiates the propagation of chains, hence inducing poor molecular weight control and broad polydispersities [77]. On the other hand, the activation energy for the elimination reaction is generally higher than that of propagation, thus maintaining the polymerization temperature at cryogenic levels (- 78°C) keeps the transfer reactions minimum [90, 91].

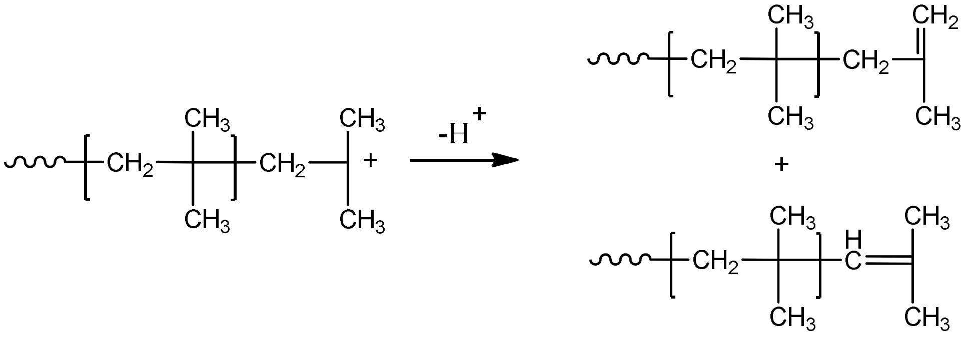

Figure 1.35. β proton elimination.

Purity of the reaction medium also plays an important role on the polymerization process. Nucleophilic impurities may abstract β protons, as stated previously, or they may react with the growing chain ends and induce termination. The activity of Lewis acid co-initiators may also be affected by the presence of such impurities [77]. To prevent such undesirable reactions, cationic polymerizations are typically conducted under inert atmosphere, namely dry N_2 or argon, at cryogenic temperatures and in the presence of purified reagents.

1.5.4. Telechelic Polyisobutylenes

The first examples of telechelic PIBs emerged in the 1980s. Kennedy group developed the “inifer” technique and accomplished the synthesis of chloride di-telechelic PIBs. The inifer process was based upon the utilization of a bifunctional initiator-transfer agent (binifer), para-dicumyl chloride, with BCl_3 as co-initiator; the reaction was conducted in the presence of polar DCM solvent at temperatures around -50 °C [92]. However, further studies on the subject revealed that an undesirable intramolecular cyclization, namely indanyl ring formation, was taking place in the presence of para-dicumyl chloride at temperatures higher than -80 °C (Figure 1.36) [93].

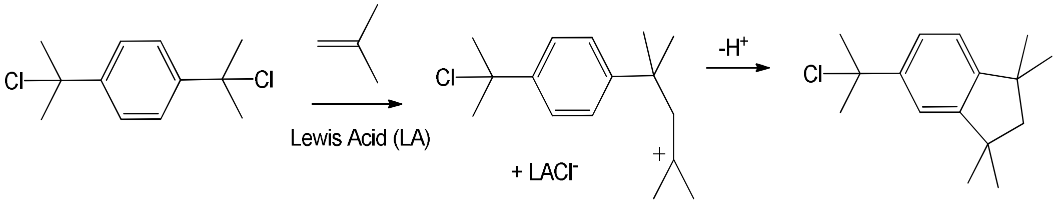

Figure 1.36. Formation of indanyl ring structure [93].

On the other hand, the same group also synthesized tri-tert chlorine telechelic PIBs at relatively high temperatures (-30 °C) by using symmetrical tricumyl chloride initiator (trinifer). The success of this synthesis was attributed to the steric hindrance of trinifer system that prevented the formation of indanyl structure. Following this proposition, steric hindrance was induced on the dicumyl chloride initiator by placing bulky tert-butyl group on the meta position. Thus, indanyl ring formation was suppressed and the synthesis of perfect di-telechelic PIBs could be accomplished at higher temperatures by using 5-tert-butyl-1,3-bis(2-chloro-2-propyl)benzene (t-Bu-m-DiCumCl) (Figure 1.37) [94].

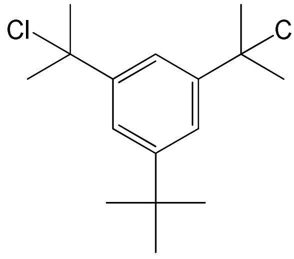

t-Bu-m-DiCumCl

Figure 1.37. Sterically hindered dicumyl chloride initiator.

Apart from cumyl chloride type initiators, cumyl methyl ethers were determined to form good initiating systems with BCl_3 and lead to synthesis of mono-, di- and tri-telechelic PIBs [95, 96]. $TiCl_4$ could also be utilized for the activation of cumyl ether, ester and chloride type initiators [75, 97]. These living cationic polymerization methods developed over the years enabled the synthesis of tertiary chloride end-functionalized PIBs. Further conversion of these chain ends rendered the synthesis of other telechelic PIBs possible. For instance, Kennedy group performed quantitative conversion of chloride chain end to yield allyl terminated PIBs, which were then utilized to form the epoxy and hydroxy derivatives [98].

Faust and coworkers discovered that PIB chain ends could be functionalized with 1,1-diphenylethylene (DPE) quantitatively. The addition of non-homopolymerizable DPE monomer results in the formation of a more stable carbenium ion than that of PIB chain end, which prevents further reaction with isobutylene units. As a result, living PIB chain ends could be quantitatively end-capped with single DPE moieties [99, 100]. This strategy was also well suited for the synthesis of block copolymers. The stable DPE carbenium ion enabled the controlled initiation of styrenic monomers [101, 102] and led to formation of PIB based triblock copolymers (Figure 1.38).

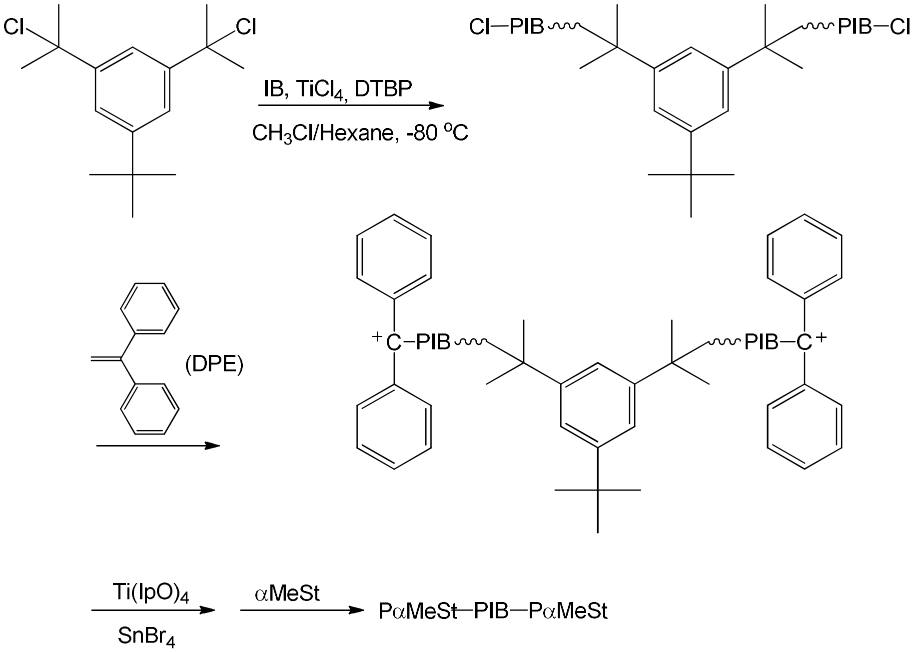

Figure 1.38. Synthesis of poly(α-methylstyrene-b-isobutylene-b-α-methylstyrene) triblock copolymers [101].

Another approach was the metallation of DPE end-functionalized PIB with cesium or Na/K alloy to make the chain end suitable to undergo further anionic polymerization with MMA and tert-butyl methacrylate monomers to obtain linear and star block copolymers [103, 104]. It was also determined that, in the presence of $TiCl_4$, the DPE capped living polymers attained the endgroup structure of 1,1-diphenyl-1-methoxy (DPOMe) (Figure 1.39) quantitatively when a methanol-ammonia mixture was utilized as quenching agent [99, 104]. On the other hand when the polymer solution was quenched with methanol and underwent no further purification, 2,2,-diphenylvinyl (DPV) end functionality was obtained quantitatively (Figure 1.39). The formation of vinylic chain end was attributed to elimination caused by the acidic nature of the medium. The reaction temperature also affected the end-capping yield; it was stated that quantitative functionalization was obtained at -78 °C whereas increasing the temperature resulted in a rapid decrease of capping yield [104].

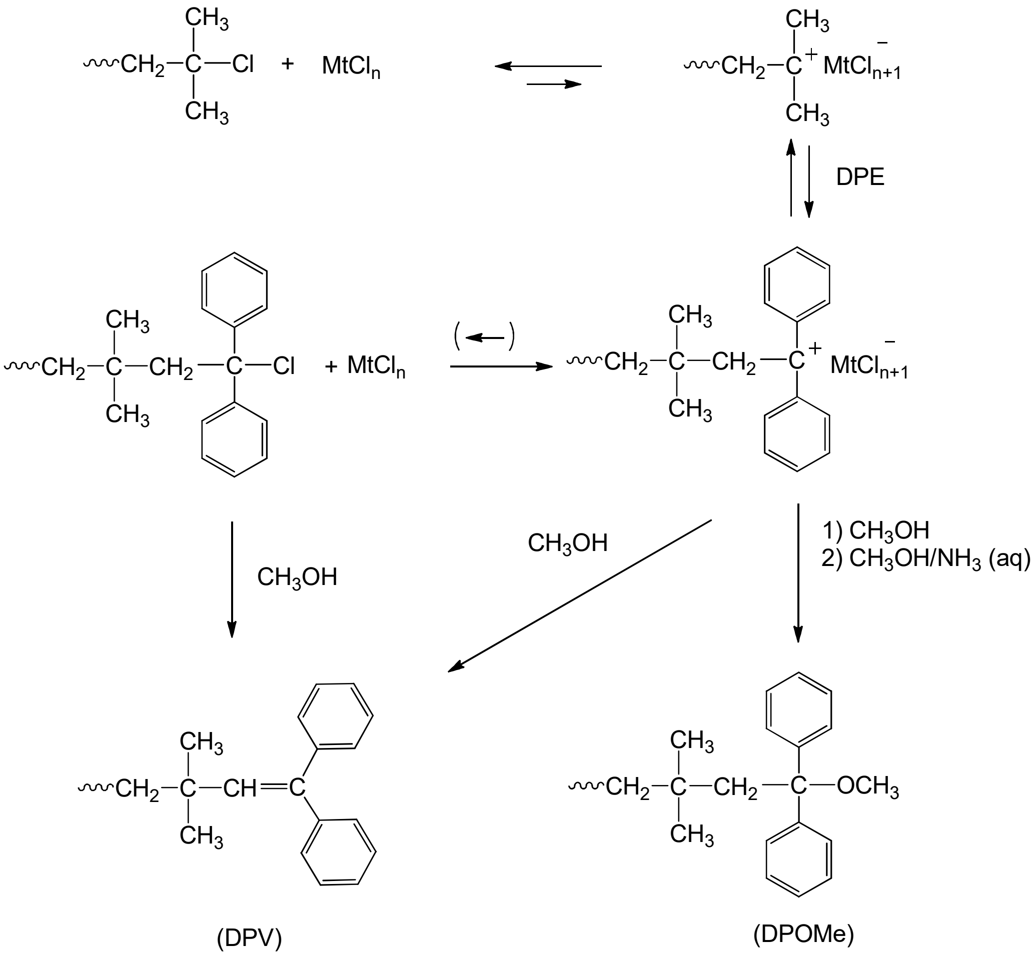

Figure 1.39. Living PIB chains end-functionalized with DPE [104].

Derivatives of DPE have also been utilized for end functionalization of PIB to yield block copolymers. Hadjikyriacou et al. employed 1,1-ditolylethylene (DTE) (Figure 1.40) as well as DPE as end-capping agents for PIB in order to obtain poly(isobutylene-*b*-methyl vinyl ether) via sequential living cationic polymerization [105]. Faust and coworkers utilized 1,4-bis(1-phenylethenyl) benzene (para-double dipehnylethylene, PDDPE) (Figure 1.41) to obtain mono and di-telechelic PIBs, which were than subjected to anionic polymerization with alkyl methacrylate monomers to yield block copolymers [106, 107].

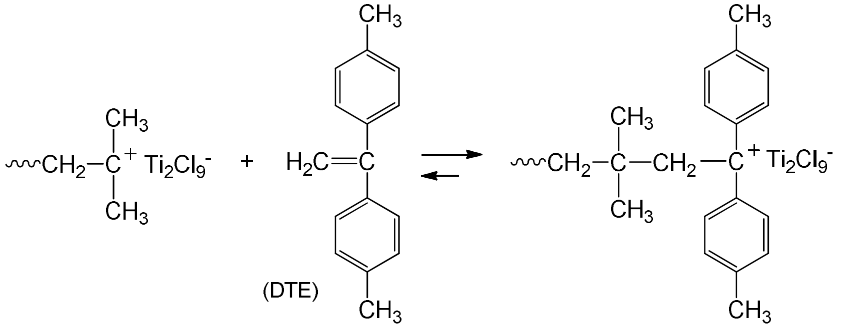

Figure 1.40. End-capping PIB chains with 1,1-ditolylethylene (DTE) [105].

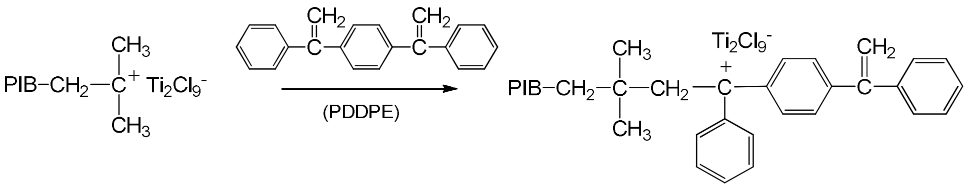

Figure 1.41. End-capping PIB chains with PDDPE [106].

2. AIM OF THE STUDY

The objective of this project is to synthesize various anthryl telechelic and di-telechelic polymers by the utilization of 1-(2-anthryl)-l-phenylethylene (APE), in order to study the reversible photocycloaddition reactions of the anthryl moieties. For this purpose, the 2-substitited anthryl compound APE is selected to be used for chain end functionalization, in order to overcome the restrictions in terms of mobility and steric hindrance induced by the more common 9-substituted anthracenes in the literature and provide ease of photocycloaddition. The initial task is to perform the three step synthesis of APE. Then, novel 1-(2-anthryl)-1-phenylethylene di-telechelic polyisobutylenes are synthesized by the utilization of difunctional cationic initiator 5-tert-butyl-1,3-bis(2-chloro-2-propyl)benzene and the in-situ addition of the non-homopolymerizable APE monomer to the chain ends. Mono and di-anthryl telechelic polystyrenes and anthryl telechelic poly(methyl methacrylate)s are also synthesized via living anionic polymerization by the incorporation of APE at initiation step or at chain end. The APE functionalized polymers are then subjected to UV irradiation at 365 nm to study the reversible [$4\pi+4\pi$] photocycloaddition of the anthryl units; and at 254 nm to examine the photoscission process. Irradiations at 365 nm are conducted to obtain chain extension of anthryl and di-anthryl telechelic polymers; initially for homopolymer solutions and then for polymer mixtures. The products are characterized in terms of change in molecular weight; as the cycloaddition of anthryl units at 365 nm lead to formation of higher molecular weight products by the coupling of polymer chains. UV irradiations of mixtures of di-anthryl telechelic polyisobutylenes and polystyrenes at 365 nm are performed in order to obtain products with possible thermoplastic elastomeric properties.

3. EXPERIMENTAL

3.1. The System

All the syntheses were carried out in a system that is isolated from the external atmosphere. The main vacuum line is equipped with a pump that is capable of reducing the pressure to 10^{-3} mmHg. High purity grade nitrogen gas (N_2) is utilized in order to create an inert atmosphere for the reactions. Additionally, the nitrogen gas is passed through traps containing molecular sieves and active materials to scavenge possible impurities such as oxygen, water vapor and peroxides; to prevent any interference with the ongoing reactions. All the glassware is dried under vacuum by heating (flaming) to eliminate the adsorbed water from glass surface, and purged with N_2 prior to utilization.

Capillary technique is utilized for the transfer of liquid reagents and solvents into reactors. The steel capillary to be used is flamed under N_2 gas flow prior to the transfer process, thereby removing possible impurities present in it. During transfer, one end of the capillary is connected to the flask, capped with a septum, containing the material to be transferred under N_2 nitrogen flow. The other end is inserted into a previously evacuated, dried and N_2 gas filled flask through a septum. When the tip of the capillary is immersed into the liquid, the pressure difference between the two flasks causes the transfer of the material through the capillary. By this method, the transferred material is stored under nitrogen atmosphere after the process.

The solvents used in the reactions are purified by distilling over appropriate desiccants. Vacuum distillation process is the preferred method since it provides fresh and highly pure distillates in a relatively short time. For this purpose; the vacuum distillation apparatus equipped with a magnetic stirrer bar is prepared. The apparatus is connected to the vacuum line with the aid of three-way glass stopcock valves bearing septums. Apiezon H grease is applied to the ground glass joints to provide insulation from external atmosphere. Then the glassware is flamed under vacuum and purged with N_2 after cooling. Next the desiccant of choice is added by briefly opening the round bottom flask of the apparatus under N_2 flush, which is once again vacuumed and purged with N_2. The compound to be purified is transferred into the round bottom flask over the desiccant via syringe or capillary technique. Prior to distillation, this flask is degassed by several freeze-pump-thaw cycles with the aid of liquid nitrogen. Then the flask to collect the distillate is immersed into a Dewar cup filled with liquid nitrogen; creating a difference in pressure between the two sides of the apparatus and thus initiating the distillation process. Once the distillation is complete, the cooling Dewar cup is removed to keep the distillate at room temperature for a while and finally N_2 gas is introduced to the system.

3.2. Materials

Anthracene, acetic anhydride, nitrobenzene, aluminum chloride ($AlCl_3$), diethyl ether (DEE), cyclohexane, phosphorous pentoxide, toluene, acetic acid (CH_3COOH), sulfuric acid (H_2SO_4), lithium chloride (LiCl), methanol (CH_3OH), magnesium sulfate ($MgSO_4$), ammonium chloride (NH_4Cl), sodium hydroxide (NaOH), hydrochloric acid (HCl), sodium bicarbonate ($NaHCO_3$), titanium tetrachloride ($TiCl_4$), calcium hydride (CaH_2), benzophenone, sodium chloride (NaCl), dichloromethane (DCM), chloroform, n-hexane, tetrahydrofuran (THF), ammonia (NH_3), 2,6-di-tert-butylpyridine (DtBP), methyl methacrylate (MMA) and styrene were purchased from Merck. Sodium (Na) and potassium (K) metals were purchased from Alfa Aesar. Calcium chloride ($CaCl_2$) anhydrous was purchased from J.T. Baker. Isobutylene (IB) was purchased from Scott Speciality Gases. Phenylmagnesium bromide (PhMgBr, 3 M solution in DEE), methylmagnesium bromide (MeMgBr, 3 M solution in DEE), *n*-butyllithium (*n*-BuLi, 1.6 M solution in hexanes), *sec*-butyllithium (*sec*-BuLi, 1.3 M solution in hexanes) triethylaluminium (1.0 M solution in hexanes) and N,N-dibutylmagnesium (0.5 M solution in heptane) were purchased from Sigma Aldrich.

3.2.1. Purification of Solvents and Reagents

Nitrobenzene was stored over molecular sieve for 1 day and then transferred into a previously flamed and nitrogen purged fractional distillation apparatus via capillary technique. Vacuum distillation was performed to obtain purified liquid.

DCM was washed with 5% NaOH and water to remove stabilizers and impurities. Then it was dried over anhydrous $CaCl_2$ and refluxed in the presence of CaH_2 under nitrogen atmosphere. Before being used in polymerization reactions, DCM was freshly distilled over phosphorous pentoxide. Phosphorous pentoxide was added to the previously flamed and nitrogen filled distillation apparatus, which was opened for a short time under nitrogen flush. Then the system was evacuated and refilled with nitrogen gas. The required amount of DCM was transferred to the distillation apparatus via capillary technique. After the liquid was degassed via consecutive freeze-pump-thaw cycles, vacuum distillation was conducted. The system was filled with nitrogen gas after purified DCM was collected.

n-Hexane was refluxed over CaH_2 under nitrogen atmosphere and freshly distilled over sodium mirror prior to use. A piece of sodium metal was placed in a previously flamed and nitrogen filled distillation apparatus under nitrogen flush. Then the system was evacuated and the flask was flamed gently until the formation of a homogeneous sodium mirror took place on the surface of the distillation flask. The required amount of n-hexane was transferred onto the sodium mirror via capillary technique. Vacuum distillation was performed following consecutive freeze-pump-thaw cycles, the apparatus was filled with nitrogen gas after the distillation was completed.

THF was purified by distillation over sodium and benzophenone. The required amount of THF was transferred into a previously flamed and nitrogen filled distillation apparatus via capillary technique. Pieces of sodium metal and benzophenone were added to the distillation flask under nitrogen flush. The mixture was allowed to stir until the colorless solution turns to dark blue; which indicates the formation of the radical anion, a scavenger of water and oxygen. Then the distillation flask was degassed via consecutive freeze-pump-thaw cycles and distillation was conducted under reduced pressure. The system was filled with nitrogen gas after purified THF was collected.

Toluene was purified by distillation over sodium and benzophenone, by the same procedure applied to THF.

Isobutylene was dried via passing through a column of anhydrous calcium sulfate, cobalt chloride, moisture sensitive color indicator and silica gel. It was collected by condensation into a flamed and nitrogen purged graduated cylinder immersed in an acetone-dry ice bath at -40 °C.

2,6-di-tert-butylpyridine (DtBP) was purified by distillation over calcium hydride (CaH_2). CaH_2 was added into a previously flamed and nitrogen filled distillation apparatus under nitrogen flush. The system was evacuated and refilled with nitrogen gas. The required amount of DtBP was transferred onto CaH_2 via a syringe equipped with a steel capillary. Degasing was done through consecutive freeze-pump-thaw cycles, distillation was performed under vacuum. The system was filled with nitrogen gas after purified DtBP was collected.

Styrene and MMA were purified by the same procedure applied to DtBP. Before polymerizations MMA was treated with triethylaluminum and distilled under vacuum, whereas styrene was distilled over N,N-dibutylmagnesium.

Naphthalene was purified by sublimation under reduced pressure. The rest of the chemicals were used as received.

3.3. Synthesis of Anthracene Functionalized Monomer 1-(2-anthryl)-1-phenylethylene (APE)

3.3.1. Synthesis of 2-acetylanthracene (A-ANT)

50 g anthracene was weighed into a previously flamed and nitrogen filled two-necked round bottom flask, equipped with a stirrer and a graduated dropper. System was evacuated and purged with nitrogen, then 100 ml distilled nitrobenzene was transferred via capillary technique. The suspension was stirred at room temperature. A separate two-necked round bottom flask was prepared in the same manner. 85 g $AlCl_3$ was transferred into this flask and 320 ml nitrobenzene was added by capillary. The mixture was stirred at room temperature. 52 ml acetic anhydride was transferred into the graduated dropper by capillary and added dropwise onto the $AlCl_3$ and nitrobenzene mixture whilst stirring in ice-bath. Then, the $AlCl_3$-acetic anhydride complex was slowly added into the anthracene suspension through the dropper by vigorous stirring over a period of 2 h and stirred at room temperature for 18 h. 500 ml benzene was transferred into the red complex that had formed, which was then filtered, washed with cold benzene and hexane. Next, hydrolysis of the red complex was performed by adding into a mixture of 100 ml HCl and 500 ml distilled water-ice. The green colored product was collected by filtration, extracted with chloroform and water, dried with $MgSO_4$ and recrystallized from DEE. The product was further dried on the high vacuum line and weighed as 11.9887 (yield= 23.9 %).

^1H NMR ($CDCl_3$): δ= 2.77 (s, 3H, CH_3), 7.48-7.60 (m, 2H), 7.96-8.09 (m, 4H), 8.44 (s, 1H), 8.58 (s, 1H), 8.66 (s, 1H).

3.3.2. Synthesis of 1-(anthracen-2-yl)-1-phenylethanol (APEOL)

11.9887 g 2-acetylanthracene was weighed into a round bottom flask equipped with a stirrer and graduated dropper. Then 2-acetyl anthracene was dissolved in 350 ml freshly distilled toluene. Grignard reaction was carried out by drop wise addition of 35 ml

PhMgBr (3M in DEE) to the solution at 0 °C under N_2 atmosphere. The reaction was continued overnight at 50 °C. Then the brown reaction content was poured onto a mixture of 46 ml HCl and 460 ml distilled water-ice. The organic layer was separated and washed with $NaHCO_3$ and water. After the extraction was completed, the organic phase was dried over $MgSO_4$ and the solids were filtered off. The solvent was evaporated on rotary evaporator and the product was further dried on the high vacuum line.

^{1}H NMR ($CDCl_3$): δ= 2.09 (s, 3H, CH_3), 7.28-7.53 (m, 8H), 7.90-8.05 (m, 3H), 8.13 (s, 1H), 8.37 (s, 1H), 8.43(s, 1H).

3.3.3. Synthesis of 1-(2-anthryl)-1-phenylethylene (APE)

All of the obtained 1-(anthracen-2-yl)-1-phenylethanol (APEOL) was dissolved in 240 ml acetic acid and refluxed at 130 °C. Then 0.2 ml concentrated H_2SO_4 was added dropwise into the solution. The mixture was cooled; the crystalline product was collected, washed with cold acetic acid and dried. The APE monomer was further purified by recrystallization ad weighed as 8.1862 g (Figure 3.1) (yield= 68.4 %, with respect to 2-acetyl anthracene).

^{1}H NMR ($CDCl_3$): δ (ppm) = 5.57 (s, 1H), 5.67 (s, 1H), 7.33-7.53 (m, 8H), 7.90 -8.05 (m, 4H), 8.37 (s, 1H), 8.41(s, 1H).

3.4. Anionic Polymerizations

3.4.1. Synthesis of Anthryl Telechelic Poly(methyl methacrylate) by Anionic Polymerization

A representative polymerization procedure for the synthesis of anthryl telechelic poly(methyl methacrylate) (PMMA-APE) was carried out as the following. Into a previously vacuumed and nitrogen purged reactor 0.4508g (1.61 x 10^{-3} mol) APE and 0.0877 g (2 x 10^{-3} mol) LiCl ligand was weighted and dried under vacuum. The system was filled with nitrogen gas and 90 ml previously purified THF was transferred into the reactor through a stainless-steel capillary and cooled to -78 ºC. A small amount of *n*-BuLi initiator was added dropwise to the reaction mixture for blank titration until the deep purple color of 1-(2-anthryl)-1-phenylhexyllithium (APHL) complex persisted (Figure 3.2). Subsequently, the required amount of n-BuLi/hexane solution to provide 4 x 10^{-4} mol initiator was added. 2.13 ml of freshly distilled MMA was added to the reactor via capillary under rapid stirring. The reaction was quenched by the addition of methanol after 90 min. Then the polymer solution was concentrated on rotary evaporator and precipitated in 400 ml hexane. Following the filtration, the obtained compound was dissolved in THF and precipitated in hexane once again. The final product was filtered through sintered glass and dried on high vacuum line.

^{1}H NMR ($CDCl_3$): δ= 0.77-1.25 (br, 3H, CH_3), 1.75-2.00 (br, 2H, CH_2), 3.50-3.68 (s, 3H, CO_2CH_3), 6.67-8.50 (m, 14H, Ar-H).

Two sets of polymerizations were carried out by changing the initiator amount in order to obtain polymers with different molecular weights, the reaction conditions are given in Table 3.1.

Table 3.1. Reaction Conditions for Anionic Polymerization of MMA

Name	APE (mol/10^{-3})	n-BuLi (mol/10^{-4})	MMA (mol/10^{-2})
$PMMA_{3k}$-APE	1.61	4.0	2.0
$PMMA_{16k}$-APE	0.78	1.56	1.88

3.4.2. Synthesis of Anthryl Telechelic Polystyrene by Anionic Polymerization

60 ml distilled THF was added into a flamed and nitrogen purged flask and cooled to -78 °C under nitrogen atmosphere. The required amount of *sec*-BuLi was added to provide 4.8×10^{-4} mol initator. Then 2.2 ml of freshly distilled styrene was added via capillary with rapid stirring. The solution was stirred at -78 °C for 90 min. Concurrently, 0.2060 g APE was weighed into a 100ml flamed and nitrogen purged flask. After it was degassed for 1 h, system was purged with nitrogen gas and 20 ml freshly distilled THF was added under nitrogen flow via capillary. A few drops of *sec*-BuLi was added into the solution until a deep purple color persisted. This solution was then added into the reaction flask via capillary at -78 °C and stirred for an additional 75 min. The reaction was terminated by the addition of 3 ml methanol. The polymer solution was concentrated on rotary evaporator and precipitated in 500 ml methanol. The product PS_{4k}-APE was filtered through sintered glass and dried on high vacuum line.

^1H NMR ($CDCl_3$): δ= 0.50-0.80 (m, 6H, CH_3, *sec*-butyl), 1.20-1.67 (br, 2H, CH_2), 1.67-2.30 (br, H, CH), 6.25-7.25 (br, 5H, Ar-H, styrene), 6.67-8.50 (m, 14H, Ar-H, APE).

3.4.3. Synthesis of Potassium Naphthalenide for Anionic Initiation

Previously sublimed naphthalene was transferred into the flamed and nitrogen purged reaction flask and excess amount of potassium metal was weighed in to the flask under nitrogen atmosphere in dry box. Freshly distilled THF was transferred into the flask via capillary. The reaction was conducted under nitrogen atmosphere at 0 °C for 2 h and a dark green solution of the radical anion initiator was obtained (Figure 3.3).

3.4.4. Synthesis of di-Anthryl Telechelic Polystyrene by Anionic Polymerization

A representative polymerization procedure for the synthesis of di-anthryl telechelic polystyrene (APE-PS-APE) was carried out as the following. Into a previously vacuumed and nitrogen purged reactor 40 ml freshly distilled THF was transferred via capillary. A small amount of potassium naphthalenide initiator solution was added dropwise to the reactor mixture for blank titration until the deep green color persisted. Subsequently, the required amount of potassium naphthalenide solution to provide 5.2×10^{-4} mol initiator was added. The reaction was conducted at -78 ^{o}C with the addition of 2.2 ml (2 g) of freshly distilled styrene to the reactor via capillary under rapid stirring, for 90 min. Concurrently, 0.3459 g APE was weighed into a 100 ml flamed and nitrogen purged flask. After it was degassed for 2 h, system was purged with nitrogen gas and 14 ml freshly distilled THF was added under nitrogen flow via capillary. A few drops of n-BuLi/hexane solution was added into the APE solution until a deep purple color persisted to ensure purification of APE. This solution was then added into the reaction flask via capillary at -78 ^{o}C and stirred for an additional 150 min. The reaction was terminated by the addition of 5 ml methanol. The polymer solution was concentrated on rotary evaporator and precipitated in 350 ml hexane. The product was filtered through sintered glass and dried on high vacuum line.

^{1}H NMR ($CDCl_3$): δ= 1.20-1.67 (br, 2H, CH_2), 1.67-2.30 (br, H, CH), 6.25-7.25 (br, 5H, Ar-H, styrene), 6.67-8.50 (m, 14H, Ar-H, APE).

Two sets of polymerizations were carried out by changing the initiator amount in order to obtain polymers with different molecular weights, the reaction conditions are given in Table 3.2.

Table 3.2. Reaction Conditions for Anionic Polymerization of Styrene and End-Functionalization with APE

Name	Potassium naphthalenide (mol/10^{-3})	Styrene (mol)	APE (mol/10^{-3})
APE-PS_{3k}-APE	0.520	0.0192	1.235
APE-PS_{13k}-APE	0.142	0.0192	0.353

3.5. Cationic Polymerizations

3.5.1. Synthesis of Carbocationic initiator

The sterically hindered di-functional initiator, 5-tert-butyl-1,3-bis(2-chloro-2-propyl)benzene (t-Bu-m-DiCumCl), was synthesized in three steps. Initially the starting compound 5-tert-butylisophthalic acid was converted to dimethyl-5-tert-butyl-1,3-benzyl dicarboxylate, which was then utilized to obtain 5-tert-butyl-1,3-dicumyl alcohol, yielding t-Bu-m-DiCumCl in the final step.

<u>3.5.1.1. Synthesis of dimethyl-5-tert-butyl-1,3-benzyl dicarboxylate.</u> Initially, 25 g 5-tert-butylisophthalic acid was subjected to esterification by refluxing for 2 days in 700 ml methanol in the presence of 47.5 ml sulfuric acid. Obtained product was stored at 0 ºC overnight, then the precipitate was filtered and washed with water, treated with NaHCO3 and extracted. After the organic phase was dried by the addition of dry MgSO4, the solvent evaporated in Rotary Evaporator after filtration step. The product dimethyl-5-tert-

butylisophthalate was further dried on the high vacuum line and weighed as 21.9606 g (yield= 87.8%).

^{1}H NMR ($CDCl_3$): δ= 1.37 (s, 9H, $C(CH_3)_3$), 3.94 (s, 6H, OCH_3), 8.20-8.55 (m, 3H, Ar-CH).

<u>3.5.1.2. Synthesis of 5-tert-butyl-1,3-dicumyl alcohol (t-Bu-m-DiCumOH).</u> 10.02 g (0.04 mol) dimethyl-5-tert-butyl-1,3-benzyl dicarboxylate was dissolved in 50 ml freshly distilled THF. 66.6 ml (0.2 mol) MeMgBr (3M in DEE) was added into this solution dropwise, at 0 ^oC under N_2 atmosphere, to carry out the Grignard reaction. The color of the solution became pinkish after the addition of a few drops of MeMgBr, which then turned into brownish orange. The reaction was continued overnight, afterwards the obtained solid product was dissolved in 50 ml DEE. This solution was added into ice-and NH_4Cl mixture while stirring. Extraction was performed with DEE and the DEE phase was dried over $MgSO_4$. Following the filtration of drying agent, the solvent was evaporated on rotary evaporator and the product was further dried on the high vacuum line. Yield =94 %

^{1}H NMR ($CDCl_3$): δ= 1.34 (s, 9H, $C(CH_3)_3$), 1.60 (s,12H, $C(CH_3)_2$),7.35-7.50 (m,3H, Ar-CH).

<u>3.5.1.3. Synthesis of 5-tert-butyl-1,3-bis(2-chloro-2-propyl)benzene (t-Bu-m-DiCumCl).</u> 5 g (0.02 mol) 5-tert-butyl-1,3-dicumyl alcohol was dissolved in DCM solvent under N_2 atmosphere. The solution was transferred into a previously prepared reactor, containing $CaCl_2$, via capillary technique. In a separate flask sulfuric acid was added dropwise onto sodium chloride, in order to generate HCl gas, which was then introduced into the abovementioned reactor by passing through polytetrafluoroethylene (PTFE) capillary tube under continuous N_2 flush (Figure 3.4). Thus HCl gas was bubbled through the alcohol solution and the reaction was conducted for 6 hours at 0 °C. After completion, the remaining HCl gas was neutralized by bubbling through a flask containing sodium hydroxide solution. The obtained solution was filtered through sintered glass and concentrated on rotary evaporator. Extraction was performed by using DEE and $NaHCO_3$

solution, then the DEE layer was dried over $MgSO_4$ and filtrated. The remaining solvent was evaporated on rotary evaporator and the obtained compound was dried on the high vacuum line. Next, the product was dissolved in hexane and stored in refrigerator for recrystallization. Then, hexane was evaporated on rotary evaporator and the final product was dried on the high vacuum line. The obtained initiator t-Bu-m-DiCumCl was stored under nitrogen atmosphere.

^{1}H NMR ($CDCl_3$): δ= 1.35 (s, 9H, $C(CH_3)_3$), 2.01 (s, 12H, $C(CH_3)_2$), 7.52-7.62 (M, 3H, Ar-CH).

3.5.2. Synthesis of di-Anthryl Telechelic Polyisobutylenes by Carbocationic Polymerization

A representative polymerization procedure of APE-PIB-APE carried out by cationic polymerization is as follows (Figure 3.5). A 500 ml round bottom flask equipped with a magnetic stirrer bar and a rubber septum was prepared by connecting to the vacuum line, flaming under vacuum and charging with nitrogen gas. The polymerization was performed in freshly distilled n-hexane/DCM (60:40 %) solvent mixture at -80 °C under nitrogen atmosphere; with t-Bu-m-DiCumCl/$TiCl_4$ initiating system and DtBP as the proton trap. Hexane (100 ml), DCM (65 ml) and t-Bu-m-DiCumCl (0.2882 g, 1.01×10^{-3} mol) were transferred into the reactor. 0.5 ml (1.66×10^{-4} mol) of a 5 ml stock solution of DtBP in hexane was added via syringe equipped with steel capillary and then the reactor was cooled to -80 °C. Isobutylene (8.2 ml, 1.08×10^{-1} mol) was condensed into a previously flamed and nitrogen filled graduated cylinder at -40 °C and added to the reactor via capillary. After the transfer of $TiCl_4$ (2.2 ml, 2.0×10^{-2} mol) the polymerization was conducted -80 °C for one hour. Then, a solution of APE (1.12 g, 4×10^{-3} mol in 60 ml DCM) added into the reactor via capillary and the reaction was continued for 3 h. Termination was performed by the addition of 5 ml methanol and the polymer solution was precipitated into excess methanol. The obtained polymer was dissolved in hexane, and washed with 5% aqueous sodium bicarbonate and water. The organic phase was dried overnight over magnesium sulfate, filtered through fine sintered glass and the solvent was evaporated on rotary evaporator. Then, the polymer was redissolved in a small amount of hexane and precipitated into acetone twice in order to remove excess APE. Finally, the polymer was further dried on high vacuum line.

^{1}H NMR ($CDCl_3$): δ= 0.77-0.80 (s, 12H, $C(CH_3)_2$), 1.03-1.22 (br, 6H, $C(CH_3)_2$), 1.35-1.46 (br, 2H, CH_2), 7.15 (s, 3H, Ar-H), 7.17-8.50 (m, 28H, Ar-H, APE).

Two sets of polymerizations were carried out by changing the initiator amount to obtain polymers with different molecular weights, the reaction conditions are given in Table 3.3.

Table 3.3. Reaction Conditions for Cationic Polymerization of IB and End-Functionalization with APE

Name	IB (mol)	t-Bu-m-DiCumCl (mol/10^{-3})	DtBP (mol/10^{-4})	$TiCl_4$ (mol/10^{-2})	APE (mol/10^{-3})
APE-PIB$_{6k}$-APE	0.11	1.01	1.66	2.0	4.01
APE-PIB$_{18k}$-APE	0.12	0.4	0.83	1.0	2.01

3.6. UV Irradiation Experiments

A custom made UV chamber was utilized for the UV irradiation experiments of the synthesized polymers. Photocycloaddition reactions of the anthryl functionalized polymers were conducted with low-pressure mercury-vapor fluorescent lamps (Philips TL 8 Watt

Blacklight Blue), with maximum emission wavelength of 365 nm. The intensity of light was measured as 10 mW/cm^2, by using UVA/B Light Meter 850009 (Sper Scientific). Photoscission reactions were performed with low-pressure mercury-vapor fluorescent lamps (8 Watt), with maximum emission wavelength of 254 nm. The intensity of light was measured as 5.5 or 11 mW/cm^2, by using UVC Light Meter 850010 (Sper Scientific). The reactions were carried out at room temperature, a fan attached to the back enabled circulation of air through the UV chamber. The photocycloaddition reactions of anthracene moieties should be conducted under inert atmosphere in order to prevent the formation of endoperoxides that occur in the presence of air [7, 10]. Therefore the polymers to be used were weighed into vials which were then crimp sealed, evacuated under vacuum and purged with nitrogen gas. Then a required amount of distilled THF was transferred into the sealed vial through capillary under N_2 atmosphere. After the reaction mixture was homogenized, the reactor vial was placed into the UV chamber and the polymer solution was stirred throughout the reaction (Figure 3.6). Sampling at different time intervals was done under nitrogen atmosphere.

3.6.1. Preparation of Polymer Films

The polymer solutions irradiated at 365 nm were concentrated by partial evaporation of the solvent and poured into a Teflon mold (3 cm x 1 cm x 0.5 cm) (Figure 3.7). The mold was covered with aluminum foil to prevent light exposure. The films were dried at room temperature for 48 h and then in vacuum oven at 45 °C for 4 h.

3.7. Characterization of Samples

3.7.1. Spectroscopic Analysis

Structural analysis of samples was performed using ^{1}H nuclear magnetic resonance (NMR) spectroscopy on Varian Gemini 400 MHz spectrometer at room temperature with deuterated chloroform (δ $CDCl_3$: 7.26 ppm) as solvent.

3.7.2. Chromatographic Analysis

The number average molecular weights (M_n) and polydispersity index (M_w/M_n) of the polymers were determined by Size Exclusion Chromatography (SEC) at 30 °C using Waters Isocratic HPLC Pump with Waters 2414 Refractive Index (RI) Detector, Waters 2487 UV absorbance detector and four Waters Styragel columns (HR 3, HR 4, HR 4E and HR 5E). Distilled THF was used as the mobile phase at a flow rate of 0.35 mL THF/min. Polystyrene standards in the range of 400-180000 were used for calibration. Samples were injected by using 100 µL Hamilton syringe. For the detection of anthracene moieties, UV absorbance detector was adjusted to 365 nm.

3.7.3. Thermal and Mechanical Analysis

Thermal gravimetric analysis (TGA) was done with a TGA-Q500 TA instrument under N_2 atmosphere. 5 mg samples were heated from 30 to 600 ^{o}C at 10 ^{o}C/min.

Differential scanning calorimetry (DSC) was performed by using DSC-Q2000 TA instrument under N_2 atmosphere. 4 mg samples were weighed in aluminum pans, sealed and heated from -90 to 105 ^{o}C at 10 ^{o}C/min in the first run and from -90 to 150 ^{o}C at 10 ^{o}C/min in the second run.

Mechanical testing of the films was performed by using Zwick/Roell Z1.0 instrument equipped with a 1 kN load cell. Samples (25 mm x 6 mm x 0.5 mm) were tested to failure at 100 mm/min crosshead speed at room temperature.

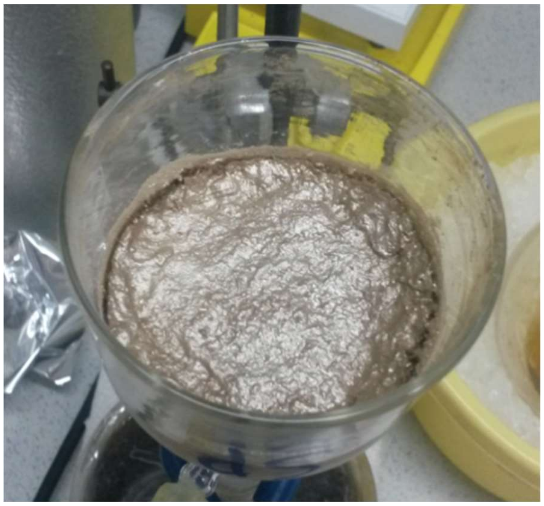

Figure 3.42. 1-(2-anthryl)-1-phenylethylene (APE).

Figure 3.2. Synthesis of anthryl telechelic poly(methyl methacrylate) by anionic polymerization.

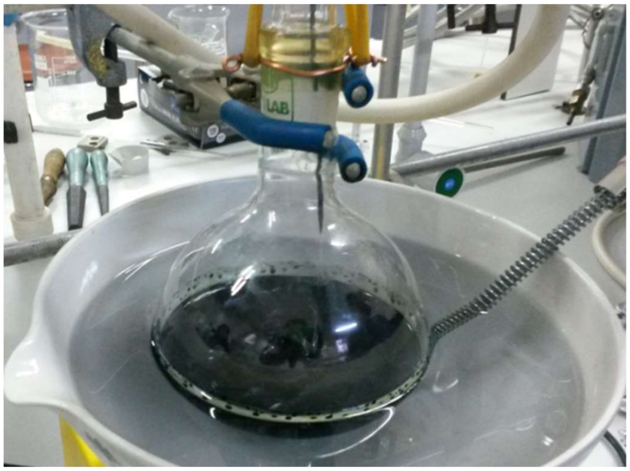

Figure 3.3. Synthesis of potassium naphthalenide for anionic initiation.

Figure 3.4. Synthesis of 5-tert-butyl-1,3-bis(2-chloro-2-propyl)benzene.

Figure 3.5. Cationic polymerization set up.

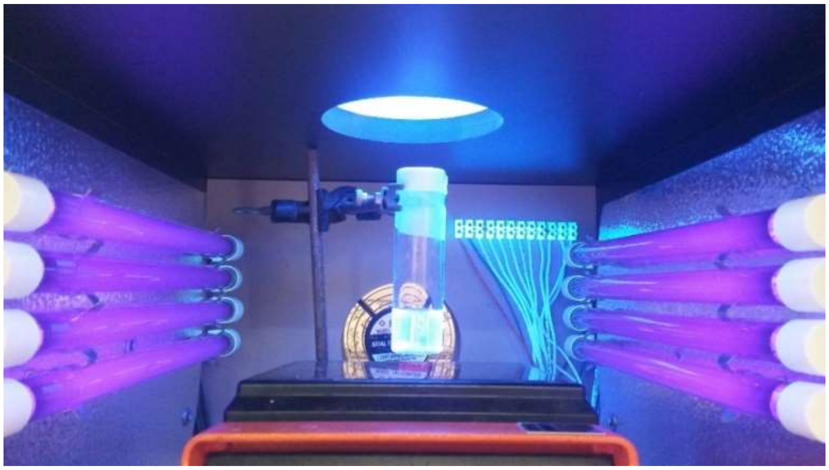

Figure 3.6. UV chamber.

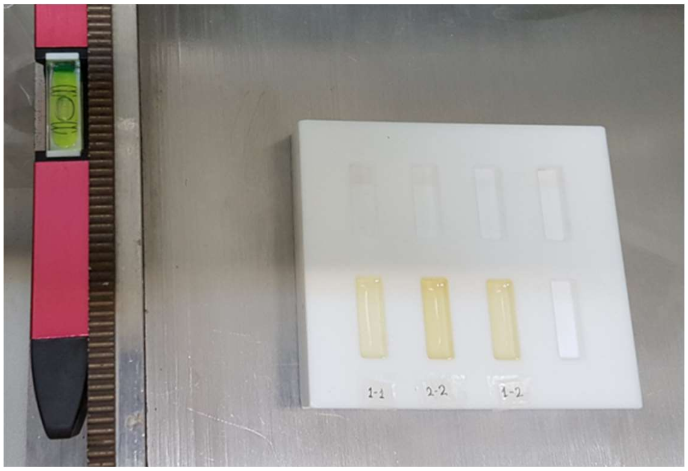

Figure 3.7. Preparation of polymer films.

4. RESULTS AND DISCUSSION

4.1. Synthesis of Anthracene Functionalized Monomer 1-(2-anthryl)-1-phenylethylene (APE)

4.1.1. Synthesis of 2-acetylanthracene (A-ANT)

The synthesis of 2-acetylanthracene (A-ANT) was done by Friedel-Crafts reaction according to the literature as shown in Figure 4.1 [60].

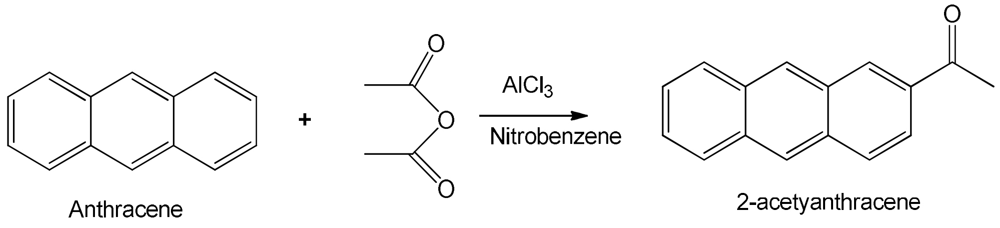

Figure 4.1. Synthesis of 2-acetylanthracene.

The Friedel-Crafts reaction was performed regioselectively by using acetic anhydride as acetylation agent and nitrobenzene as solvent, in order to obtain the 2-acetylanthracene product. These conditions were previously utilized to avoid the formation of side products such as 9- or most commonly 1-acetylanthracene [108].

The initial trial led to the synthesis of very little amount of 2-acetylanthracene, the obtained compound was highly contaminated with side products. This was attributed to the quality of the $AlCl_3$ that was used in the reaction; it was inspected this reactant contained a large amount of aluminum hydroxide due to oxidation. Following the utilization of freshly acquired $AlCl_3$, the desired 2-acetylanthracene was obtained with an improved yield. Moreover, side products such as 1-acetylanthrecene or diacetylanthracenes were removed from the final product.

The ^{1}H NMR spectrum of 2-acetylanthracene in Figure 4.4 shows the methyl protons at 2.77 ppm and the aromatic protons of the anthryl group between 7.48 and 8.66 ppm, with an integration ratio of 1:3, as stated previously [108]. The rest of the signals arise from solvents; DEE at 1.21 and 3.48 ppm, water at 1.56 ppm and acetone at 2.17 ppm. Peaks corresponding to 9- or 1-acetyl and diacetyl side products were not observed [109].

4.1.2. Synthesis of 1-(anthracen-2-yl)-1-phenylethanol (APEOL)

The synthesis of 1-(anthracen-2-yl)-1-phenylethanol (APEOL), which is the interim product in the synthesis of APE, was done by the Grignard reaction of 2-acetylanthracene as described previously (Figure 4.2) [60].

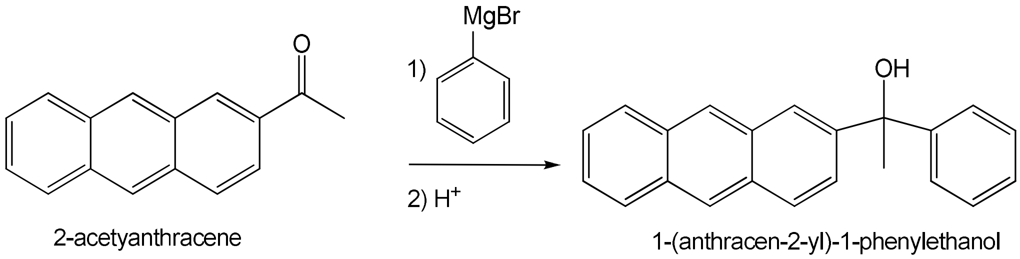

Figure 4.2. Synthesis of 1-(anthracen-2-yl)-1-phenylethanol.

^{1}H-NMR spectrum in Figure 4.5 shows the presence of APEOL with methyl protons at 2.09 ppm and the aromatic protons of the anthryl group between 7.28 and 8.43 ppm. Consumption of the starting compound 2-acetylanthracene was confirmed by the disappearance of corresponding methyl peak at 2.77 ppm. The peak at 1.56 ppm is due to the presence of water. The peaks at 5.57 and 5.67 ppm corresponds to vinyl hydrogens of the final product APE. This indicates that some amount of elimination reaction took place readily before the designated next step of the reaction was performed, which was observed by Hruska et al. as well [62]. Integration ratio of the above mentioned vinylic hydrogen peak at 5.57 ppm and methyl peak at 2.09 ppm shows that the obtained compound consists of 75 % APEOL, the interim product, and 25 % APE. All of this product will be utilized and converted into APE in the next step of the reaction.

4.1.3. Synthesis of 1-(2-anthryl)-1-phenylethylene (APE)

The final step of APE synthesis was performed as described in the literature (Figure 4.3) [60]. The obtained 1-(anthracen-2-yl)-1-phenylethanol (APEOL) was converted into APE via elimination in acidic medium.

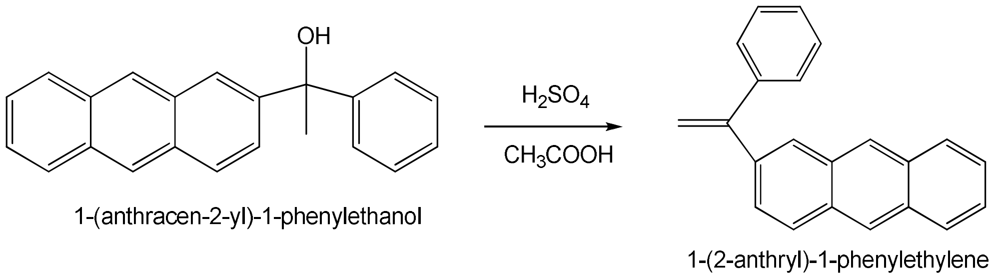

Figure 4.3. Synthesis of 1-(2-anthryl)-1-phenylethylene.

Figure 4.6 shows the ^{1}H-NMR spectrum of the synthesized APE. Consumption of the starting compound APEOL in elimination reaction was confirmed by the disappearance of corresponding methyl peak at 2.09 ppm. The characteristic peaks of APE monomer appear at 5.57 ppm and 5.67 ppm for vinylic hydrogens and between 7.33-8.41 ppm for the aromatic hydrogens of the anthryl moiety [108]. The peak at 1.56 ppm is due to the presence of water. Overall yield of the APE synthesis, with respect to the initial starting compound 2-acetylanthracene, is 68.4 %; ^{1}H-NMR spectrum also indicates that the desired final product APE was successfully synthesized and purified.

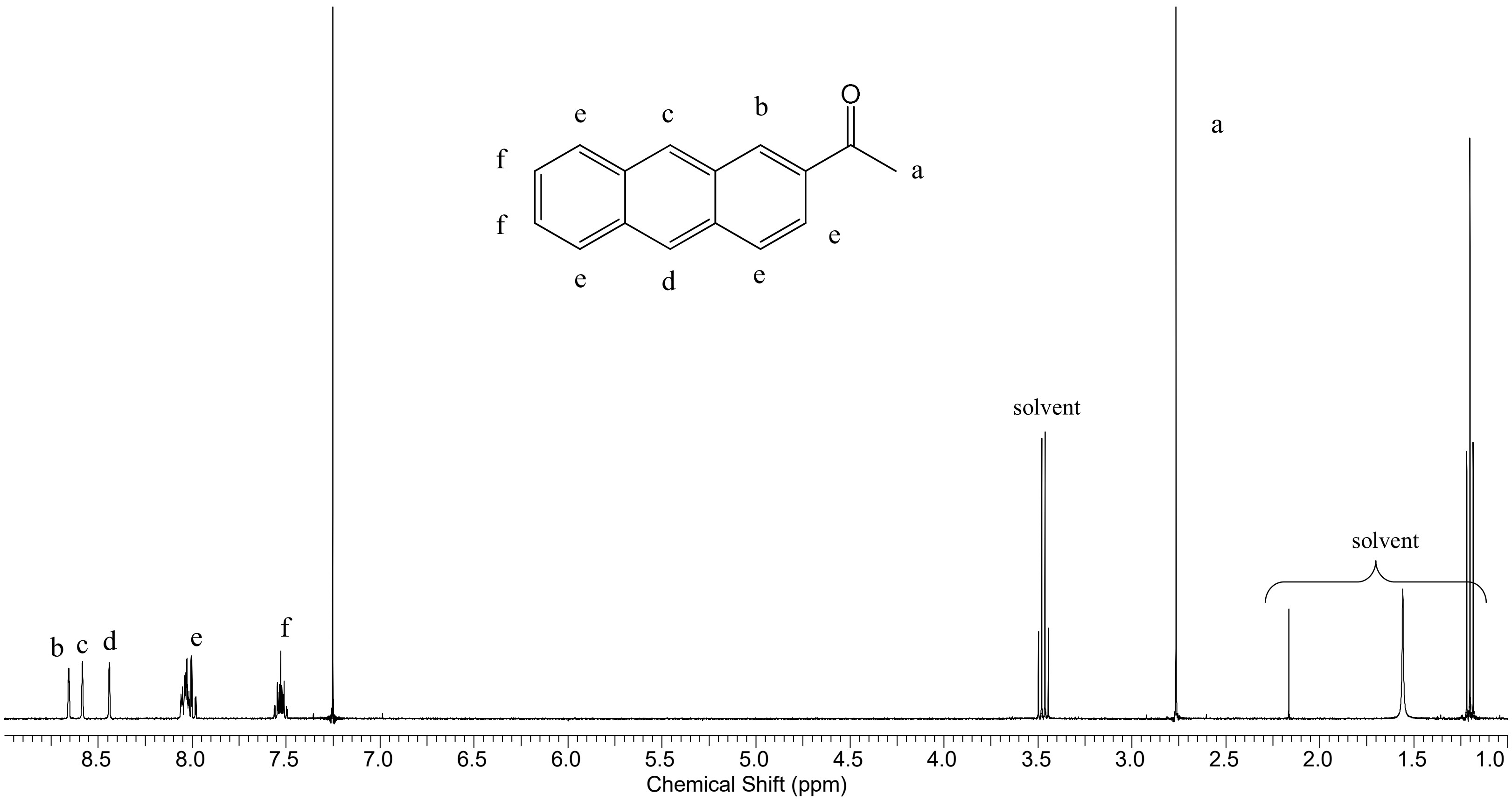

Figure 4.4. ^{1}H NMR spectrum of 2-acetylanthracene.

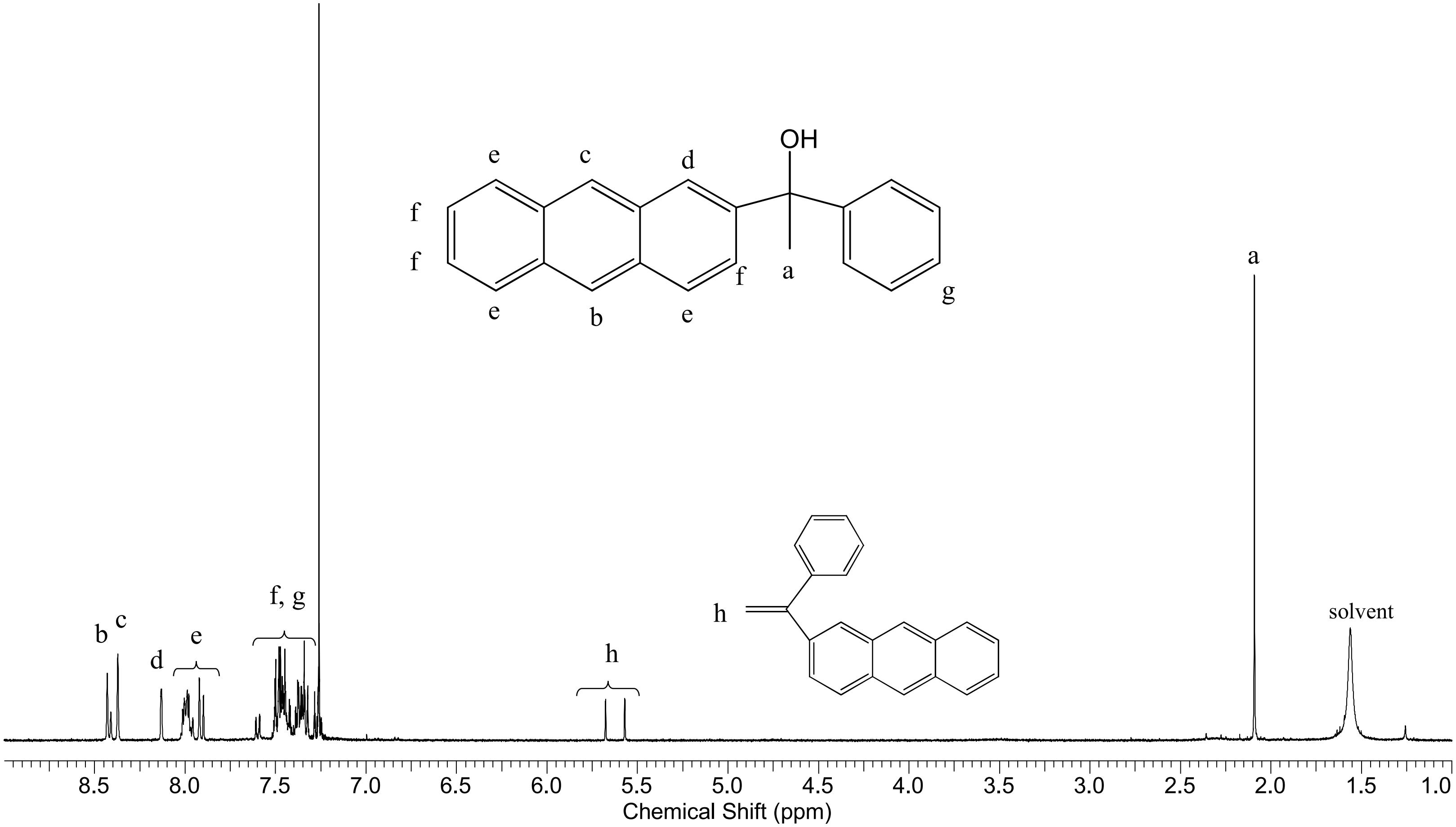

Figure 4.5. ^{1}H NMR spectrum of 1-(anthracen-2-yl)-1-phenylethanol.

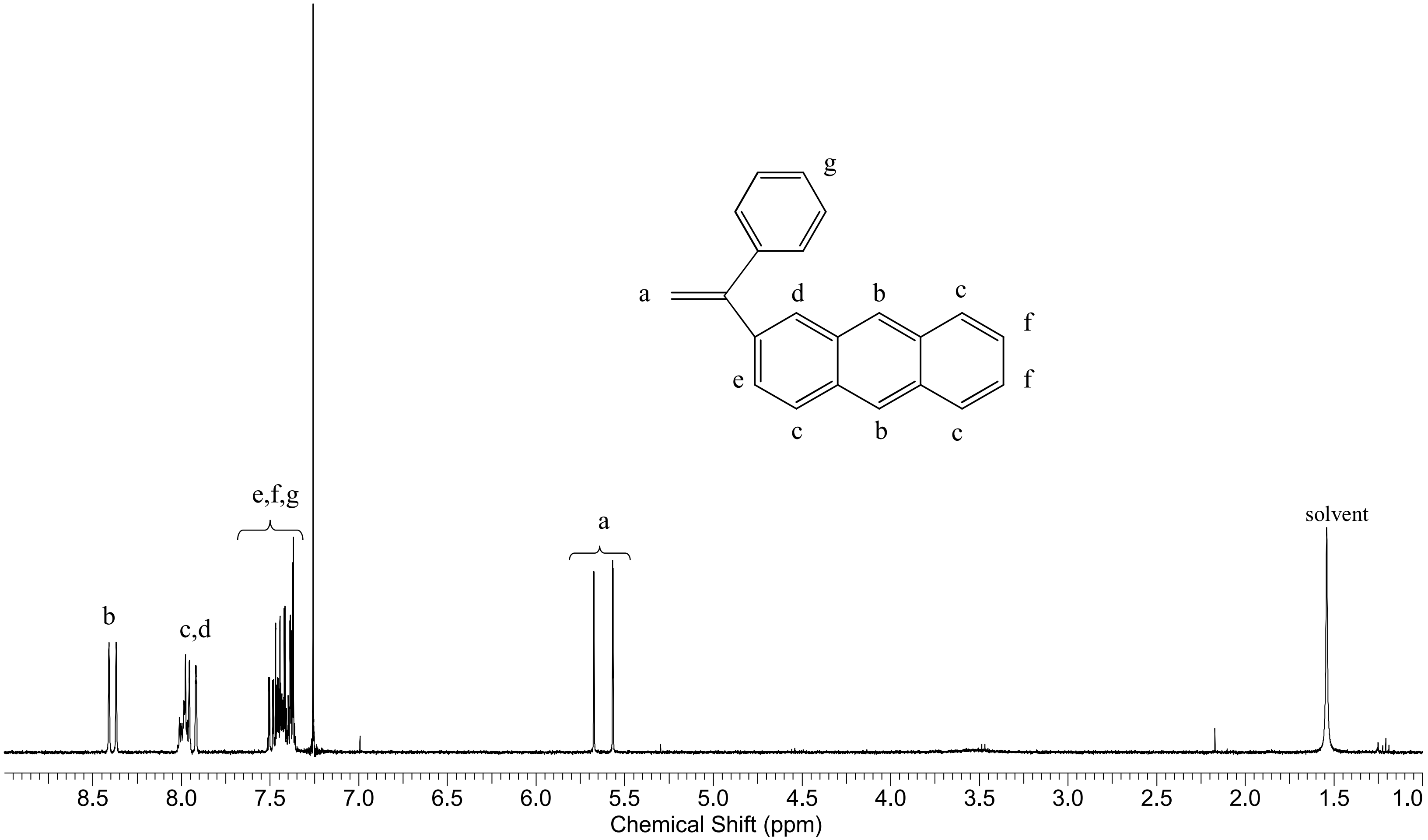

Figure 4.6. ^{1}H NMR spectrum of 1-(2-anthryl)-1-phenylethylene.

4.2. Anionic Polymerizations

4.2.1. Synthesis of Anthryl Telechelic Poly(methyl methacrylate) by Anionic Polymerization

For the synthesis of anthryl telechelic PMMA, first the initiator 1-(2-anthryl)-1-phenylhexyllithium (APHL) was synthesized by the reaction of APE with *n*-BuLi (Figure 4.7). The process is applicable due to the fact that APE monomer can not homopolymerize, therefore the reaction with *n*-BuLi leads to the formation of a sterically hindered APHL initiator bearing a single APE moiety [72, 73]. This bulky initiator, in the presence of LiCl, was utilized for the anionic polymerization of MMA to yield anthryl telechelic PMMA (PMMA-APE) (Figure 4.7).

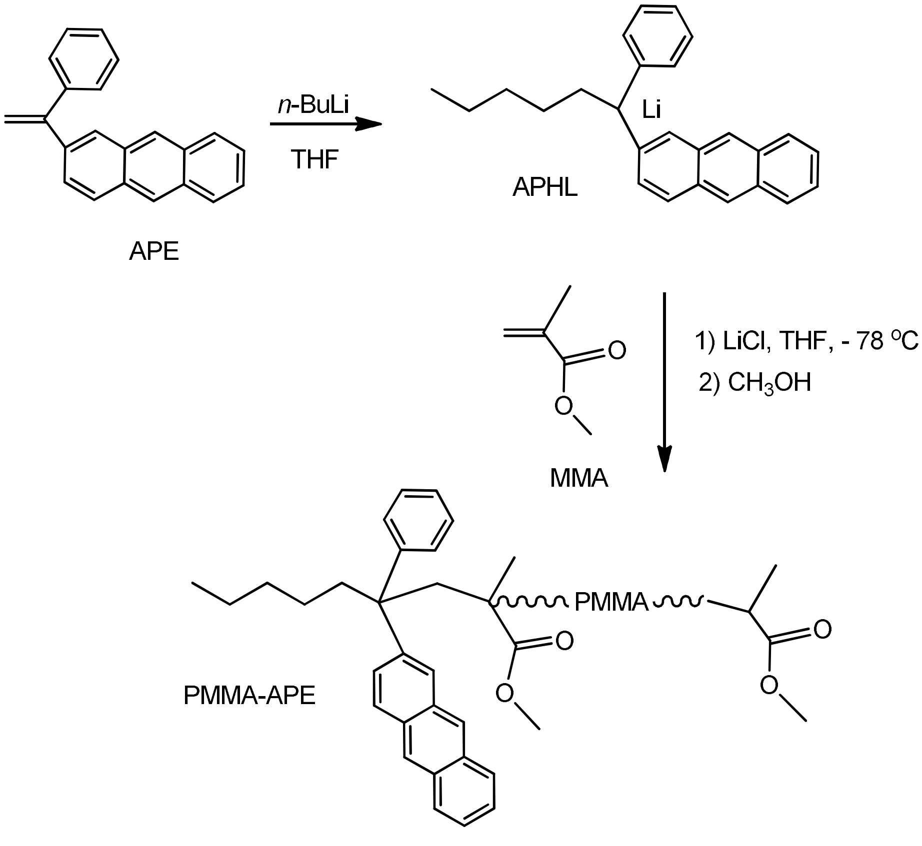

Figure 4.7. Synthesis of PMMA-APE.

Two polymerizations were done by changing the initiator amount in order to obtain polymers with different molecular weights. Table 4.1

Table 4.1. Molecular Weight Analysis data of di-anthryl telechelic PMMAs.

Name	M_n *a*	M_n *b*	M_p *b*	M_w/M_n *b*
$PMMA_{3k}$-APE	3556	3426	3751	1.07
$PMMA_{16k}$-APE	16279	16134	17278	1.05

a calculated by ^{1}H NMR

b calculated by SEC

The ^{1}H-NMR spectra of $PMMA_{3k}$-APE (Figure 4.8) and $PMMA_{16k}$-APE (Figure 4.9) display the characteristic PMMA peaks, with methylene protons of the backbone appearing between 1.75-2.00 ppm, methyl protons between 0.77-1.25 ppm and methyl acrylate protons between 3.50-3.68 ppm. The signals at 6.67-8.50 ppm correspond to the anthryl and phenyl groups of APE moiety, which indicate quantitative functionalization of the polymer chains via initiation with 1-(2-anthryl)-1-phenylhexyllithium. For both polymers, the methyl protons of polymer backbone (0.77-1.25 ppm) and the two protons at the 9- and 10- position on the anthryl ring (8.25-8.50 ppm) were utilized for the calculation of M_n values (Table 4.1). For $PMMA_{3k}$-APE it is possible to identify the terminal proton of the chain (2.30-2.40 ppm) for comparison; however this can not be detected in $PMMA_{16k}$-APE due to low intensity of the terminal group signals in the relatively greater molecular weight product.

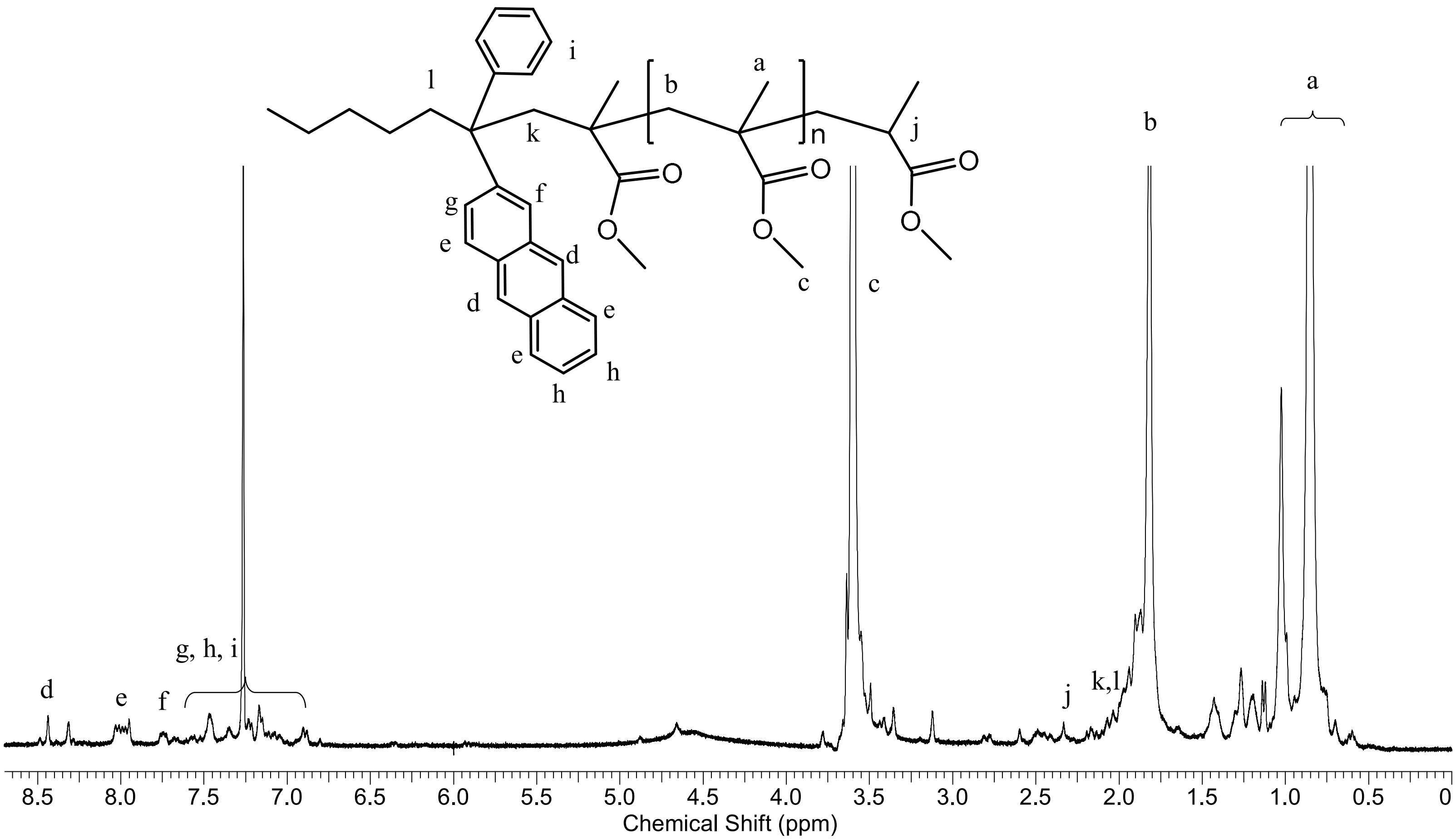

Figure 4.8. ^{1}H NMR spectrum of PMMA$_{3k}$-APE.

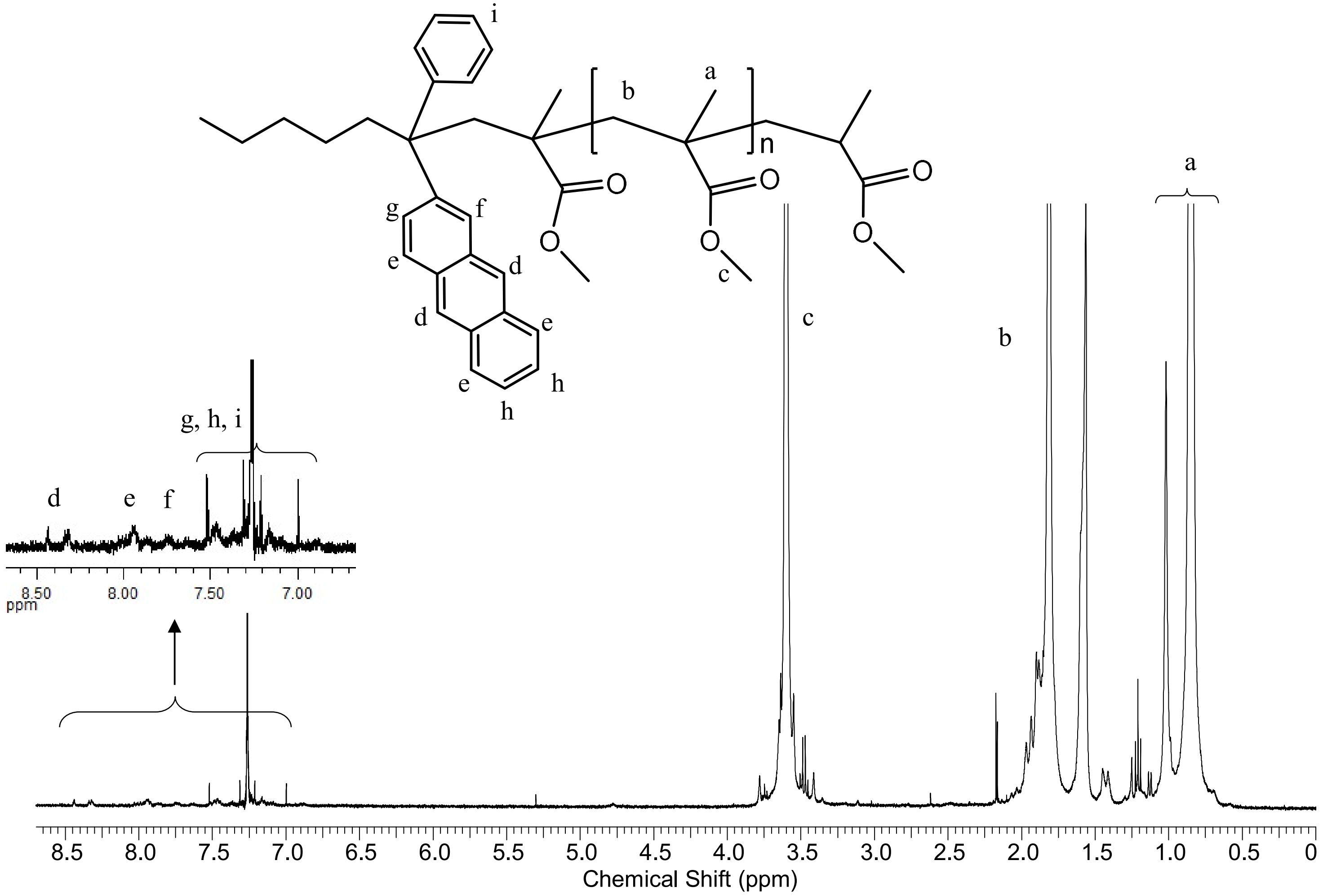

Figure 4.9. ^{1}H NMR spectrum of PMMA$_{16k}$-APE.

The corresponding SEC data for the synthesized polymers are demonstrated in Figures 4.10 and Figure 4.11 respectively. UV absorbance detector at 365 nm was utilized alongside the refractive index detector in order to monitor the presence of the anthracene moieties on the polymer chains. The overlap in the chromatograms indicates that the polymer chains were successfully functionalized with APE.

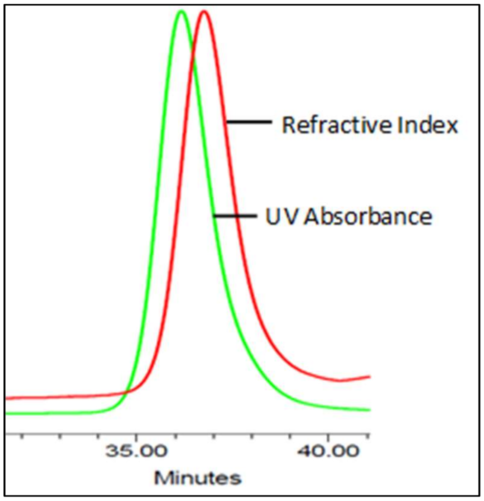

Figure 4.10. SEC data of APE-PMMA$_{3k}$-APE recorded by UV absorbance and RI detectors.

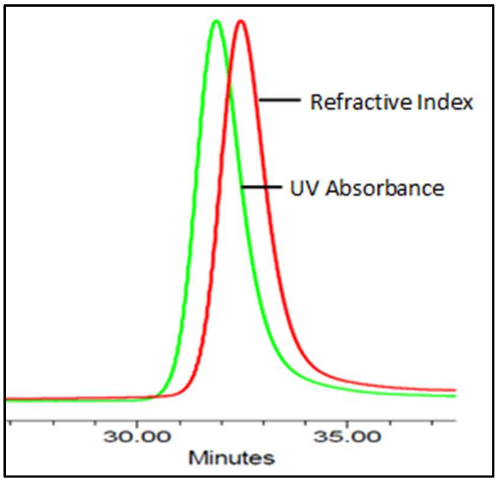

Figure 4.11. SEC data of APE-PMMA$_{16k}$-APE recorded by UV absorbance and RI detectors.

4.2.2. Synthesis of Anthryl Telechelic Polystyrene by Anionic Polymerization

The synthesis of anthryl telechelic polystyrene (PS-APE) was conducted by the anionic polymerization of styrene with *sec*-BuLi, followed by the functionalization of living polystyryl chain ends with APE. Due to the fact that APE monomer can not homopolymerize, the PS chains get labelled with one APE moiety (Figure 4.12) [60, 73].

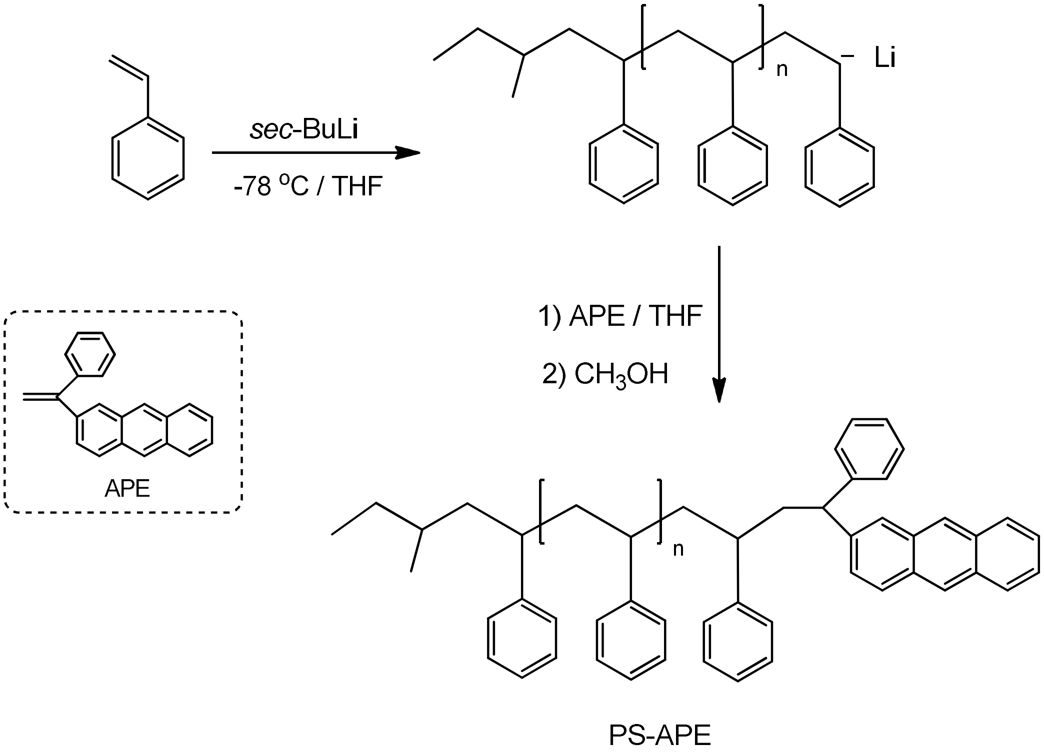

Figure 4.12. Synthesis of PS-APE.

Table 4.2. Molecular Weight Analysis data of anthryl telechelic PS.

Name	M_n *a*	M_n *b*	M_p *b*	M_w/M_n *b*
PS_{4k}-APE	4345	4054	4335	1.08

a calculated by ^{1}H NMR

b calculated by SEC

The ^{1}H-NMR spectrum of PS_{4k}-APE (Figure 4.13) displays the characteristic polystyrene peaks, with methylene protons of the backbone appearing between 1.20-1.67 ppm, methine protons between 1.67-2.30 ppm and aromatic protons between 6.25-7.25 ppm. The signals corresponding to the anthryl and phenyl groups of APE moiety fall to the region of 6.67-8.50 ppm, therefore superimposing to a degree with the large aromatic signals of polystyrene. On the other hand, the two protons at the 9- and 10- position on the anthryl ring (8.20-8.45 ppm) can be detected apart from the rest of the anthryl protons and therefore utilized to estimate the chain end functionalization. The aromatic protons of polymer backbone (0.77-1.25 ppm) and the methyl signals of *sec*-butyl head group (0.50-0.80) were used for the calculation of M_n value (Table 4.2). The aforementioned two protons of anthryl unit were used to calculate successful end functionalization with 97.5% yield.

The corresponding SEC data for the synthesized polymer is demonstrated in Figure 4.14. UV absorbance detector at 365 nm was utilized alongside the refractive index detector in order to monitor the presence of the anthracene moieties on the polymer chains. The overlap in the chromatograms indicates that the polymer chains were successfully functionalized with APE.

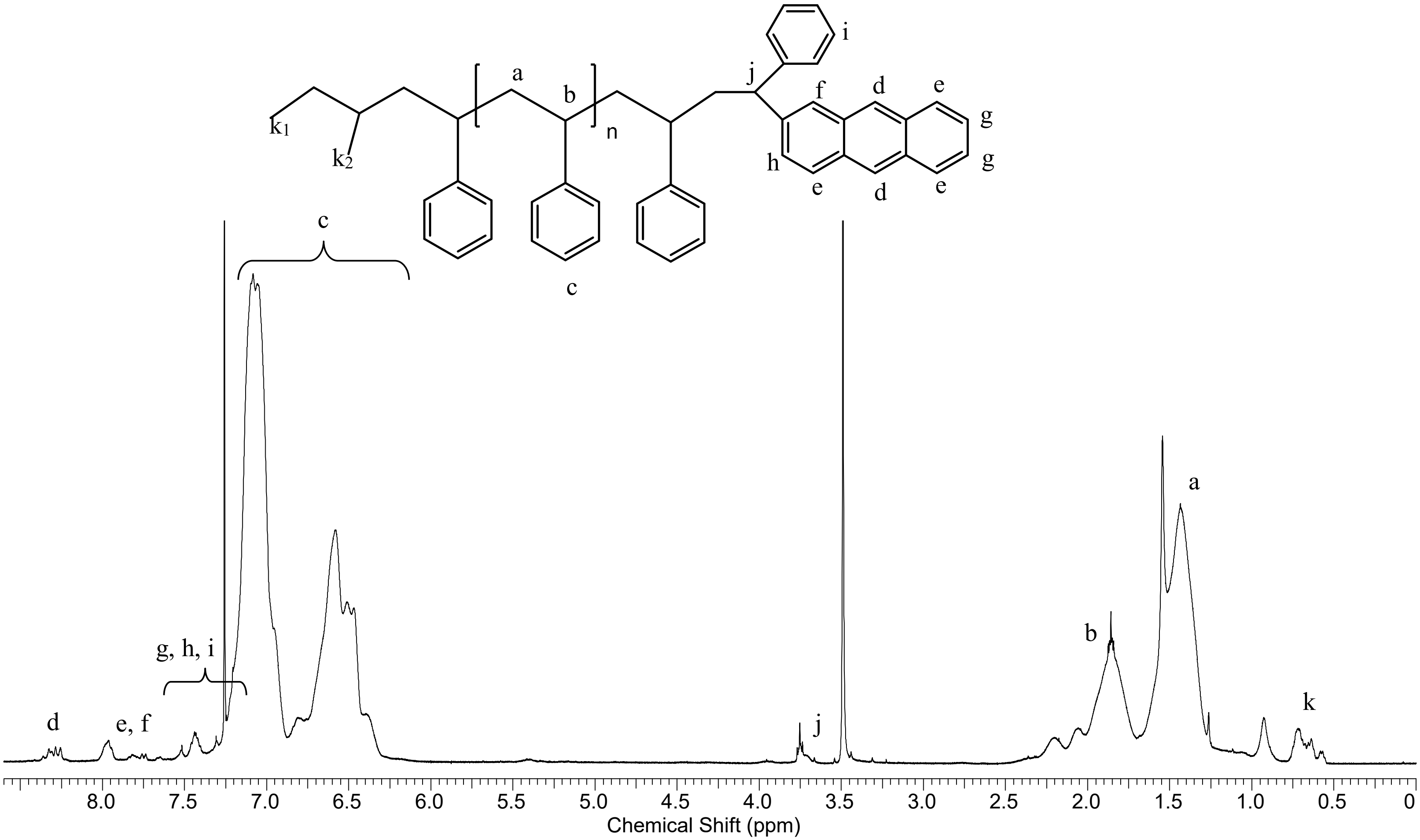

Figure 4.13. ^{1}H NMR spectrum of PS_{4k}-APE.

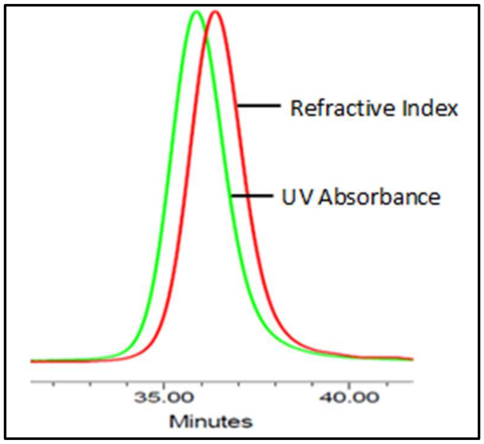

Figure 4.14. SEC data of APE-PS$_{4k}$-APE recorded by UV absorbance and RI detectors.

4.2.3. Synthesis of di-Anthryl Telechelic Polystyrene by Anionic Polymerization

For the synthesis of di-anthryl telechelic polystyrene (APE-PS-APE), the initiator potassium naphthalenide was prepared by the reaction of naphthalene and potassium metal under nitrogen atmosphere (Figure 4.15).

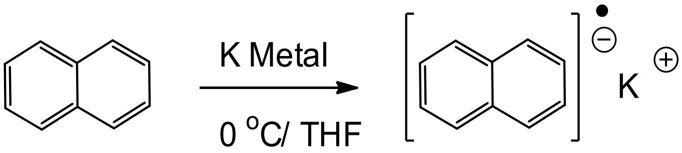

Figure 4.15. Synthesis of potassium naphthalenide initiatior.

The aromatic radical anion type initiator was then utilized for the anionic polymerization of styrene. Next, the living bifunctional polystyryl chain ends were reacted with APE. Since the APE monomer can not homopolymerize, only one unit of it is added to each living chain end, leading to the formation of di-anthryl telechelic PS chains after quenching (Figure 4.16) [60, 73].

Two polymerizations were done by changing the initiator amount in order to obtain polymers with different molecular weights. Table 4.3.

Table 4.3. Molecular Weight Analysis data of di-anthryl telechelic PSs.

Name	M_n *a*	M_n *b*	M_p *b*	M_w/M_n *b*
APE-PS$_{3k}$-APE	3638	3223	2994	1.52
APE-PS$_{15k}$-APE	14878	15755	14106	1.33

a calculated by ^{1}H NMR

b calculated by SEC

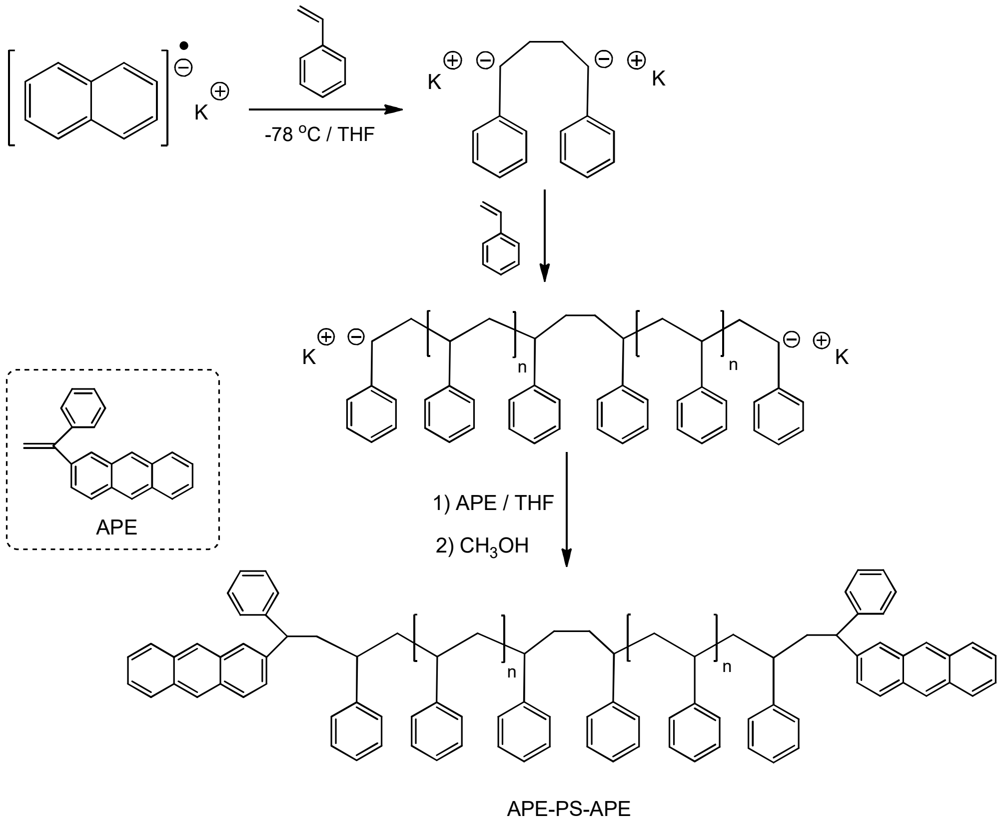

Figure 4.16. Synthesis of APE-PS-APE.

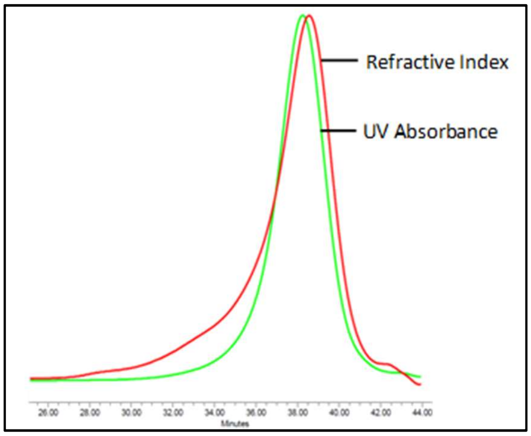

Figure 4.17. SEC data of APE-PS$_{3k}$-APE recorded by UV absorbance and RI detectors.

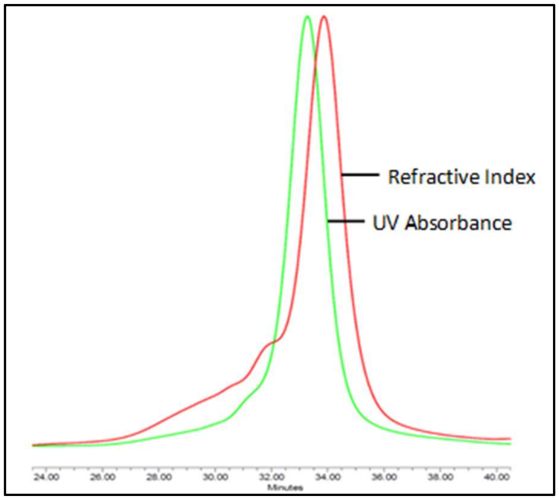

Figure 4.18. SEC data of APE-PS$_{15k}$-APE recorded by UV absorbance and RI detectors.

The corresponding SEC data for the synthesized polymers are demonstrated in Figure 4.17 and Figure 4.18 respectively. Both SEC RI data show molecular weight distributions that are broader than expected. Before the synthesis in question was performed, three trials with the potassium naphthalenide initiator was done for the polymerization of styrene solely, without end-functionalization, in order to investigate the efficiency. The first two reactions yielded products with bimodal and broad molecular weight distributions ($M_w/M_{n\ 1}$: 2.05, $M_w/M_{n\ 2}$: 1.55). This was attributed to the presence of unreacted potassium metal in the initiator solution. Therefore, filtration was performed on the prepared potassium naphthalenide initiator before further use. The following third polymerization reaction yielded polystyrene product with narrow and monomodal distribution ($M_w/M_{n\ 3}$: 1.14), hence the synthesis of di-anthryl telechelic polystyrene was conducted afterwards. However, a similar problem has emerged, which indicates the presence of multiple active species in the reaction medium. In the previous chapter, formation of different propagating species in anionic polymerization was discussed [42, 48]. When a polar solvent such as THF is utilized; free ions, solvent separated ion pairs and contact ion pairs are in equilibrium. A slow exchange between these different active species results in broad molecular weight distributions [44] since they have different propagation rates, with free ions having much greater propagation rate constants than ion pairs [42]. A high solvating medium, which is necessary for the preparation of radical anion type initiator, may shift the equilibrium towards the formation of free ions [49]. As a result, the presence of potassium metal and the formation of free ions in polar solvent may have lead broad molecular weight distribution in the final product. Nevertheless, the functionalization of polymer chains with anthracene moieties was detected by the overlap chromatograms obtained by UV absorbance detector at 365 nm and RI detector.

On the other hand, SEC RI data of APE-PS_{15k}-APE displays a small shoulder with M_p: 27796 approximately twice the M_p value of actual polymer peak, which points to the presence of small amount of “dimeric” PS units in the product. Corresponding SEC UV data also shows a small increase in absorbance at this region, which suggests that the dimeric PS units are also functionalized with APE. Goldbach et al. had also reported the detection of 5% dimeric polystyrene impurity in their synthesis of APE end-capped polystyrene by anionic polymerization [29]. This finding was attributed to a side reaction; the nucleophilic attack of the polystyryl anion to the anthracene unit of an APE functionalized polystyrene. It was stated that after rearomatization a dimeric polystyryl impurity with an anthracene functionality in the middle was obtained (Figure 4.19).

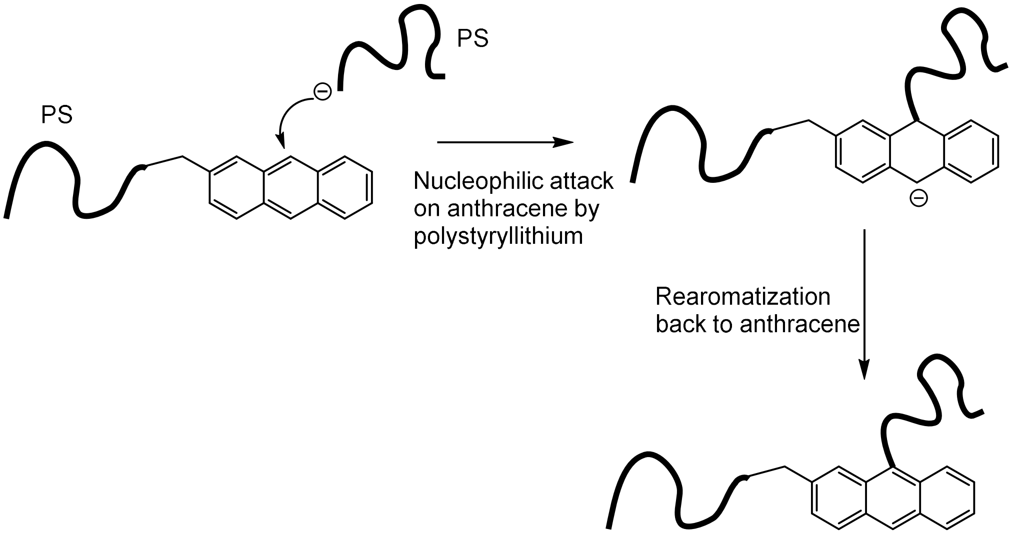

Figure 4.19. Proposed mechanism of side reaction leading to dimeric polystyrene with anthracene middle group [29].

The ^{1}H-NMR spectra of APE-PS$_{3k}$-APE and APE-PS$_{15k}$-APE (Figure 4.20 and Figure 4.21, respectively) display the characteristic polystyrene peaks, with methylene protons of the backbone appearing between 1.20-1.67 ppm, methine protons between 1.67-2.30 ppm and aromatic protons between 6.25-7.25 ppm. The signals corresponding to the anthryl and phenyl groups of APE moiety fall to the region of 6.67-8.50 ppm, therefore superimposing to a degree with the large aromatic signals of polystyrene. On the other hand, the two protons at the 9- and 10- position on the anthryl ring (8.20-8.40 ppm) can be detected separately from the rest of the anthryl protons and therefore utilized to estimate the chain end functionalization. For APE-PS$_{3k}$-APE a very small peak corresponding to methylene protons of the non-functionalized chain end at 2.62-2.64 ppm was observed; the aforementioned protons of anthryl unit were used to determine successful end functionalization with 98.4% yield. The same chain end methylene peak could not be observed in APE-PS$_{15k}$-APE, which points to very low amount of non-functionalized chains. The aromatic protons of polymer (6.25-7.25 ppm) and aforementioned anthryl protons (8.20-8.40 ppm) were utilized for the calculation of M$_n$ values (Table 4.3).

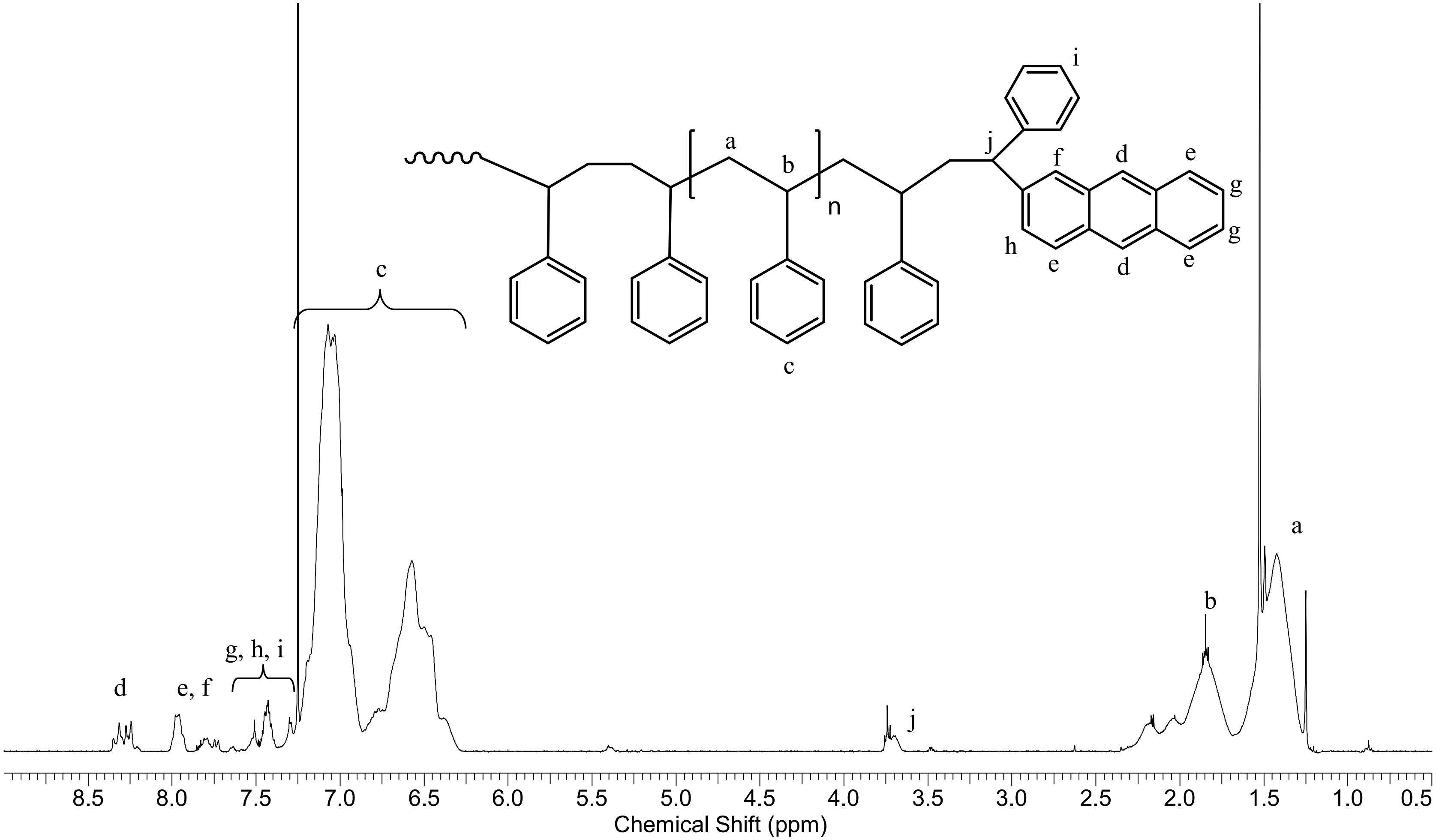

Figure 4.20. ^{1}H NMR spectrum of APE-PS$_{3k}$-APE.

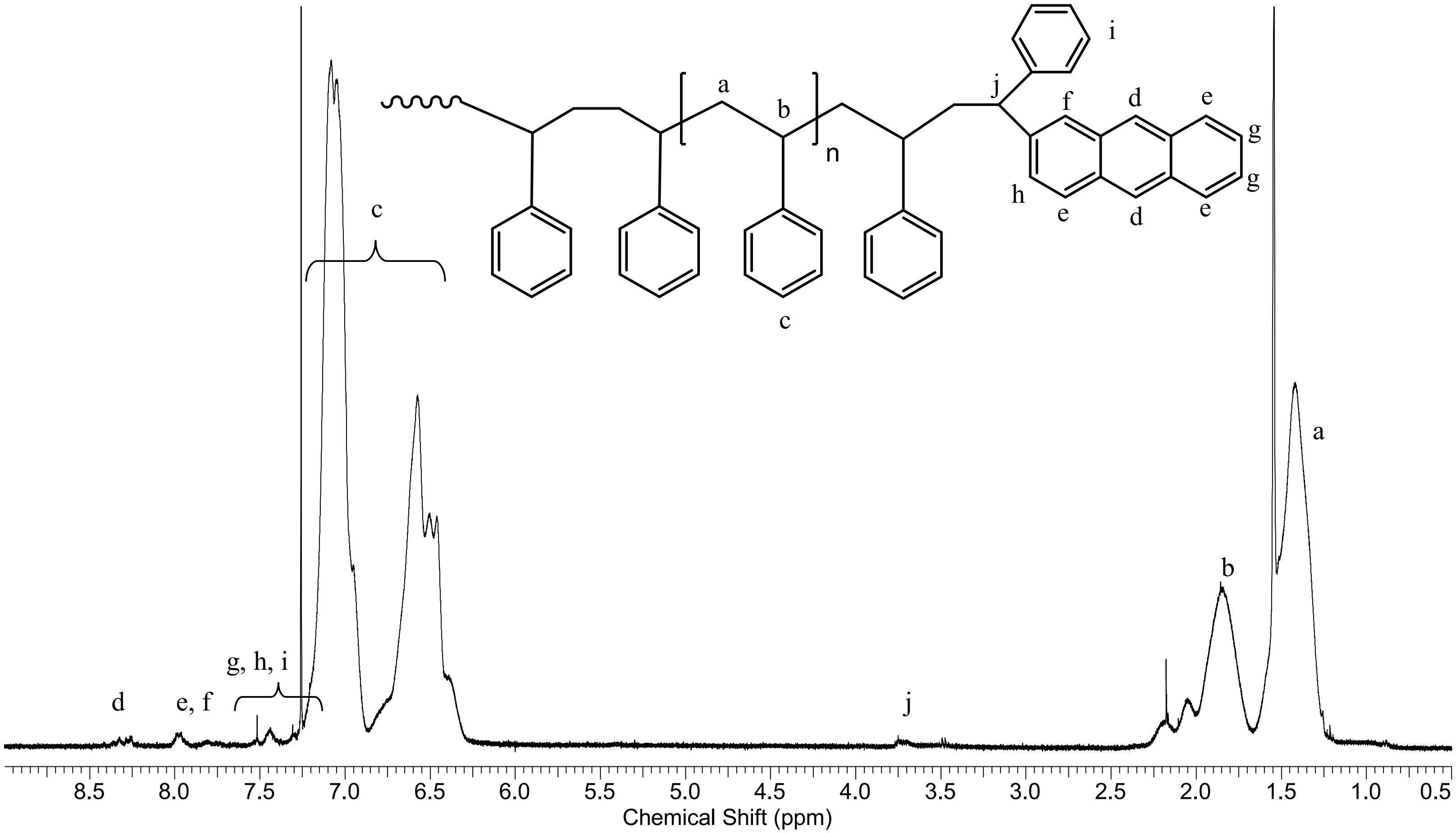

Figure 4.21. ^{1}H NMR spectrum of APE-PS$_{15k}$-APE.

4.3. Synthesis of carbocationic initiator (t-Bu-m-DiCumCl)

4.3.1. Synthesis of dimethyl-5-tert-butyl-1,3-benzyl dicarboxylate

Dimethyl-5-tert-butyl-1,3-benzyl dicarboxylate was synthesized as described in the literature (Figure 4.22) [110].

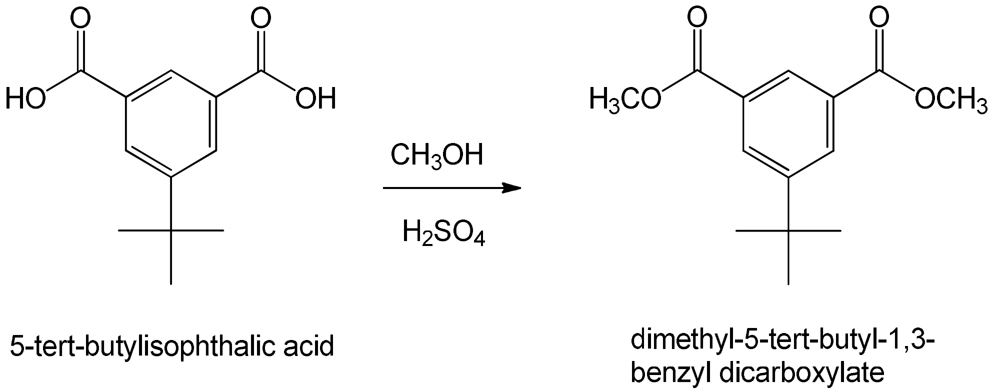

Figure 4.22. Esterification of 5-tert-butylisophthalic acid.

The ^1H NMR spectrum displays methyl protons of t-butyl group at 1.37 ppm, methyl protons of ester groups at 3.94 ppm and the aromatic protons between 8.2-8.5 ppm (Figure 4.23). The integration ratio of 3:2 for the methyl protons of t-butyl and ester groups confirms the quantitative conversion of the diacid compound to the corresponding diester.

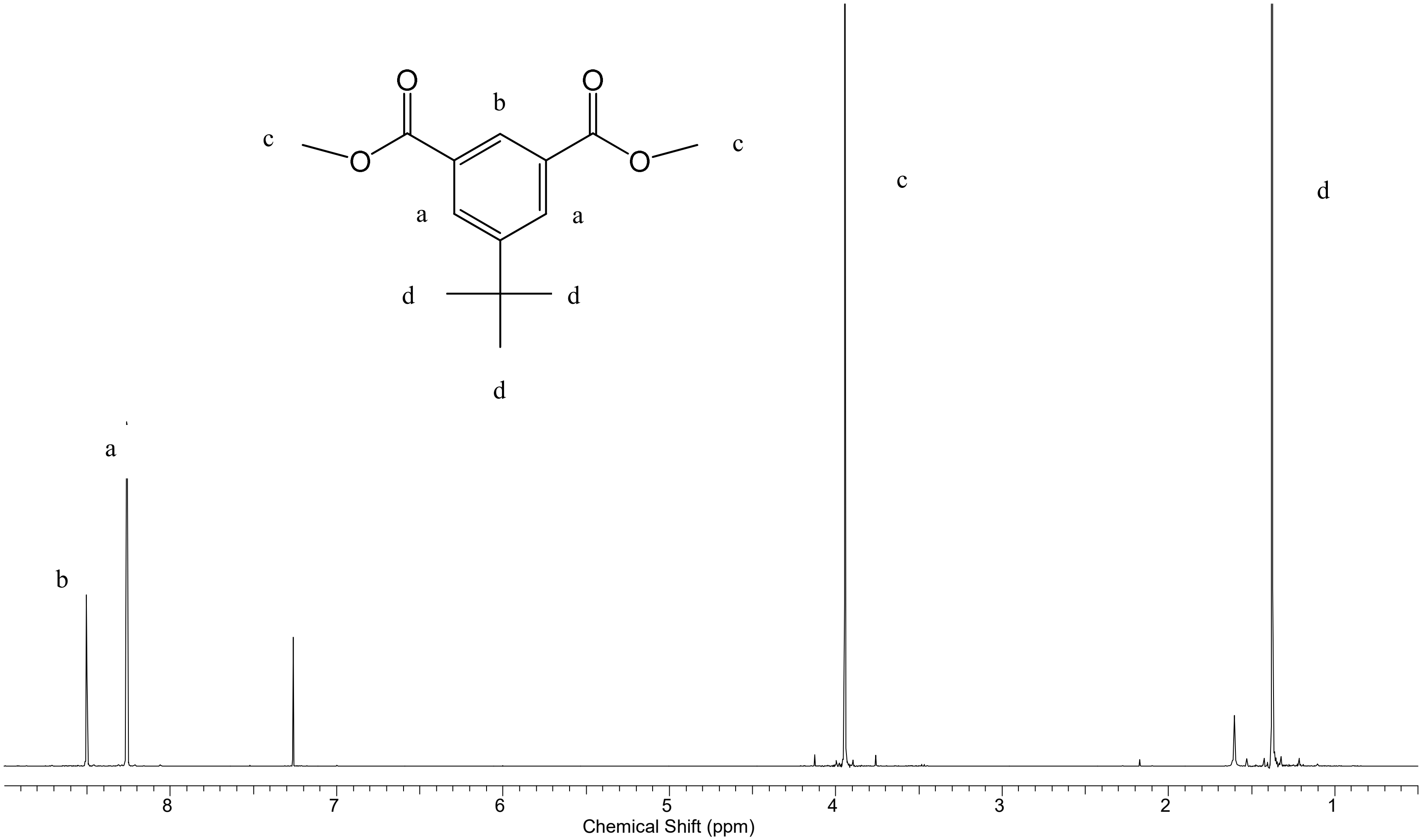

Figure 4.23. ^{1}H NMR spectrum of dimethyl-5-tert-butyl-1,3-benzyl dicarboxylate.

4.3.2. Synthesis of 5-tert-butyl-1,3-dicumyl alcohol (t-Bu-m-DiCumOH)

5-tert-butyl-1,3-dicumyl alcohol was prepared according to the literature, as shown in Figure 4.24 [110].

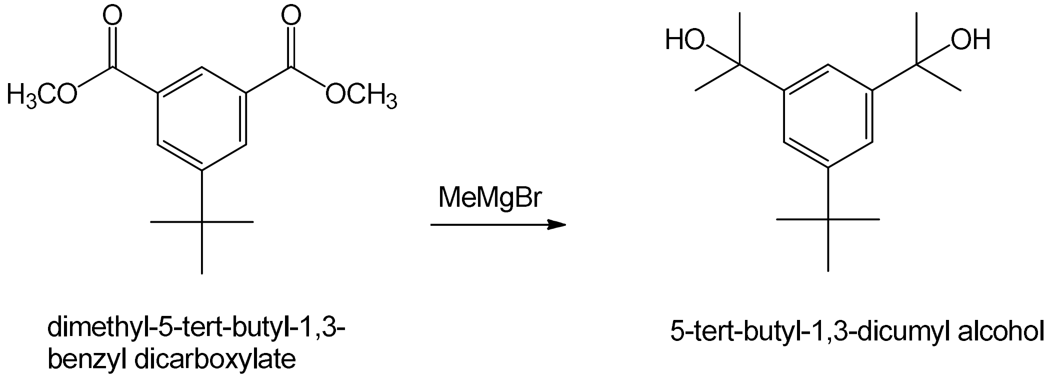

Figure 4.24. Synthesis of 5-tert-butyl-1,3-dicumyl alcohol.

^{1}H NMR spectrum of 5-tert-butyl-1,3-dicumyl alcohol shows that after Grignard reaction the methyl protons of the diester at 3.94 ppm were replaced by methyl protons of isopropyl groups at 1.60 ppm (Figure 4.25). Also the aromatic protons have shifted upfield to 7.35-7.50 ppm.

The integration ratio of 4:3 for methyl protons of isopropyl and t-butyl groups were utilized to confirm quantitative conversion.

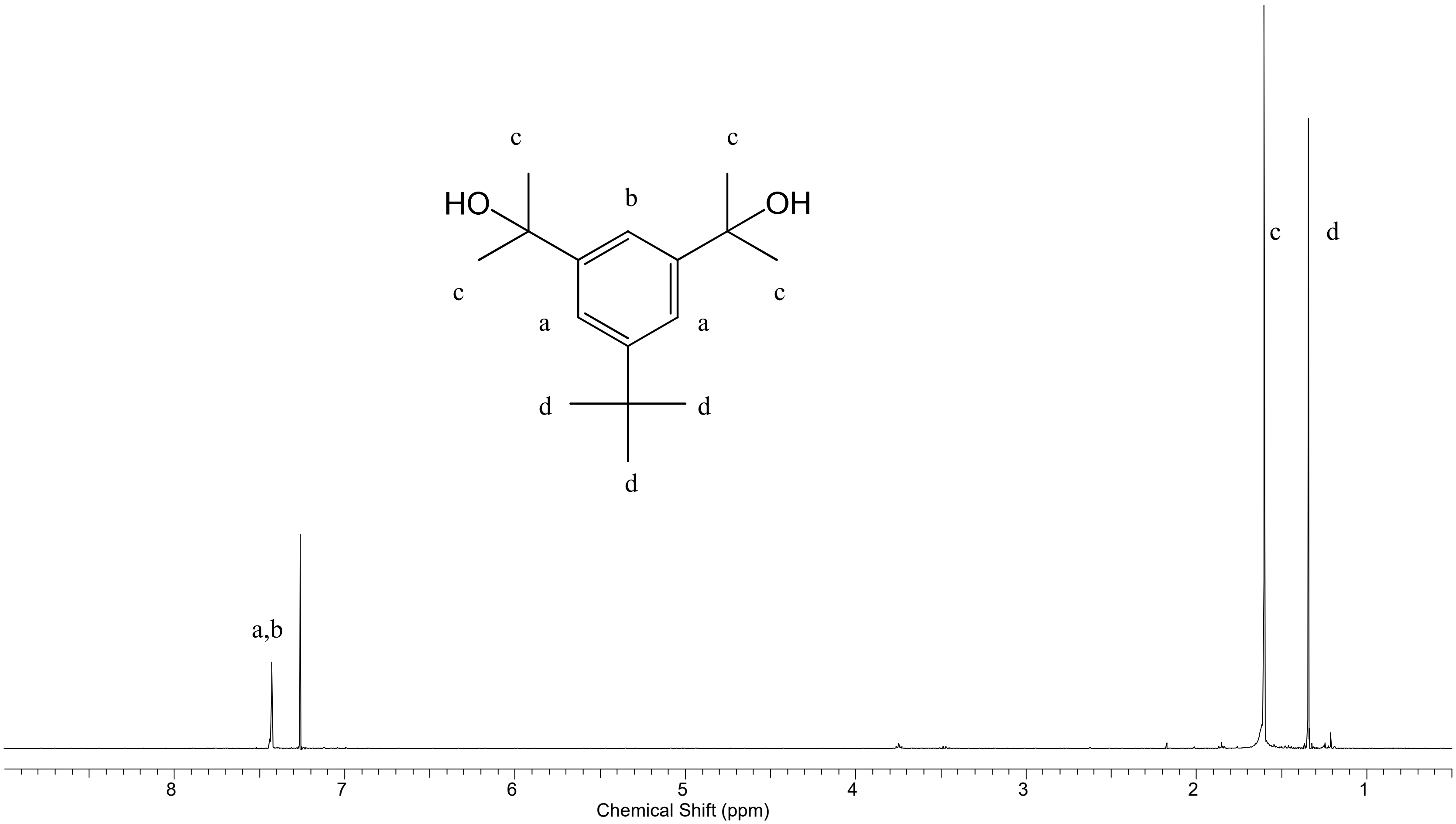

Figure 4.25. ^{1}H NMR spectrum of 5-tert-butyl-1,3-dicumyl alcohol (t-Bu-m-DiCumOH).

4.3.3. Synthesis of 5-tert-butyl-1,3-bis(2-chloro-2-propyl)benzene (t-Bu-m-DiCumCl)

5-tert-butyl-1,3-bis(2-chloro-2-propyl)benzene was synthesized in a similar manner to previously described method (Figure 4.26) [111]. Previously obtained t-Bu-m-DiCumOH was chlorinated in the presence of NaCl and H_2SO_4 to obtain the desired dicumyl chloride initiator.

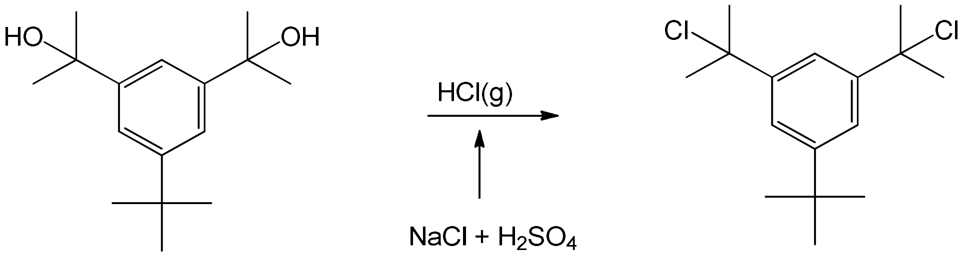

5-tert-butyl-1,3-dicumyl alcohol

t-Bu-m-DiCumCl

Figure 4.26. Synthesis of t-Bu-m-DiCumCl.

During the chlorination of the dicumyl alcohol, undesired elimination reactions leading to the formation of exo-olefinic products may occur. Such an outcome would create an inept cationic initiator, jeopardizing the success of further polymerization reactions. However vinylic hydrogen peaks at 5 and 5.35 ppm, indicating the presence of exo-olefin groups, were not detected in the ^{1}H NMR spectrum (Figure 4.27). The methyl protons of isopropyl group shifted from 1.60 to 2 ppm after the chlorination reaction.

The dicumyl chloride initiator was obtained with high yield and purity, the integration ratio of 4:3 for the methyl protons of isopropyl and t-butyl groups indicates that quantitative conversion was reached.

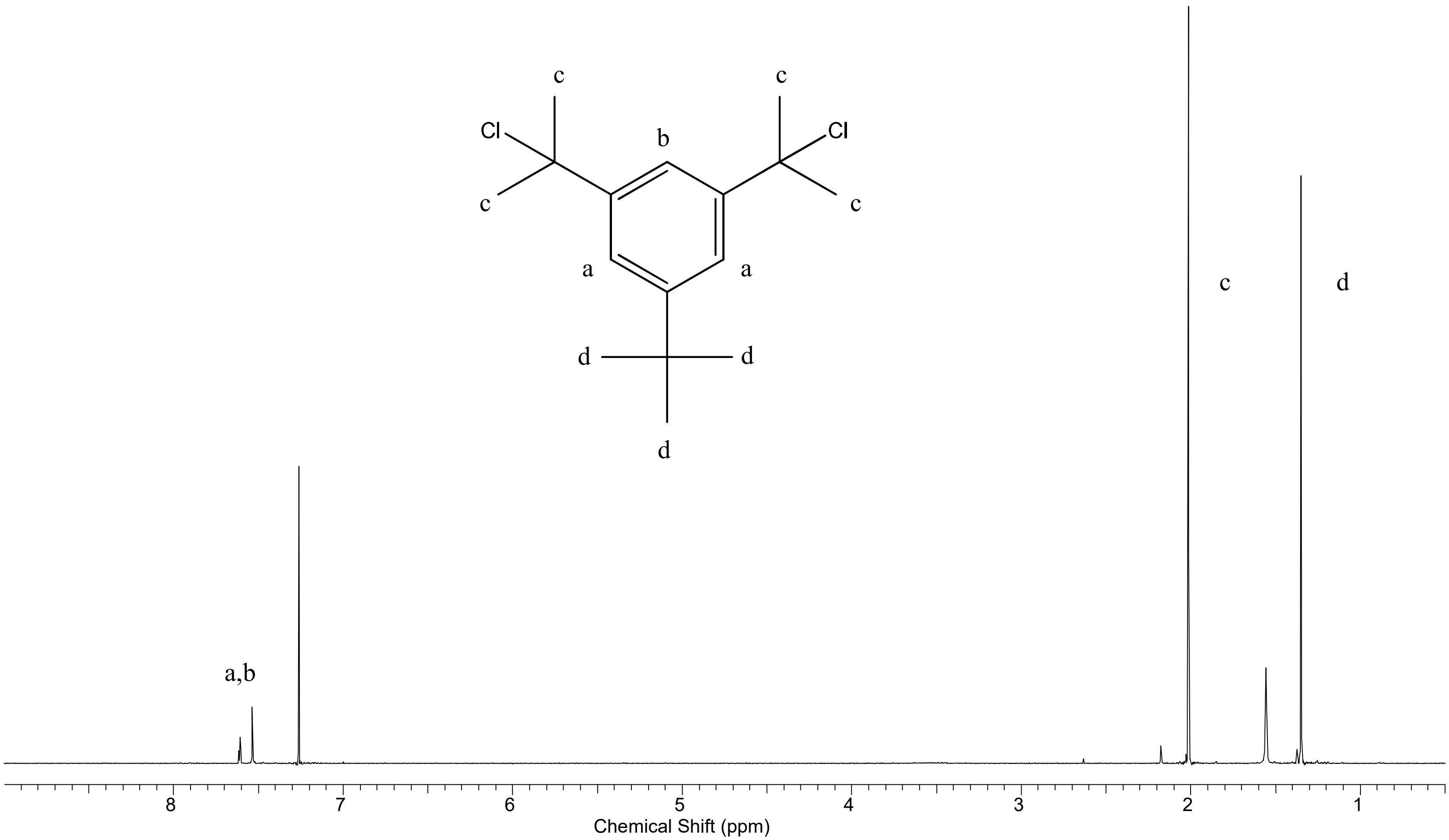

Figure 4.27. ^{1}H NMR spectrum of 5-tert-butyl-1,3-bis(2-chloro-2-propyl)benzene (t-Bu-m-DiCumCl).

4.4. Cationic Polymerizations

4.4.1. Synthesis of di-Anthryl Telechelic Polyisobutylenes by Carbocationic Polymerization

A series of polymerizations were conducted in order to obtain the optimum reaction conditions to yield the desired well defined IB polymers. Addition of the APE monomer to the reaction medium was performed on the selected system. t-Bu-m-DiCumCl was used as the difunctional initiator in the cationic polymerization process to yield di-anthryl telechelic PIBs (APE-PIB-APE) (Figure 4.28). Two polymerizations were done by changing the initiator amount in order to obtain polymers with different molecular weights (Table 4.4) [28].

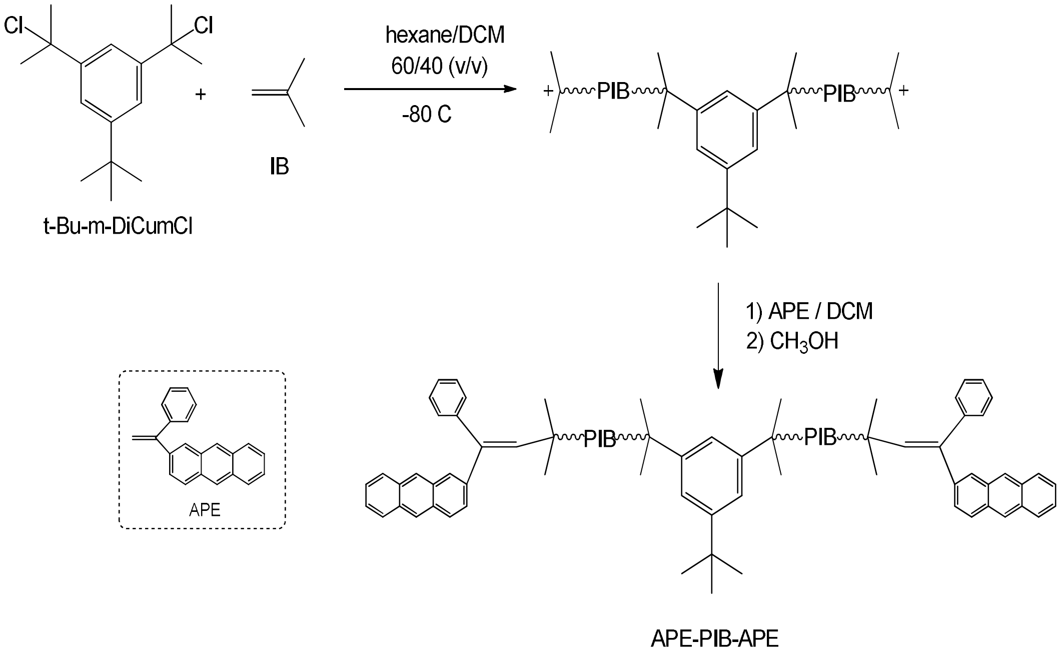

Figure 4.28. Synthesis of di-anthryl telechelic PIB via cationic polymerization.

The ^{1}H-NMR spectrum of APE-PIB$_{6k}$-APE (Figure 4.29) displays the characteristic polyisobutylene peaks, with methylene protons of the backbone appearing between 1.35-1.46 ppm and methyl protons between 1.03-1.22 ppm. The signals at 7.2-8.5 ppm correspond to the anthryl and phenyl groups of APE moieties, which indicate successful end functionalization with 97.2% yield. The remaining 2.8% is attributed to tert-chloride chain end, which is observed by the gem-dimethyl protons at 1.68 ppm. The peak at 3.5 ppm corresponds to the methoxy protons of 1-(2-anthryl)-1-methoxy-1-phenyl chain end with 3.8% yield. The signals at 6.2-6.4 ppm arise from the formation of vinylic hydrogen of 2-(2-anthryl)-2-phenlyvinyl type chain end, with 93.4% yield, which is expected due to the termination conditions; addition of methanol to the highly acidic reaction mixture induces the formation of elimination product [104]. The higher molecular weight polymer APE-PIB$_{18k}$-APE also displays the aforementioned characteristic peaks and shows 88.1% end functionalization calculated from ^{1}H-NMR spectrum (Figure 4.30). For both polymers, the methyl protons of polymer backbone (1.03-1.22 ppm) and the methyl protons of the first isobutylene units attached to the bifunctional initiator (0.78 ppm) were utilized for the calculation of M_n values (Table 4.4) [28].

Table 4.4. Molecular Weight Analysis data of di-anthryl telechelic PIBs.

Name	M_n *a*	M_n *b*	M_p *b*	M_w/M_n *b*
APE-PIB$_{6k}$-APE	6357	6893	7456	1.20
APE-PIB$_{18k}$-APE	17545	18005	20288	1.18

a calculated by ^{1}H NMR

b calculated by SEC

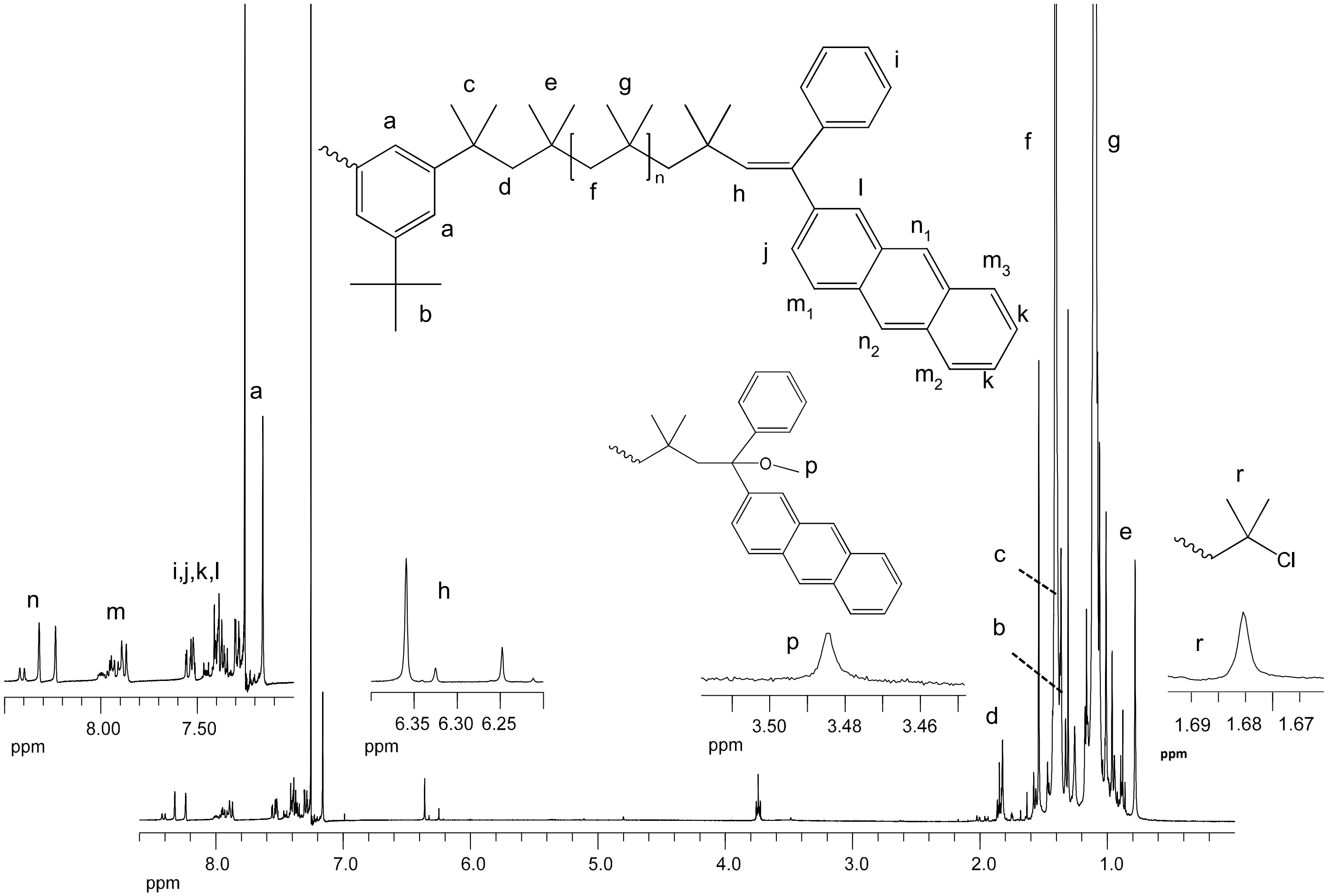

Figure 4.29. ^{1}H NMR spectrum of APE-PIB$_{6k}$-APE.

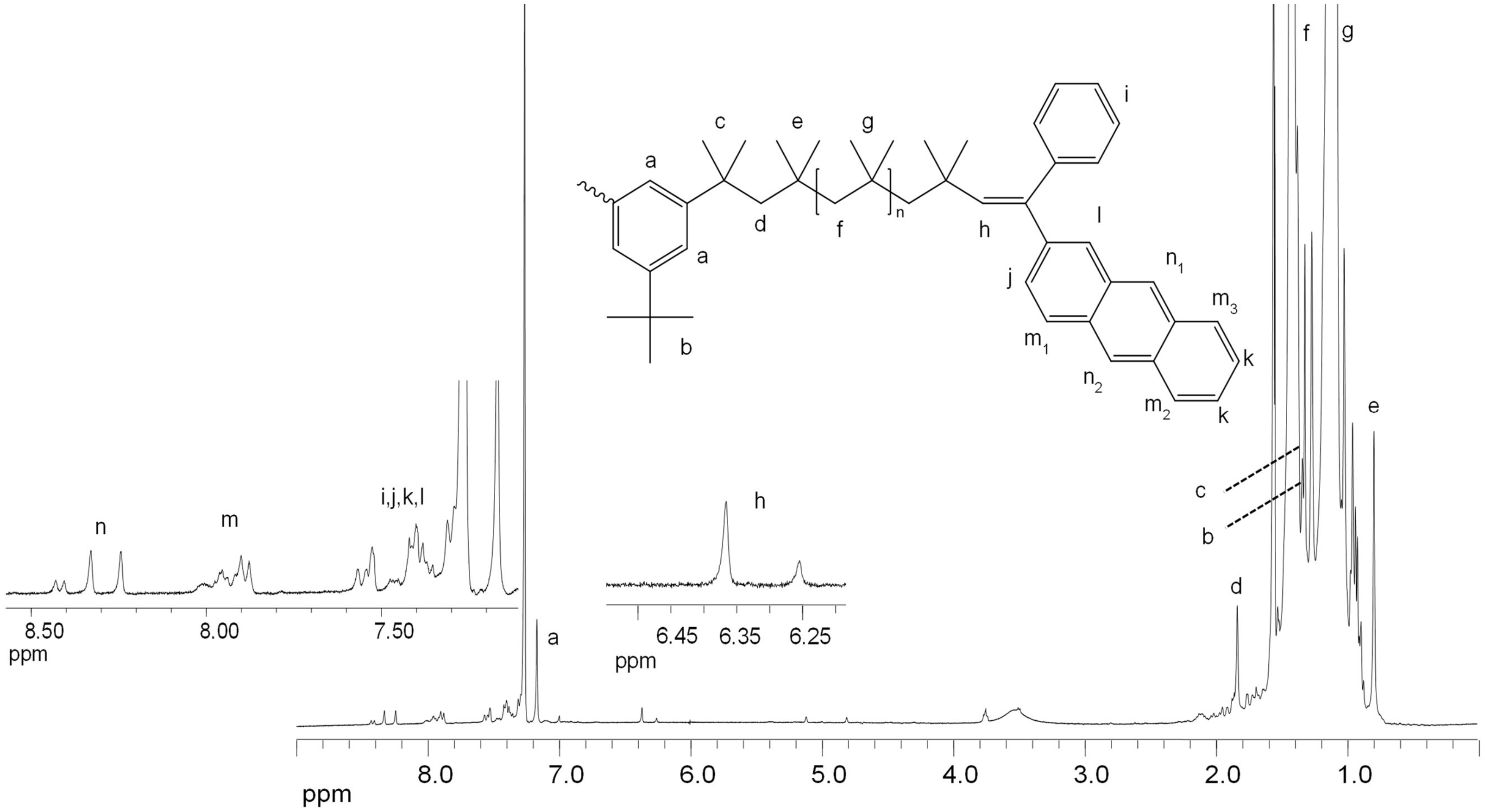

Figure 4.30. ^{1}H NMR spectrum of APE-PIB$_{18k}$-APE.

The corresponding SEC data for the synthesized polymers APE-PIB$_{6k}$-APE and APE-PIB$_{18k}$-APE are demonstrated in Figure 4.31 and Figure 4.32 respectively. UV absorbance detector at 365 nm was utilized alongside the refractive index (RI) detector in order to monitor the presence of the anthracene moieties on the polymer chains. The overlap in the chromatograms indicates that the polymer chains were successfully functionalized with APE [28].

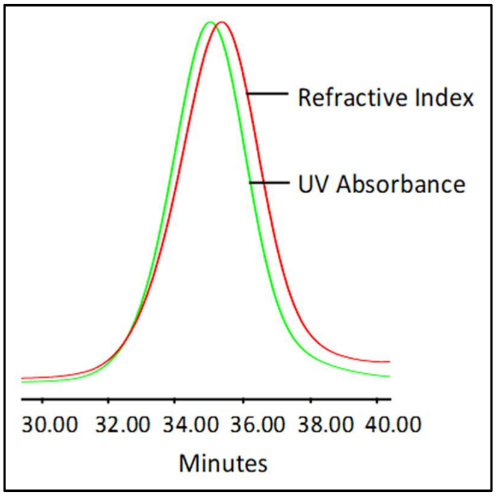

Figure 4.31. SEC data of APE-PIB$_{6k}$-APE recorded by UV absorbance and RI detectors.

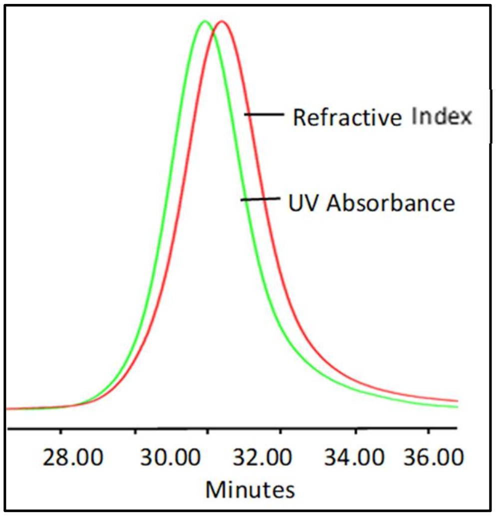

Figure 4.32. SEC data of APE-PIB$_{18k}$-APE recorded by UV absorbance and RI detectors.

4.5. UV Irradiation Studies

The synthesized anthryl and di-anthryl telechelic polymers were utilized in UV irradiation experiments in order to examine the photocycloaddition reactions that induce chain extension and formation of higher molecular weight products. Upon irradiation with UV light at 365 nm, polymer chains having APE units at the chain ends would couple via [4π+4π] cycloaddition of anthracene moieties (Figure 4.33). The reversibility of the process was also examined by irradiation of the photocoupled products under 254 nm UV light, which induces photoscission of the polymer chains and conversion of APE units to original state (Figure 4.33).

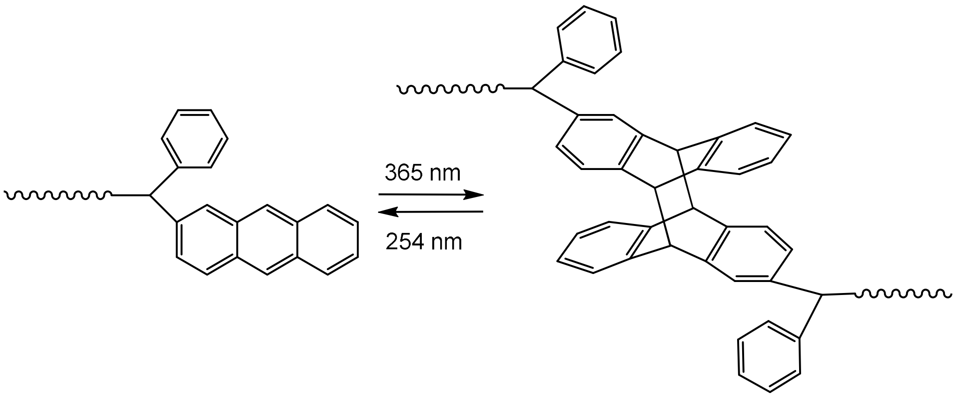

Figure 4.33. Reversible photocycloaddition of anthracene functionalized polymers.

Depending on the experimental conditions such as concentration, molecular weight and solvent; the di-anthryl telechelic polymers may undergo intermolecular interactions leading to chain extension or intramolecular interactions that result in the formation of cyclic polymers (Figure 4.34) [28]. The chain extension process is predominant in the case of high polymer concentrations and utilization of high molecular weight polymers, since both conditions increase the probability of intermolecular interactions among polymer chains [112].

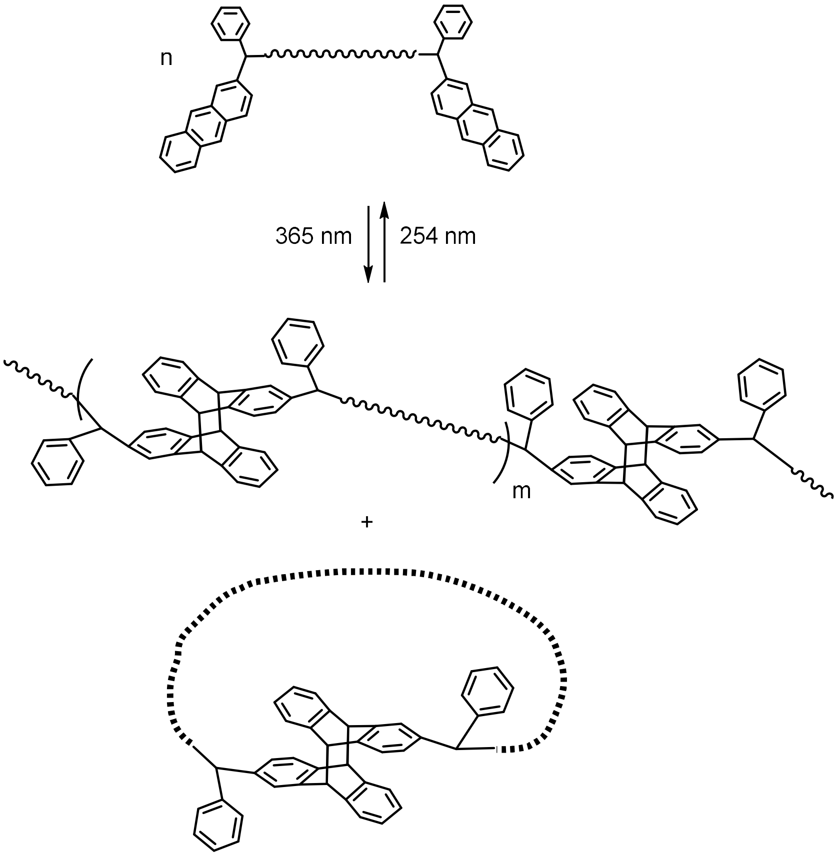

Figure 4.34. Photocycloaddition reactions of di-anthryl telechelic polymers.

The chain extension of APE functionalized polymers can be monitored by SEC analysis through the increase in the molecular weight with respect to reaction time. Subsequent decrease in absorbance in the UV chromatograms at 365 nm by the photocoupling of anthracene units can also be observed; owing to the fact that photodimerization of the anthracene units cause a disruption in the conjugation of the π system and the resulting photodimers no longer absorb light of wavelengths greater than 300 nm [6]. The reversal of the photocycloaddition reaction can also be monitored via SEC analysis. Photoscission of polymer chains via irradiation at 254 nm leads to shift of polymer peak molecular weight to lower values and recovery of anthracene moieties at the chain ends, which can be observed by the increase in the UV absorbance at 365 nm.

The reversible photocycloaddition reactions of anthracene moieties should be conducted under inert atmosphere in order to prevent the formation of anthracene-9,10-endoperoxide that occurs in the presence of air (Figure 4.35) [1, 7, 10, 13]. This aromatic endoperoxide may undergo further reactions thermally or via UV irradiations to yield a number of different products [113]. Therefore to prevent possible side reactions, all experiments were performed in sealed vials under N_2 atmosphere.

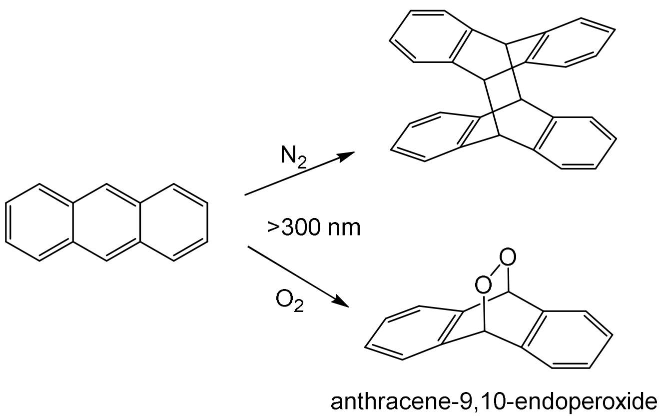

Figure 4.35. Irradiation of anthracene in air and nitrogen atmosphere [7].

4.5.1. Photodimerization Reactions of Anthryl Telechelic Polystyrene and Poly(methyl methacrylate)

<u>4.5.1.1. PS$_{4k}$-APE.</u> Irradiation of PS$_{4k}$-APE at 365 nm leads to the decrease of the original polymer peak with M_p: 4559 and the simultaneous growth of the peak M_p: 8718 of the forming PS-dimer with the doubled molecular weight [27]. Maximum conversion of 78% is reached at 24 h of irradiation (Figure 4.36).

Consequently, SEC UV absorbance data recorded at 365 nm shows a decrease in the absorption peak corresponding to the original PS$_{4k}$-APE with the increase in irradiation time (Figure 4.37). As the anthracene units undergo photodimerization, the conjugation of the π system is disrupted and the resulting photodimers no longer absorb light of wavelengths greater than 300 nm [6]. Therefore, the formation of PS-dimers by the photocoupling of anthracene units lead to a decrease in the absorption value.

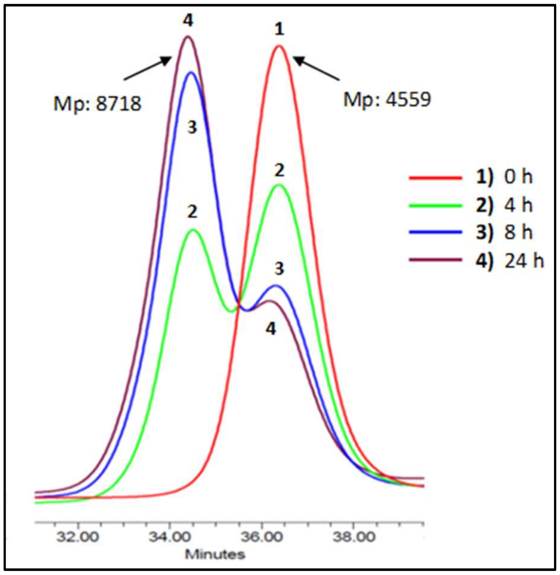

Figure 4.36. SEC data of PS_{4k}-APE recorded by RI detector at specific reaction times.

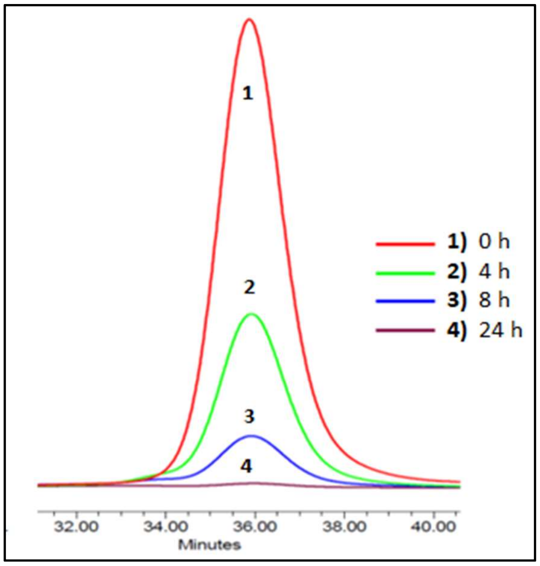

Figure 4.37. SEC data of PS_{4k}-APE recorded by UV absorbance detector at specific reaction times.

Irradiation was continued up to 48h, however after the maximum conversion was reached at 24 h, a reversal of the process was detected; by the decrease of the high molecular peak along with the increase of the low molecular peak. UV absorption value did not show any increase during this time period, which suggested that recovery of the PS-APE was not the reason for this event. Reversion of the photocycloaddition reaction would lead to the formation of free anthracene units, which would increase the absorbance, therefore the increase in the low molecular weight fraction might be due to formation of side products. Insertion of small amount oxygen into the reactor during the samplings might alter the photodimerization process and cause side reactions [7, 10, 13, 113].

Next, photoscission experiment was conducted by using 254 nm UV light. Irradiation under shortwave UV light leads to reversal of the photocycloaddition reaction, converting the photocoupled APE units to original state and resulting in the photoscission of polymer chains (Figure 4.33). The process can be monitored via SEC analysis by the shift of polymer peak molecular weight to lower values and the increase in the UV absorbance at 365 nm arising from the recovery of anthracene moieties at the chain ends [27].

Upon comparison of the absorbance value of the nonirradiated initial polymer (Figure 4.38, Line 1) the sample irradiated at 254 nm for 3 h and 5 h exhibited a 16 % recovery of anthryl units (Figure 4.38, Line 4-5) determined by comparison of the areas under the absorbance curves. SEC RI data also showed a decrease in the dimer peak accompanied by the increase in the original polymer peak due to photoscission of the chains (Figure 4.39). The experiment was repeated by using 290 nm UV light for comparison. Irradiation with 290 nm light did not cause any difference in the photoscission efficiency; at 3 h the recovery of anthryl units was approximately the same and there was a very small decrease at 5 h.

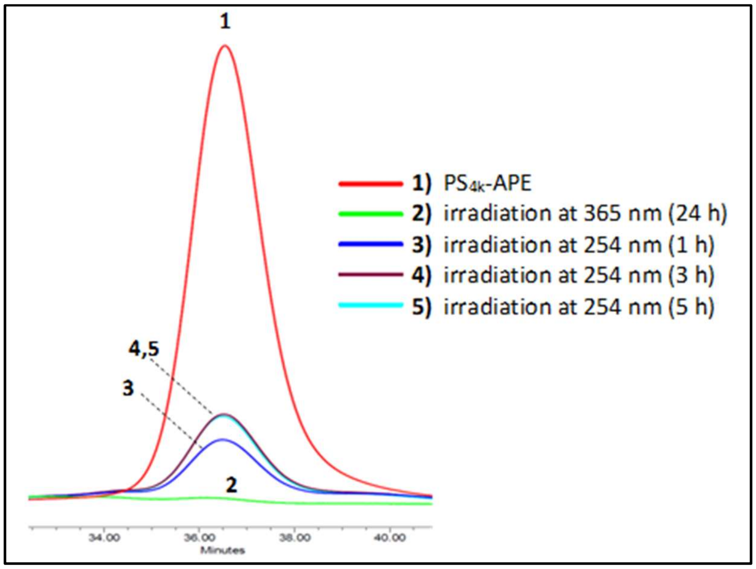

Figure 4.38. SEC data of PS_{4k}-APE recorded by UV absorbance detector: before irradiation (1), after irradiation at 365 nm for 24 h (2), after irradiation at 254 nm for 1 h (3), after irradiation at 254 nm for 3 h (4), after irradiation at 254 nm for 5 h (5).

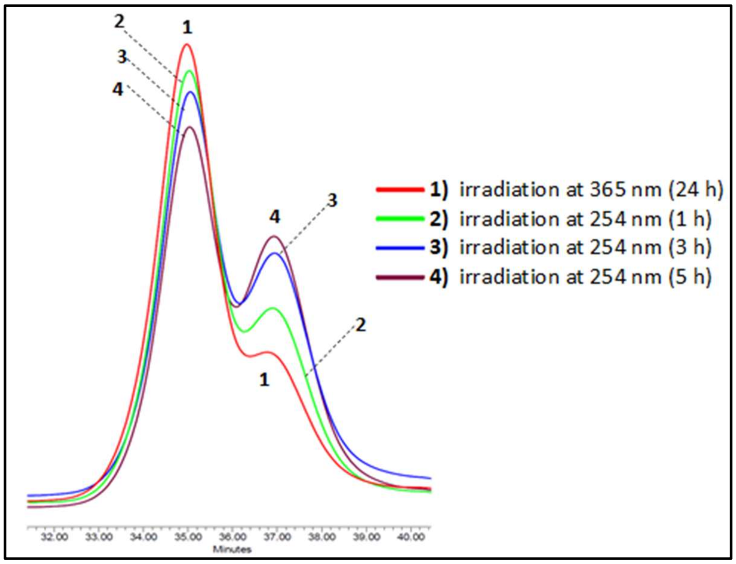

Figure 4.39. SEC RI data of PS_{4k}-APE: after irradiation at 365 nm for 24 h (1), after irradiation at 254 nm for 1 h (2), after irradiation at 254 nm for 3 h (3), after irradiation at 254 nm for 5 h (4).

<u>4.5.1.2. PMMA$_{3k}$-APE.</u> Irradiation of PMMA$_{3k}$-APE at 365 nm leads to the decrease of the original polymer peak of Mp: 3785 and the growth of the high molecular weight peak (M_p: 6916) of the forming PMMA-dimer with the doubled molecular weight [56]. Maximum conversion of 51% was reached at 24 h of irradiation (Figure 4. 40). SEC UV data alsa diplayed a decrease in the absorbance at 365 nm due to the photocycloaddition of anthryl moieties (Figure 4.41).

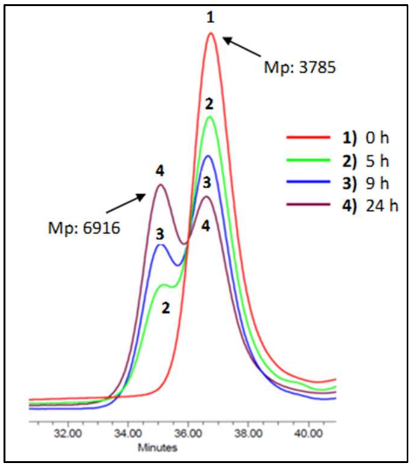

Figure 4.40. SEC data of PMMA$_{3k}$-APE recorded by RI detector at specific reaction times.

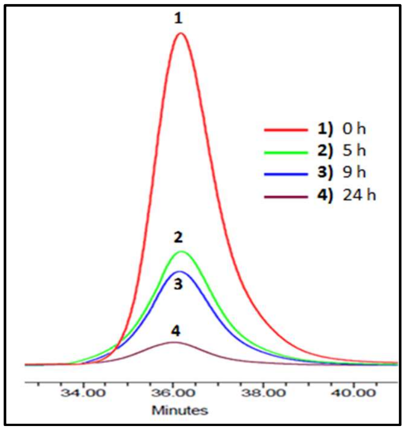

Figure 4.41. SEC data of PMMA$_{3k}$-APE recorded by UV absorbance detector at specific reaction times.

Irradiation of the polymer sample at 365 nm was continued up to 144 h, as previously reported by Goldbach et al. [29], but a reversal of the photodimerization process was observed as again, similar to the PS_{4k}-APE experiment. Further sampling after the maximum conversion at 24h showed a decrease in the high molecular weight peak and an increase in the low molecular weight peak.

4.5.1.3. $PMMA_{16k}$-APE. Irradiation of $PMMA_{16k}$-APE at 365 nm leads to the decrease of the original polymer peak of Mp: 17607 and the growth of the high molecular weight peak, M_p: 33792, of the forming PMMA-dimer with the doubled molecular weight (Figure 4.42). Upon 24 h of irradiation, the maximum conversion is 23%, which is quite lower than the low molecular weight counterpart $PMMA_{3k}$-APE. This could be expected since the rate of photocoupling depends on the molecular weight of the polymers; the induced mobility restrictions of the high molecular weight samples resulting in the unability of the longer chains to combine at these conditions [56, 114].

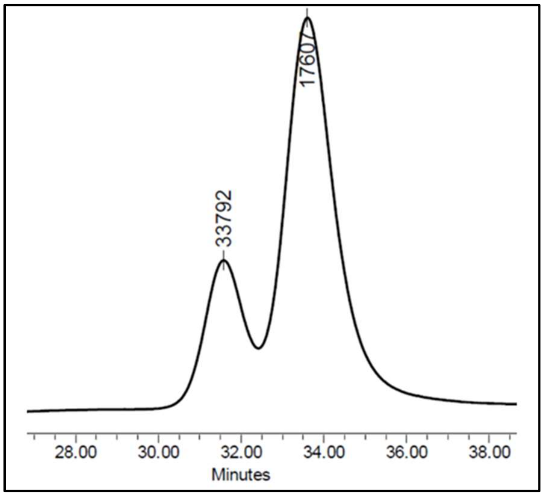

Figure 4.42. SEC data of $PMMA_{16k}$-APE recorded by RI detector after irradiation at 365 nm for 24 h.

4.5.1.4. PMMA$_{16k}$-APE and PS$_{4k}$-APE. Goldbach et al. stated that irradiation of a polymer mixture containing APE functionalized PMMA and PS above 300 nm lead to the formation of photodimerized PMMA and PS homopolymers, with doubled molecular weights, and a small percentage of PMMA-PS diblock copolymers [29]. We also investigated the photocoupling dynamics of APE functionalized PS and PMMA.

Our previous experiments showed that the irradiation of these polymers of similar M_n values lead to a faster formation of PS-dimer than PMMA-dimer. Within 4h, conversion of the PS-dimer reached 42% (Figure 4.36), whereas conversion of the PMMA-dimer was 20% at 5h (Figure 4.40). Therefore, rather than the irradiation of a polymer mixture, the prepared PS$_{4k}$-APE solution was injected into the PMMA$_{16k}$-APE solution in three portions, reaching to 1:1 molar ratio in 8h. This was performed in order to increase the yield of diblock copolymer formation. Since the detection of two polymers with similar M_n values would be problematic in SEC analysis, PMMA$_{16k}$-APE sample was utilized for this experiment. As stated in the previous part, photodimerization of this sample has a lower rate than that of the low molecular weight PMMA; the mobility of the polymer chains decreases with increasing molecular weight.

Figure 4.43 shows the SEC RI data for the irradiation of PMMA$_{16k}$-APE and PS$_{4k}$-APE mixture. The reaction was started with 1:0.25 molar ratio of PMMA:PS and sampling was done at 4 h. Then the second portion of PS was added to increase the molar ratio to 1:0.5 PMMA:PS, and sampling was done at 8 h. Afterwards the remaining portion of PS was added to have 1:1 molar ratio, which was sampled at 24 h. The decrease in the PMMA$_{16k}$-APE peak was observed within 4 h, along with the formation of the high molecular weight of the PMMA-dimer. The beginning of PS-dimer formation took place after 8 h, which was observed clearly at 24 h sample.

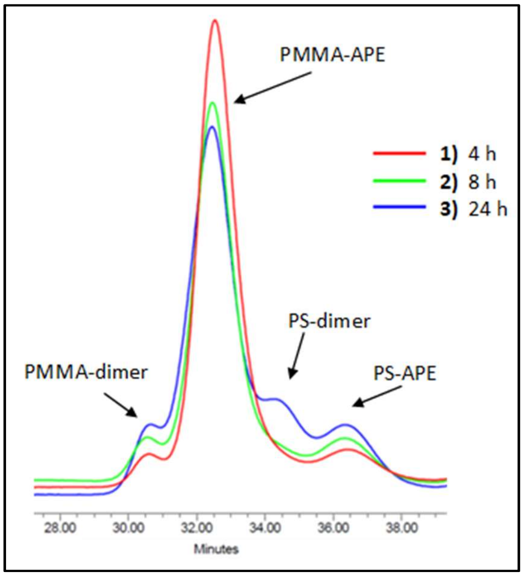

Figure 4.43. SEC data of $PMMA_{16k}$-APE and PS_{4k}-APE mixture recorded by RI detector at specific reaction times.

Figure 4.44 shows the corresponding peak molecular weights of the APE functionalized polymers and polymer dimers at 24 h. Diblock copolymer of PMMA and PS would have an approximate M_n of 20400, which might fall onto the region around M_p: 21000-22000. Unfortunately, such a peak could not be observed in the SEC data; which suggests that either the formation of block copolymer did not occur in these conditions, or the yield was very small and the corresponding low intensity peak could not be observed due to the overlapping high intensity PMMA-APE peak. Irradiation was continued up to 144 h, no significant change was observed. Goldbach et al. similarly obtained a very small yield of diblock copolymers, furthermore the homopolymers had to be removed via several treatments with selective solvents [29]. This process necessitated the usage of large quantities of labelled polymers for the UV irradiation experiments to yield enough diblock product for further studies; therefore it is not ideal for small scale experiments.

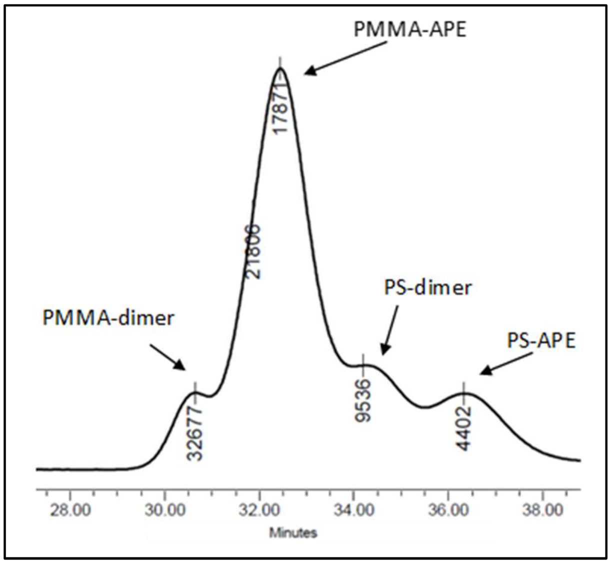

Figure 4.44. SEC data of $PMMA_{16k}$-APE and PS_{4k}-APE mixture recorded by RI detector at 24 h.

4.5.2. Reversible Photocycloaddition Reactions of di-Anthryl Telechelic Polyisobutylenes [28]

4.5.2.1. APE-PIB_{6k}-APE. Figure 4.45 shows the SEC curves of APE-PIB_{6k}-APE prior to and after UV irradiation at 365 nm for different reaction times. As the anthracene moieties at the chain ends undergo intermolecular photocycloaddition, the molecular weight of polymer chains increases which is evident in the shift to shorter retention time in SEC analysis (Line 1 vs. 6 in Figure 4.45). Concurrently, absorbance of the polymer samples monitored by the UV detector at 365 nm decreases gradually (Figure 4.46) following the depletion of anthracene units by photocycloaddition reaction.

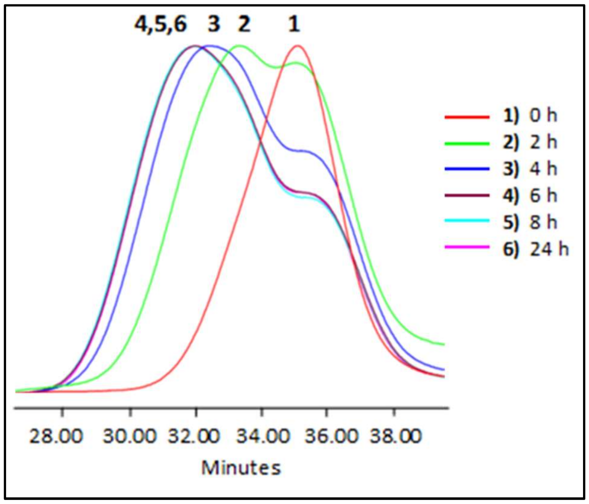

Figure 4.45. SEC data of APE-PIB$_{6k}$-APE recorded by RI detector: before irradiation (1), after irradiation at 365 nm for 2 h (2), after irradiation at 365 nm for 4 h (3), after irradiation at 365 nm for 6 h (4), after irradiation at 365 nm for 8 h (5), after irradiation at 365 nm for 24 h (6).

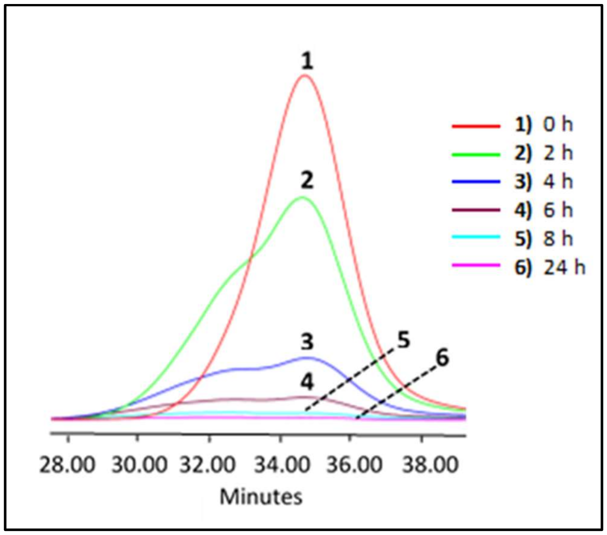

Figure 4.46. SEC UV absorbance data of APE-PIB$_{6k}$-APE recorded by UV absorbance detector: before irradiation (1), after irradiation at 365 nm for 2 h (2), after irradiation at 365 nm for 4 h (3), after irradiation at 365 nm for 6 h (4), after irradiation at 365 nm for 8 h (5), after irradiation at 365 nm for 24 h (6).

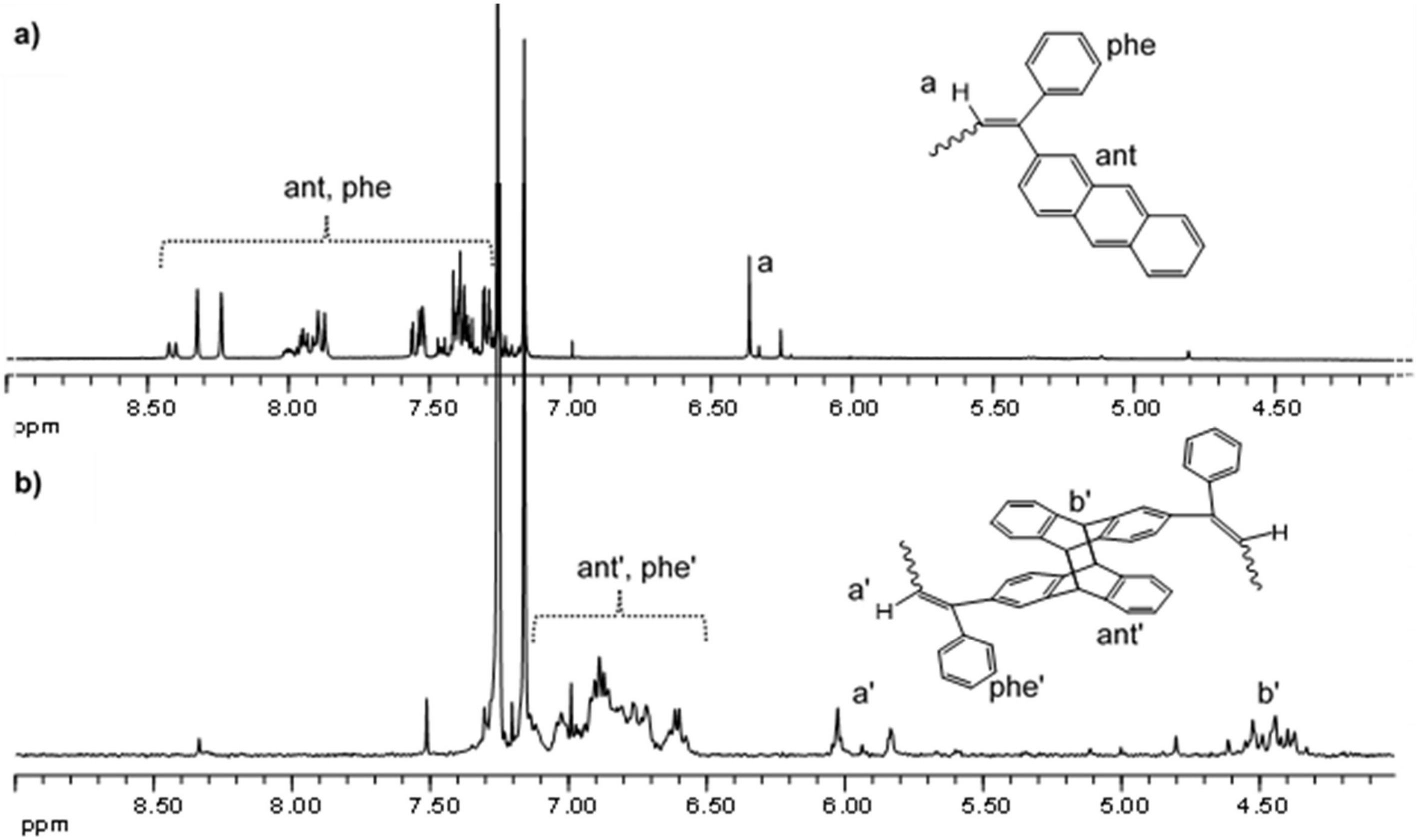

Figure 4.47. ^{1}H-NMR spectrum of APE-PIB$_{6k}$-APE (a) before irradiation (b) after irradiation at 365 nm.

^{1}H NMR spectrum of APE-PIB$_{6k}$-APE prior to and after irradiation at 365 nm is demonstrated in Figure 4.47. The comparison of the two spectra shows that the anthryl and phenyl proton peaks of the original polymer chain end at 7.2-8.5 ppm disappear upon UV treatment and new peaks corresponding to the aromatic groups of the cycloaddition product appear at 6.5-7.1 ppm. The bridgehead protons of the coupled structure are also visible at 4.3-4.6 ppm, which indicates successful photodimerization of anthracene units.

To gain insight on the effect of concentration on the degree of chain extension, four samples of APE-PIB$_{6k}$-APE with different precursor polymer concentrations ([P]: 2.4 x 10^{-5} M, 7.4 x 10^{-4} M, 2.4 x 10^{-3} M, 7.4 x 10^{-3} M) were subjected to UV irradiation of 365 nm. The formation of higher molecular weight peaks is observed in all four by the shift of the retention time to lower values, following the trend of increasing concentration as shown in Figure 4.48. The final M$_n$ and M$_p$ (M$_{p2}$ Max) values reached after irradiation at 365 nm for 24 h are listed in Table 4.5 as well as the initial M$_{n1}$ and M$_{p1}$ value of APE-PIB$_{6k}$-APE for comparison.

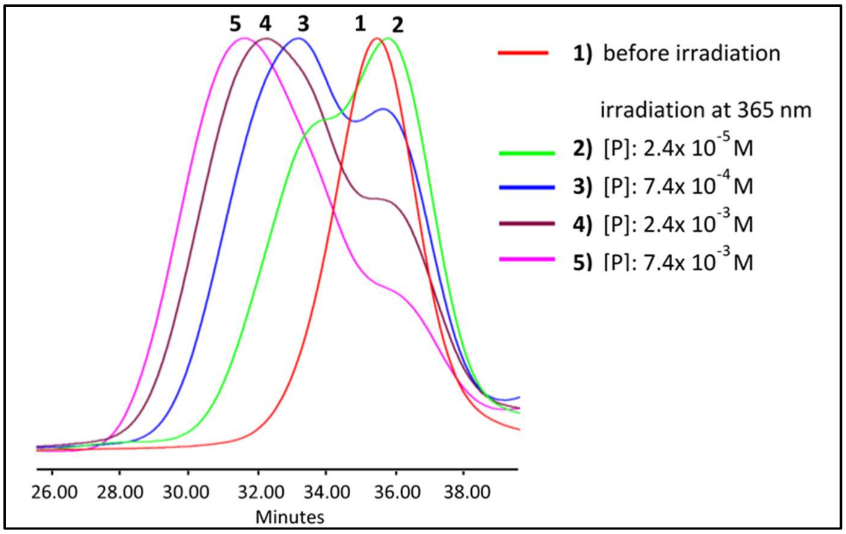

Figure 4.48. SEC data of APE-PIB$_{6k}$-APE recorded by RI detector; before irradiation (1) and after irradiation at 365 nm for 24 h with different precursor polymer concentrations: [P]: 2.4 x 10^{-5} M (2), 7.4 x 10^{-4} M (3), 2.4 x 10^{-3} M (4), 7.4 x 10^{-3} M (5).

Table 4.5. SEC RI data of APE-PIB$_{6k}$-APE irradiated at 365 nm for 24 h depicted in Figure 4.48.

	[P]: (M)	M_n Final	M_{p2} Max	M_{p1} Final	M_{p1} Initial	M_{n1} Initial
Line 2	2.4×10^{-5}	7871	12857	6745	7456	6893
Line 3	7.4×10^{-4}	10179	16212	6975	7456	6893
Line 4	2.4×10^{-3}	12212	21906	6989	7456	6893
Line 5	7.4×10^{-3}	15516	27382	6989	7456	6893

It was observed that the sample of [P]: 7.4×10^{-4} M shows an approximately two-fold increase in the M_p value compared to the original polymer within 24 h. Sample [P]: 2.4 x 10-3 M reaches a three-fold M_p value; whereas in the most concentrated sample of [P]: 7.4 x 10-3 M, the average M_p value is approximately four times the original polymer. Within 24 h of irradiation the M_n value increases from 6893 to 15516, for the most concentrated sample. This indicates that precursor polymer concentration directly affects the degree of chain extension; higher amount of APE-PIB$_{6k}$-APE in solution allows the chains to undergo intermolecular interactions and leads to the formation of tetrameric structures in the most concentrated sample. On the other hand, the original polymer peak (Figure 4.48, Line 1) does not disappear within 24 h, meaning that not all polymer chains undergo extension. Furthermore, the M_p value of this peak shifts to longer retention time throughout the reaction. This shows that the remaining polymer units that are unable to participate in chain extension may undergo intramolecular interactions instead and form unicyclic products. These cyclic polymers appear at longer retention times compared to their linear counterparts, due to their compact structures and smaller hydrodynamic volumes [112, 114-116]. The UV absorbance value of the abovementioned peak diminishes in time, which also points to the depletion of anthracene units via cyclization. The most distinct shift to longer retention time is observed for the relatively dilute sample

(Figure 4.48, Line 5). This indicates that the formation of unicyclic product is prominent for the least concentrated sample as expected, since low polymer concentration increases the probability of intramolecular interactions [112, 117]. The formation of a high molecular weight shoulder for this sample implies that chain extension could not be avoided even in the most dilute condition. However, it should be pointed out that cyclization occurs predominantly in dilute media, and chain extension does not go beyond the formation of a dimer for the most dilute sample. For the rest of the samples; the diminishing UV absorbance values suggest that intramolecular interactions leading to formation of cyclic products are also taking place in some extent during the chain extension process.

Next, photoscission experiments were conducted by using the photocoupled samples of APE-PIB$_{6k}$-APE, obtained by irradiation at 365 nm for 24 h, at concentrated conditions to yield the highest molecular weight starting products. Irradiation of these samples under UV light at 254 nm leads to reversal of the photocycloaddition reaction, converting the photocoupled APE units to original state and resulting in the photoscission of polymer chains (Figure 4.34). Reactions were once again performed in THF under inert atmosphere. The process can be monitored via SEC analysis by the shift of polymer peak molecular weight to lower values and the increase in the UV absorbance at 365 nm arising from the recovery of anthracene moieties at the chain ends. When two samples with different precursor polymer concentrations [P]: 10^{-3} M (Figure 4.49, Line 2) and [P]: 10^{-4} M (Figure 6, Line 3) were subjected to irradiation at 254 nm (I: 5.5 mW/cm^2) for 2 h, the greater shift to lower molecular weight region took place with the relatively dilute sample (Figure 4.49, Line 3). Evidently, the original polymer was recovered via photoscission at a higher degree in dilute conditions, which provide enhanced mobility to the polymer chains and facilitate photocleavage [7, 23]. When the intensity of light was increased to 11 mW/cm^2 and the initial polymer concentration was adjusted to 10^{-4} M, SEC data showed the furthest shift of the molecular weight to lower values (Figure 4.49, Line 4). The final M_n and M_p (M_{p2} Max) values reached after irradiation at 254 nm are listed in Table 6. For comparison, the M_n and M_{p2} values corresponding to the sample irradiated at 365 nm for

24 h are also present. These data show that irradiation with high light intensity and dilute conditions induces the largest change of M_n; from 15516 to 9576.

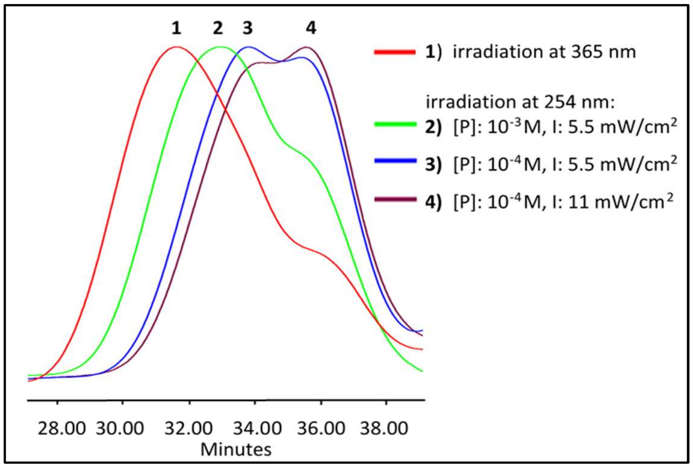

Figure 4.49. SEC RI data of APE-PIB$_{6k}$-APE; after irradiation at 365 nm for 24 h (1), followed by irradiation at 254 nm for 2 h with different precursor polymer concentrations and light intensities: [P]: 10^{-3} M, I: 5.5 mW/cm^2 (2), [P]: 10^{-4} M, I: 5.5 mW/cm^2 (3), [P]: 10^{-4} M, I: 11 mW/cm^2 (4).

Table 4.6. SEC RI data of photocoupled APE-PIB$_{6k}$-APE irradiated at 254 nm for 2 h depicted in Figure 4.49.

		[P] (M)	I (mW/cm^2)	M_n Final	M_{p2} Max	M_{p1} Final	M_{p1} Initial	M_{n1} Initial
Line 1	365 nm	-	-	15516	27382	6989	7456	6893
Line 2	254 nm	10^{-3}	5.5	10977	17952	7996	7456	6893
Line 3		10^{-4}	5.5	10743	16101	7903	7456	6893
Line 4		10^{-4}	11	9576	14120	7853	7456	6893

The dynamics of the photoscission reaction was further investigated by examining the correlation between irradiation time and change in absorbance at 365 nm (Figure 4.50). SEC UV data in Figure 4.51 demonstrates that the absorbance value increases with irradiation time due to the regeneration of anthryl moieties via photocleavage under 254 nm UV light. The highest recovery of APE units was observed upon 6 h irradiation at 254 nm (Figure 4.51, Line 8). When compared to the absorbance value of the nonirradiated initial polymer (Figure 4.51, Line 1) and the following decrease to minimum via irradiation at 365 nm (Figure 4.51, Line 2), the sample irradiated at 254 nm for 6 h exhibited a 78% recovery of anthryl units (Figure 4.51, Line 8) determined by comparison of the areas under the absorbance curves. SEC RI data is also consistent with these results, exhibiting a shift of polymer molecular weight to lower values due to chain scission (Figure 4.52, Line 3). On the other hand as the sample was exposed to further UVC treatment, extending the irradiation time to 8 h and then 24 h, the absorbance value decreased (Figure 4.50). These results show that an optimum irradiation dose has been reached within 6 h beyond which the photocleavage and photocycloaddition reactions are at dynamic equilibrium. Similar phenomena have been reported in previous studies for both anthracene [18, 26] and coumarin [118, 119] functionalized polymeric systems. After the maximum absorbance recovery is reached, prolonged irradiation at 254 nm renders the anthryl moieties susceptible to irreversible photocoupling [26].

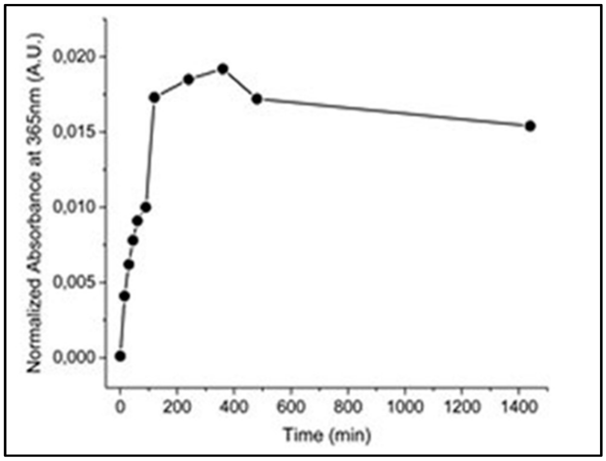

Figure 4.50. Absorbance at 365 nm versus time under irradiation at 254 nm, recorded by SEC UV detector (the sample APE-PIB$_{6k}$-APE had been previously exposed to 365 nm UV light for 24 h for maximization photocycloaddition).

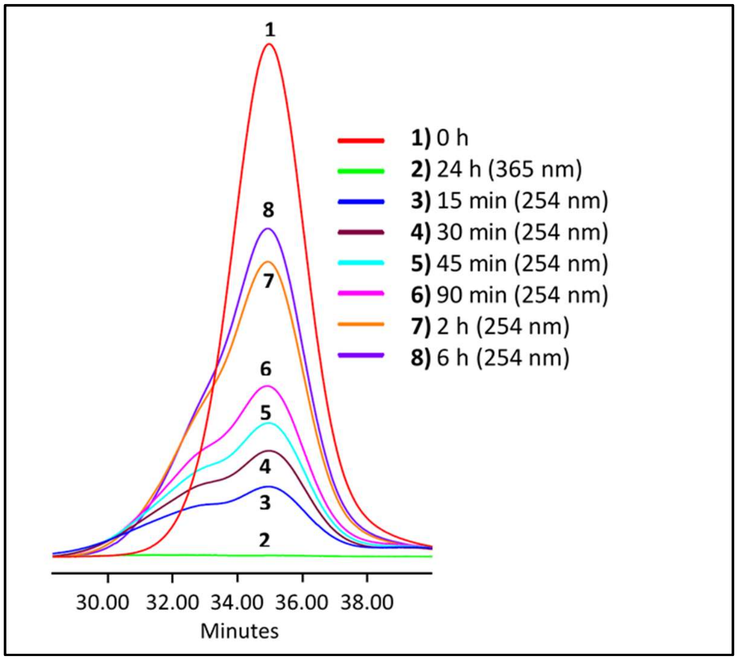

Figure 4.51. Absorbance of APE-PIB$_{6k}$-APE at 365 nm recorded by SEC UV detector; before irradiation (1), after irradiation at 365 nm for 24 h (2), followed by irradiation at 254 nm (3-8).

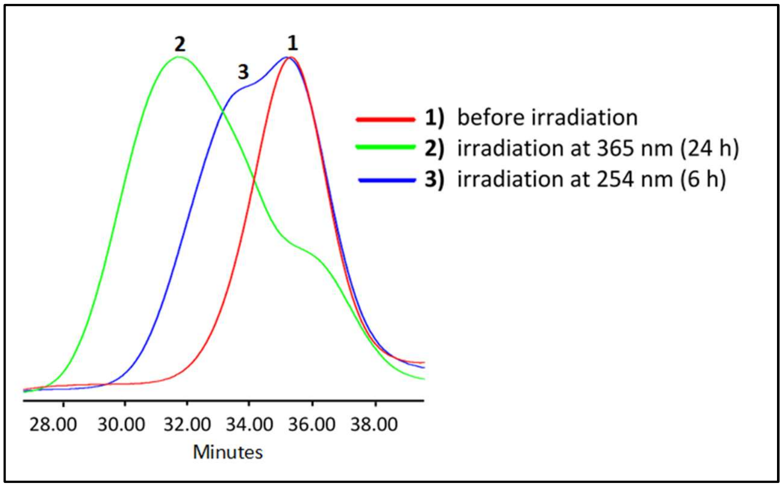

Figure 4.52. SEC data of APE-PIB$_{6k}$-APE recorded by RI detector; before irradiation (1), after irradiation at 365 nm for 24 h (2), followed by irradiation at 254 nm for 6 h (3).

The photocleaved sample was then subjected to 365 nm irradiation once again in order to investigate the viability of the photocycloaddition of anthryl units. Upon 24 h exposure to 365 nm light a shift to shorter retention time was observed in SEC RI data (Figure 4.53, Line 4), indicating that the polymer chains are undergoing photocoupling again to form higher molecular weight products.

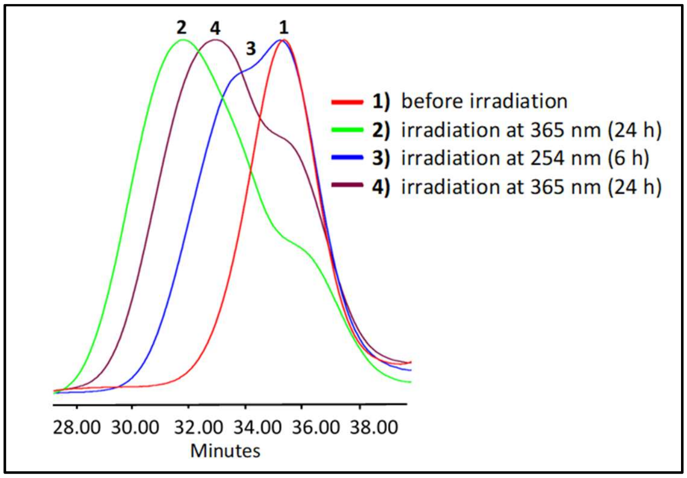

Figure 4.53. SEC data of APE-PIB$_{6k}$-APE recorded by RI detector; before irradiation (1), after irradiation at 365 nm for 24 h (2), followed by irradiation at 254 nm for 6 h (3), followed by irradiation at 365 nm for 24 h (4).

Then this sample was subjected to a second irradiation at 254 nm in order to examine the revival of anthryl units. Samples taken at 1, 2, 3 and 4 hours showed an increase in the UV absorbance at 365 nm (Figure 4.54); indicating that the photocoupled anthracenes are once again undergoing photoscission and being recovered. Accompanying SEC RI data also shows a shift to longer retention as a result of the photoscissioned chains (Figure 4.55, Line 5). Expectedly, the second 254 nm irradiation is not as efficient as the initial one, due to the loss of active anthryl units during the prolonged irradiations via possible oxidations [10, 13, 113], irreversible photocouplings and aforementioned dynamic equilibrium state of the compound in 254 nm treatment [18, 26]. The sample re-irradiated at 254 nm for 4 h exhibited a 26 % recovery of anthryl units. The overall changes in the M_n and M_p values of the polymer samples recorded by SEC RI detector are given in Table 4.7.

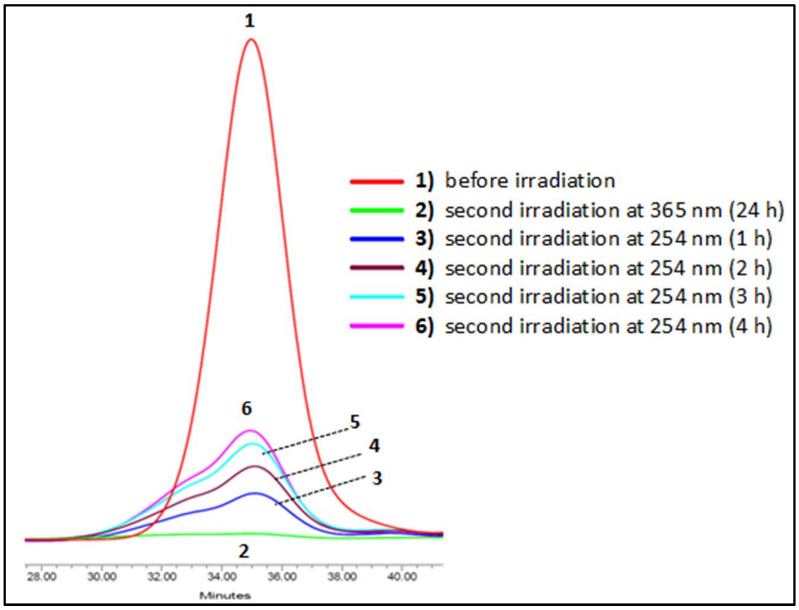

Figure 4.54. Absorbance of APE-PIB$_{6k}$-APE at 365 nm recorded by SEC UV detector; before irradiation (1), after second irradiation at 365 nm for 24 h (2), followed by second irradiation at 254 nm (3-6).

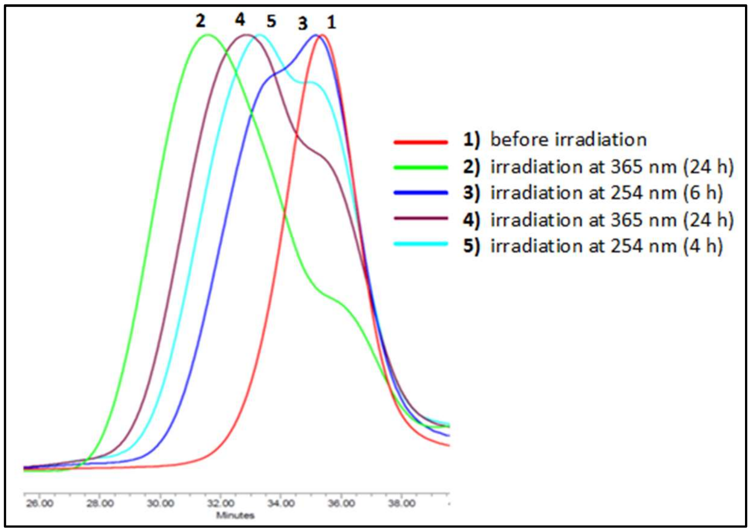

Figure 4.55. SEC data of APE-PIB$_{6k}$-APE recorded by RI detector; before irradiation (1), after irradiation at 365 nm for 24 h (2), followed by irradiation at 254 nm for 6 h (3), followed by irradiation at 365 nm for 24 h (4), followed by irradiation at 254 nm for 4 h (5).

Table 4.7. SEC RI data of APE-PIB$_{6k}$-APE depicted in Figure 4.55.

	APE-PIB$_{6k}$-APE	M_n	M_p Max
Line 1	Before irradiation	6893	7456
Line 2	365 nm (24 h)	15516	27382
Line 3	254 nm (6 h)	8893	13217
Line 4	365 nm (24 h)	11191	18148
Line 5	254 nm (4 h)	11400	17013

4.5.2.2. APE-PIB$_{18k}$-APE. High molecular weight APE-PIB$_{18k}$-APE was also subjected to UV irradiation at 365 nm, with precursor polymer concentration [P]: 6 x 10^{-3} M. Formation of higher molecular weight peak was observed, but the shift to higher molecular weights was not as prominent as the low molecular weight counterpart APE-PIB$_{6k}$-APE. SEC RI data show only an approximately two-fold increase in the M_p value with respect to the original polymer within 8 h (Figure 4.56), even at high precursor polymer concentration. Longer polymer chains tend to undergo physical restrictions and diffusion problems that reduce their mobility. It has been previously stated that the mobility of anthryl group is crucial to enable the photocycloaddition reaction [8, 114], therefore a lesser degree of chain extension might be expected for the high molecular weight polymer sample. The absorbance of the polymer samples monitored by the UV detector at 365 nm decreases gradually (Figure 4.57), following the depletion of anthracene units by photocycloaddition reaction.

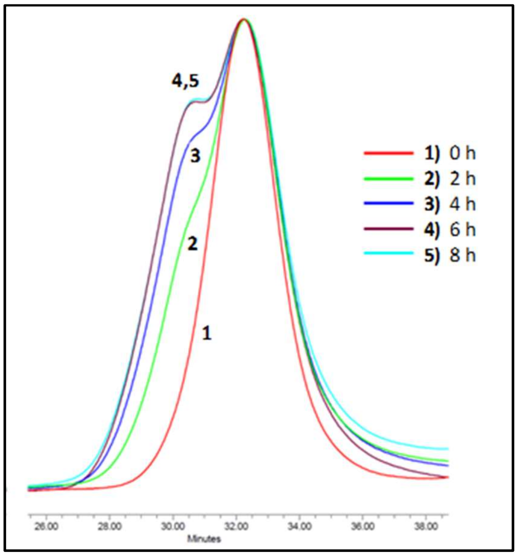

Figure 4.56. SEC data of APE-PIB$_{18k}$-APE recorded by RI detectors: before irradiation (1), after irradiation at 365 nm for 2 h (2), after irradiation at 365 nm for 4 h (3), after irradiation at 365 nm for 6 h (4), after irradiation at 365 nm for 8 h (5).

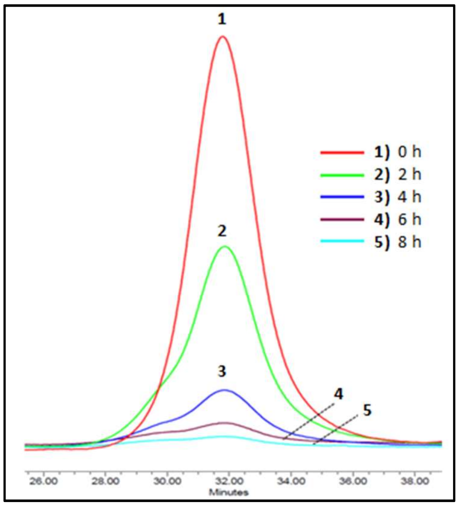

Figure 4.57. SEC data of APE-PIB$_{18k}$-APE recorded by UV absorbance detectors: before irradiation (1), after irradiation at 365 nm for 2 h (2), after irradiation at 365 nm for 4 h (3), after irradiation at 365 nm for 6 h (4), after irradiation at 365 nm for 8 h (5).

A second sample of APE-PIB$_{18k}$-APE was irradiated at 365 nm for 24 h, which was then subjected to photoscission experiments. The prepolymer concentration was again kept low (2 x 10^{-4} M) to provide mobility to the high molecular weight chains. Within 1 h of irradiation at 254 nm, the peak corresponding to the photocoupled PIB chains diminish (Figure 4.58, Line 3), indicating that these chains are undergoing photoscission. The irradiation is continued to 3 h and then 6 h, but no significant change is observed in the RI data. When the corresponding SEC UV data is examined (Figure 4.59), the increase in the absorbance value with irradiation time due to the regeneration of anthryl moieties via photocleavage under 254 nm UV light can be observed. Upon comparison of the absorbance value of the nonirradiated initial polymer (Figure 4.59, Line 1) and the decrease to minimum via irradiation at 365 nm (Figure 4.59, Line 2), the sample irradiated at 254 nm for 1 h exhibited a 47.5 % recovery of anthryl units (Figure 4.59, Line 3) determined by comparison of the areas under the absorbance curves. The photoscission recovery is lower for APE-PIB$_{18k}$-APE with respect to the low molecular weight counterpart APE-PIB$_{6k}$-APE, which could be expected due to the relatively restricted mobility of the longer polymer chains [7, 23]. For APE-PIB$_{6k}$-APE, optimum irradiation time at 254 nm was determined as 6 h. On the other hand, maximum increase in absorbance value was recorded at 1 h for APE-PIB$_{18k}$-APE. No significant difference was observed for 3 h (Figure 4.59, Line 4); however, further irradiation to 6 h displayed a slight decrease in UV absorbance at 365 nm (Figure 4.59, Line 5). These data suggest that optimum irradiation time for the photocoupled APE-PIB$_{18k}$-APE at 254 nm is about 1 h.

The photocleaved sample was then subjected to a second 365 nm to investigate the viability of the photocycloaddition of anthryl units. Upon 24 h exposure to 365 nm light a shift to shorter retention time was observed in SEC RI data (Figure 4.60, Line 4), indicating that the polymer chains are undergoing photocoupling again to form higher molecular weight products. The final M_n and M_p (M_p Max) values reached after irradiations at 365 nm and 254 nm are listed in Table 4.8, as well as the initial M_n and M_p value of APE-PIB$_{18k}$-APE for comparison.

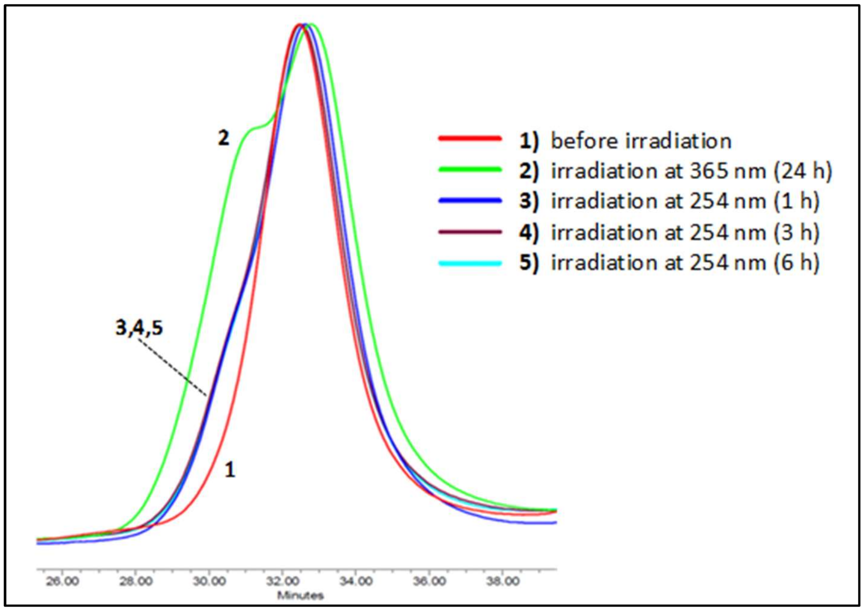

Figure 4.58. SEC data of APE-PIB$_{18k}$-APE recorded by RI detector; before irradiation (1), after irradiation at 365 nm for 24 h (2), followed by irradiation at 254 nm for 1 h (3), irradiation at 254 nm for 3 h (4) and irradiation at 254 nm for 6 h (5).

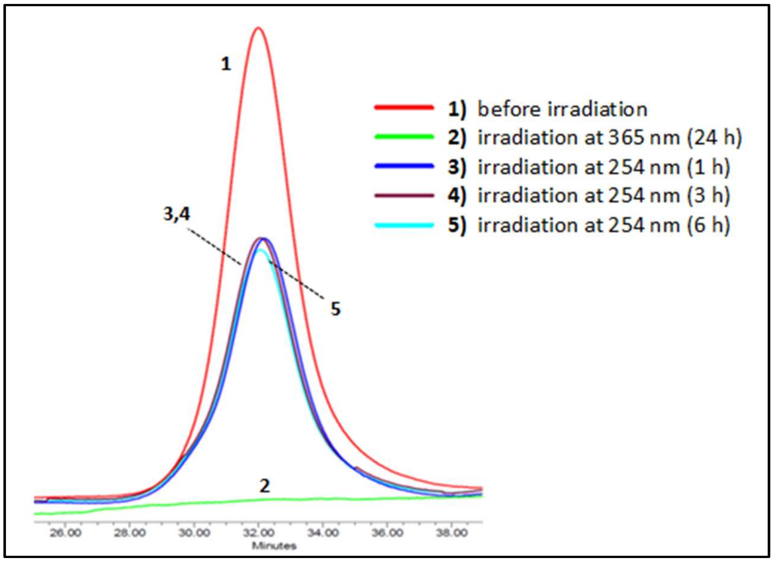

Figure 4.59. Absorbance of APE-PIB$_{18k}$-APE at 365 nm recorded by SEC UV detector; before irradiation (1), after irradiation at 365 nm for 24 h (2), followed by irradiation at 254 nm for 1 h (3), irradiation at 254 nm for 3 h (4) and irradiation at 254 nm for 6 h (5).

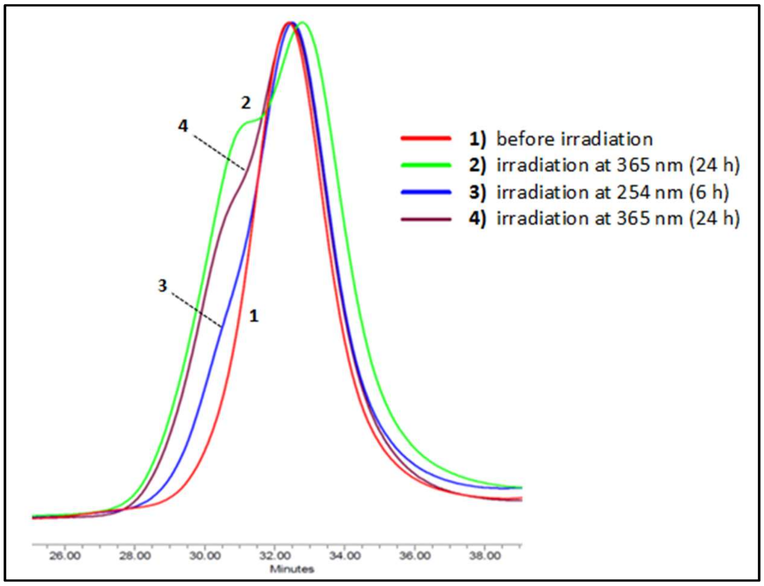

Figure 4.60. SEC data of APE-PIB$_{18k}$-APE recorded by RI detector; before irradiation (1), after irradiation at 365 nm for 24 h (2), followed by irradiation at 254 nm for 6 h (3), followed by irradiation at 365 nm for 24 h (4).

Table 4.8. SEC RI data of APE-PIB$_{18k}$-APE depicted in Figure 4.60.

	APE-PIB$_{18k}$-APE	M_n	M_p Max
Line 1	Before irradiation	18005	20288
Line 2	365 nm (24 h)	21276	34157
Line 3	254 nm (6 h)	20655	33421
Line 4	365 nm (24 h)	22114	35681

4.5.3. Reversible Photocycloaddition Reactions of di-Anthryl Telechelic Polystyrenes

4.5.3.1. APE-PS_{3k}-APE. Irradiation of APE-PS_{3k}-APE with precursor polymer concentration [P]: 2.34 x 10^{-3} M leads to the formation of higher molecular weight peaks observed by the shift of the retention time to lower values (Figure 4.61). Within 24 h the average M_p value has increased seven-fold with respect to the original polymer (Figure 4.61, Line 6) as shown in Table 4.9, which indicates that chain extension is in progress.

Table 4.9. SEC RI data of APE-PS_{3k}-APE irradiated at 365 nm for 24 h depicted in Figure 4.61.

	365 nm irradiation time	M_n Final	M_p Max	M_p Final	M_p Initial	M_n Initial
Line 2	2 h	3767	6034	2701	2994	3223
Line 3	4 h	4063	7606	2471	2994	3223
Line 4	6 h	4446	12923	2383	2994	3223
Line 5	8 h	4945	17913	2468	2994	3223
Line 6	24 h	5017	22044	2385	2994	3223

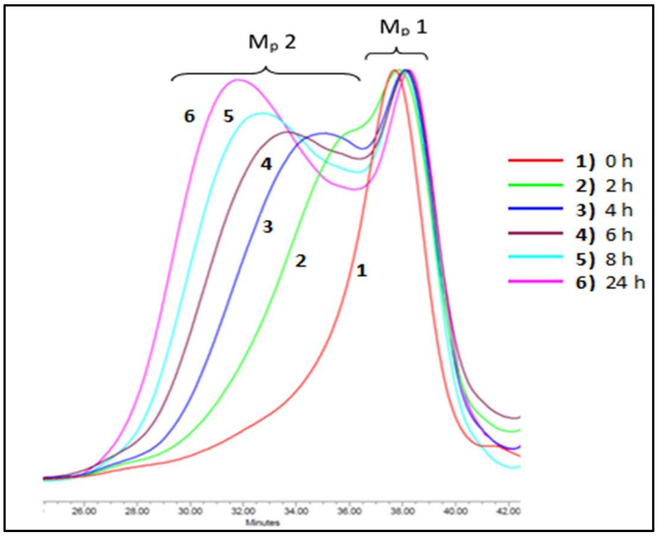

Figure 4.61. SEC data of APE-PS$_{3k}$-APE recorded by RI detector: before irradiation (1), after irradiation at 365 nm for 2 h (2), at 365 nm for 4 h (3), at 365 nm for 6 h (4), at 365 nm for 8 h (5), at 365 nm for 24 h (6).

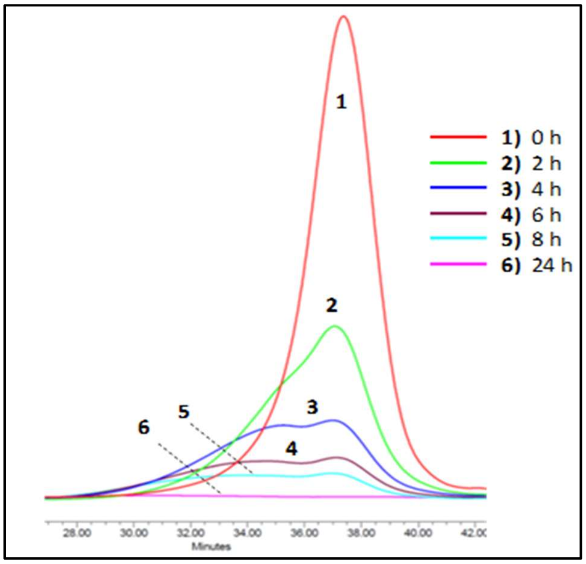

Figure 4.62. SEC data of APE-PS$_{3k}$-APE recorded by UV absorbance detector: before irradiation (1), after irradiation at 365 nm for 2 h (2), at 365 nm for 4 h (3 at 365 nm for 6 h (4), at 365 nm for 8 h (5), at 365 nm for 24 h (6).

Subsequently, UV absorbance value corresponding to original polymer decreases in time as shown in Figure 4.62. As the anthracene units undergo photodimerization, the conjugation of the π system is disrupted and the resulting photodimers no longer absorb light of wavelengths greater than 300 nm [3]. On the other hand, new absorbance peak at high molecular weight region appears at 2 h and beyond via the formation of higher molecular weight polymers with APE functionality at chain ends through coupling reaction. The original polymer peak denoted as M_p 1 in Figure 4.61 does not disappear within 24 h, meaning that not all polymer chains undergo extension. However, the M_p values of this peak shift to longer retention time throughout the reaction, which suggests that some extent of cyclization is also taking place. The UV absorbance value of abovementioned peak and the higher molecular weight peak corresponding to extended chains diminishes in time (Figure 4.62), which also points to the depletion of anthracene units via formation of cyclic products.

The photocoupled samples of APE-PS_{3k}-APE were then subjected to photoscission experiments at 254 nm UV light. The prepolymer solution of APE-PS_{3k}-APE irradiated at 365 nm for 24 h was prepared for the photoscission experiment, with a relatively low concentration of 3×10^{-4} M to increase mobility. Within 1 h of irradiation at 254 nm the peak denoted as M_p 2 corresponding to the photocoupled PS chains shifts to lower molecular weight region (Figure 4.63, Line 1), indicating that these chains are undergoing photoscission. The average M_p value decreases from 22044 to 10557 due to the light induced scission of the light molecular weight chains to lower molecular weight portions.

The accompanying UV absorbance data also displays an increase in the absorbance at this region, arising from the newly freed APE units of the obtained smaller chains (Figure 4.64). The UV absorbance of original APE-PS_{3k}-APE peak also increases with time, due to the recovery of APE end functionalities. This phenomenon may be caused by the detachment of APE-PS_{3k}-APE chains form photocoupled product and the possible decyclization of previously formed PS_{3k} unicycles. The irradiation is continued to 3 h and then 6 h.

Upon comparison of the absorbance value of the nonirradiated initial polymer (Figure 4.64, Line 1) and the decrease to minimum via irradiation at 365 nm (Figure 4.64, Line 2), the sample irradiated at 254 nm for 6 h exhibited a 38.9 % recovery of anthryl units (Figure 4.64, Line 5) determined by comparison of the areas under the absorbance curves. Extending the irradiation time to 9 h caused a decrease in the absorbance value (data not shown). The photoscission recovery is relatively lower for APE-PS$_{3k}$-APE, which could be expected due to the fact that 254 nm UV light gets absorbed by the PS chains initially and then transferred to the anthryl dimers [27, 120].

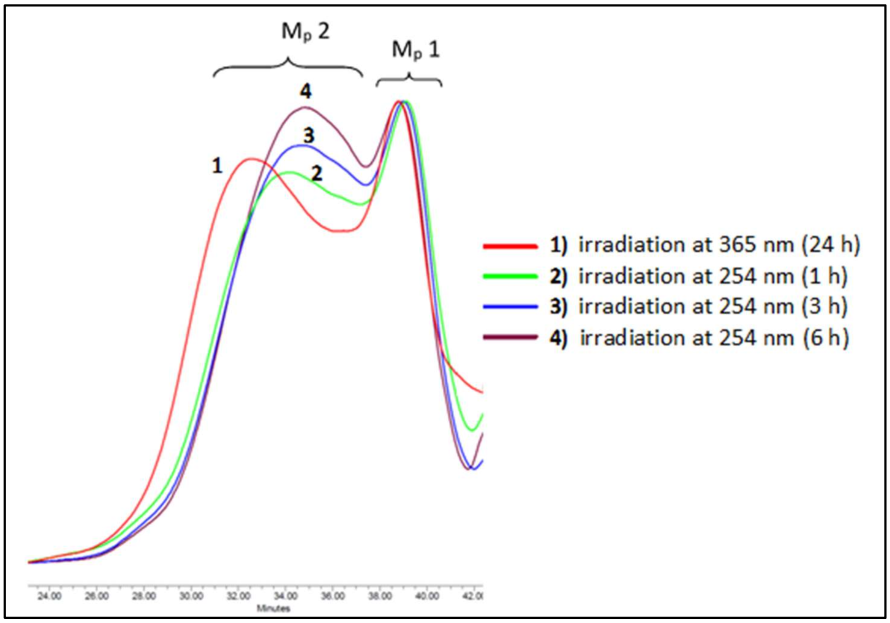

Figure 4.63. SEC data of APE-PS$_{3k}$-APE recorded by RI detector: after irradiation at 365 nm for 24 h (1), after irradiation at 254 nm for 1 h (2), after irradiation at 254 nm for 3 h (3), after irradiation at 254 nm for 6 h (4).

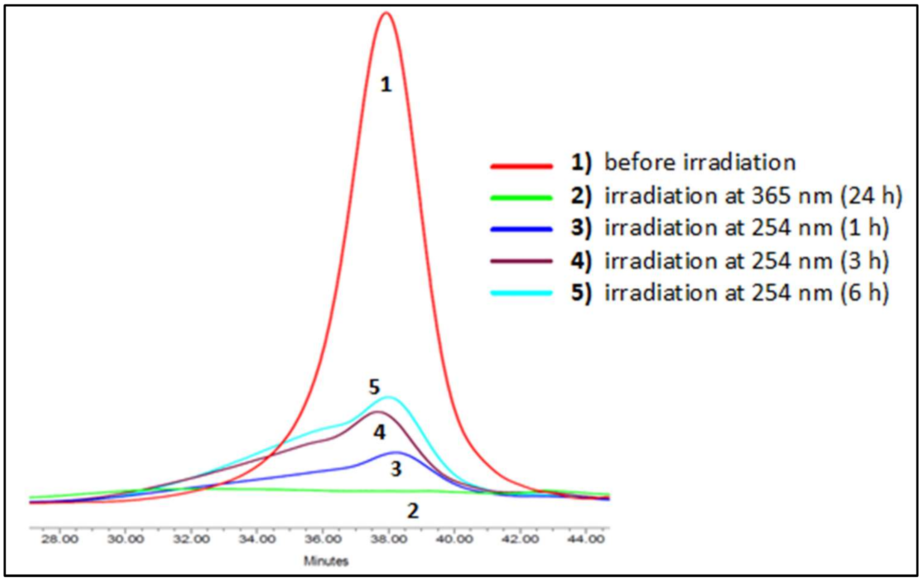

Figure 4.64. SEC data of APE-PS$_{3k}$-APE recorded by UV absorbance detector: before irradiation (1), after irradiation at 365 nm for 24 h (2), after irradiation at 254 nm for 1 h (3), after irradiation at 254 nm for 3 h (4), after irradiation at 254 nm for 6 h (5).

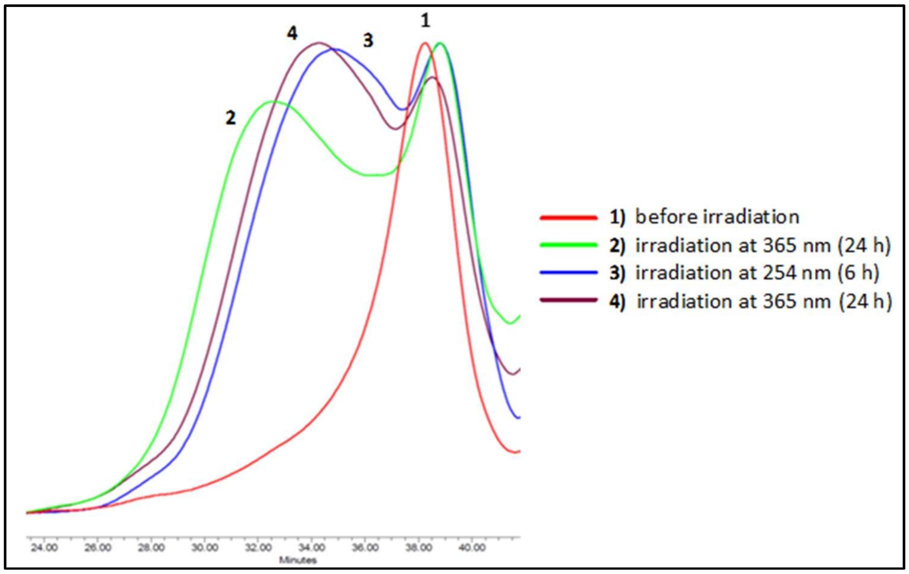

Figure 4.65. SEC data of APE-PS$_{3k}$-APE recorded by RI detector; before irradiation (1), after irradiation at 365 nm for 24 h (2), followed by irradiation at 254 nm for 6 h (3), followed by irradiation at 365 nm for 24 h (4).

When the photocleaved sample was irradiated at 365 nm once again for 24 h, only a slight shift to shorter retention time was observed in SEC RI data (Figure 4.65, Line 4). The final M_n and M_p (M_p Max) values reached after irradiations at 365 nm and 254 nm are listed in Table 4.10, as well as the initial M_n and M_p value of APE-PS$_{3k}$-APE for comparison.

Table 4.10. SEC RI data of APE-PS$_{3k}$-APE depicted in Figure 4.65.

	APE-PS$_{3k}$-APE	M_n	M_p Max
Line 1	Before irradiation	3223	2994
Line 2	365 nm (24 h)	5017	22044
Line 3	254 nm (6 h)	4655	10557
Line 4	365 nm (24 h)	5490	12398

4.5.3.2. APE-PS$_{15k}$-APE. Irradiation of APE-PS$_{15k}$-APE with precursor polymer concentration [P]: 2.3 x 10^{-3} M leads to the formation of higher molecular weight peaks observed by the shift of the retention time to lower values, which indicates that chain extension is in progress (Figure 4.66). In 2 h the peak corresponding to PS dimer (M_p 2: 29547) has increased due to the coupling of chains; a third peak with M_p approximately three times the original PS peak is has also emerged (M_p 3: 43495). This peak can be observed more clearly in the 4 h sample, depicted as M_p 3, growing as a separate peak next to the highest peak molecular weight shoulder M_p 4. This might be due the coupling of the initial PS dimer with another polymer unit to yield a trimeric structure. Within 8 h the average M_p value has increased four-fold with respect to the original polymer (Figure 4.66, Line 5) as shown in Table 4.11.

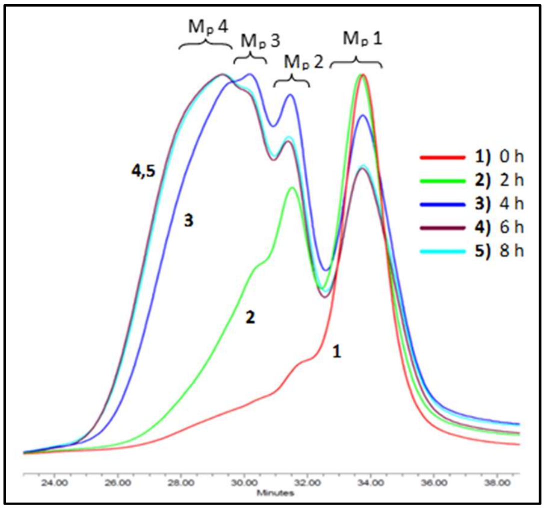

Figure 4.66. SEC data of APE-PS$_{15k}$-APE recorded by RI detector: before irradiation (1), after irradiation at 365 nm for 2 h (2), after irradiation at 365 nm for 4 h (3), after irradiation at 365 nm for 6 h (4), after irradiation at 365 nm for 8 h (5).

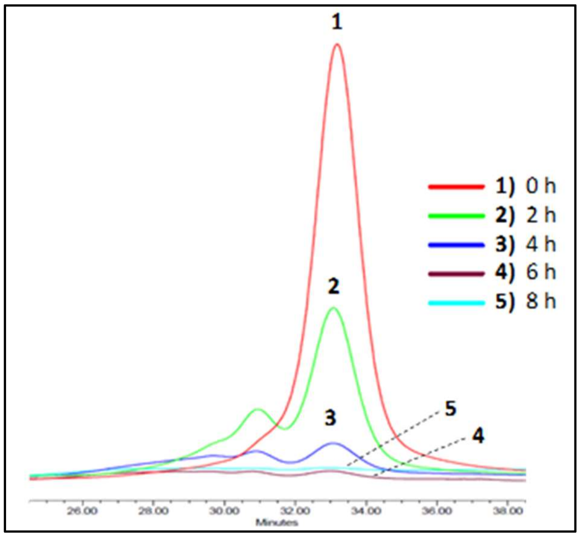

Figure 4.67. SEC data of APE-PS$_{15k}$-APE recorded by UV absorbance detector: before irradiation (1), after irradiation at 365 nm for 2 h (2), after irradiation at 365 nm for 4 h (3), after irradiation at 365 nm for 6 h (4), after irradiation at 365 nm for 8 h (5).

Subsequently, UV absorbance value corresponding to original polymer decreases in time, while new absorbance peaks emerge at high molecular weight region due to the newly formed dimers and trimers, as shown in Figure 4.67.

Table 4.11. SEC RI data of APE-PS$_{15k}$-APE irradiated at 365 nm for 8 h depicted in Figure 4.66.

	365 nm irradiation time	M_p 4	M_p 3	M_p 2	M_p 1	M_n
Line 1	0 h	-	-	27796	14106	15755
Line 2	2 h	-	43495	29547	14557	19376
Line 3	4 h	54418	43980	29182	13956	25341
Line 4	6 h	57219	46177	29793	14033	28397
Line 5	8 h	56304	4571	29273	13729	28128

4.5.4. Photocycloaddition Reaction of Anthryl Telechelic Poly(methyl methacrylate) and di-Anthryl Telechelic Polyisobutylene

APE-PIB$_{18k}$-APE and PMMA$_{3k}$-APE and mixture in THF with concentration [P]: 3 x 10^{-3} M was prepared and subjected to UV irradiation at 365 nm for 24 h. Figure 4.68 shows the SEC RI data comparison with the previously photocoupled APE-PIB$_{18k}$-APE sample. It can be observed that the mixture peak has shifted to shorter retention time with respect to photocoupled APE-PIB$_{18k}$-APE (M_p: 19792) and has a greater M_p: 23243. This indicates that there is a degree of coupling between the PIB and PMMA chains, with the possible addition of one PMMA unit to PIB chains. A shoulder has also appeared on high molecular weight region, which might correspond to APE-PIB$_{18k}$-APE dimer or a unit of PMMA coupled with the PIB dimer. However this shoulder is relatively small with respect to that in photocoupled APE-PIB$_{18k}$-APE (Figure 4.68, Line 1), which renders the detection of this second M$_p$ difficult. SEC UV data displays that after 24 h irradiation there is still absorbance at 365 nm in the region corresponding to PMMA$_{3k}$-APE, which states that unreacted PMMA is remaining in the mixture. This could be expected since previous experiments had shown that photodimerization reaction of anthryl telechelic PMMAs were relatively slow.

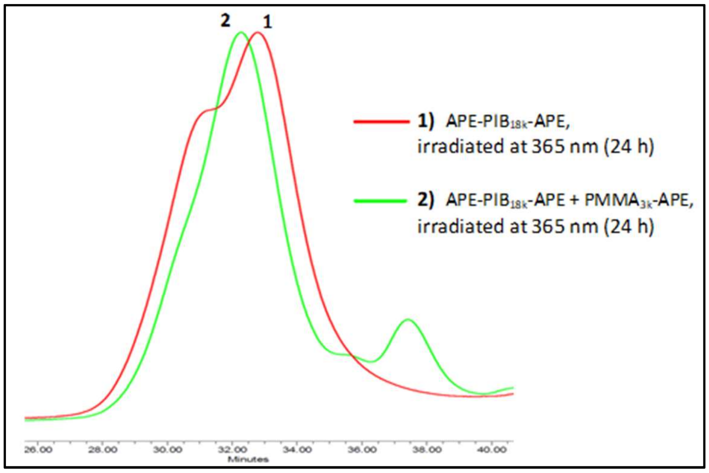

Figure 4.68. SEC RI data of photocycloaddition reaction: APE-PIB$_{18k}$-APE irradiated at 365 nm for 24 h (1), APE-PIB$_{18k}$-APE and PMMA$_{3k}$-APE mixture irradiated at 365 nm for 24 h (2).

4.5.5. Reversible Photocycloaddition Reactions of di-Anthryl Telechelic Polystyrene and Polyisobutylene

APE-PIB-APE and APE-PS-APE samples were mixed with 1:1 molar ratios in THF and subjected to irradiation at 365 nm in concentrated conditions. The two di-anthryl telechelic polymers are expected to couple in a random fashion, leading to the formation of multiblock copolymers with alternating or homogeneous regions in the overall chain extension process (Figure 4.69).

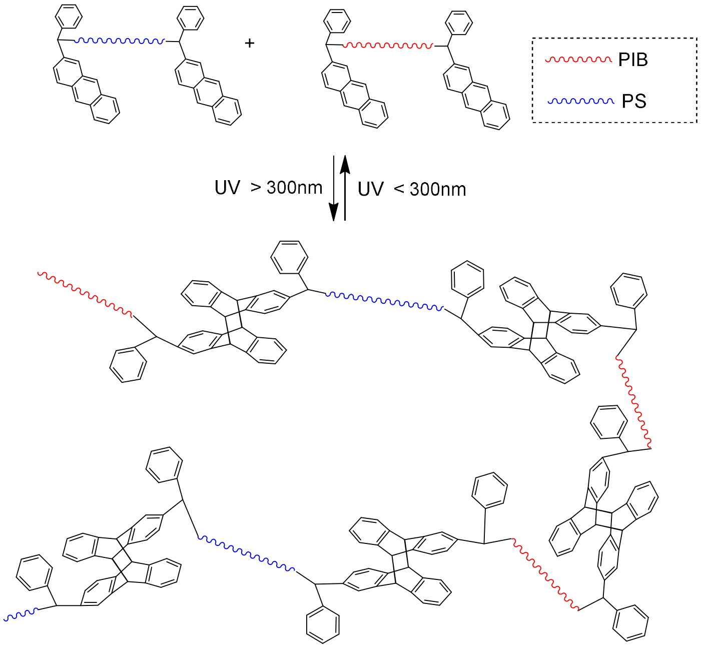

Figure 4.69. Photocoupling of APE-PS-APE and APE-PIB-APE chains under UV irradiation.

4.5.5.1. APE-PS$_{3k}$-APE and APE-PIB$_{6k}$-APE. APE-PS$_{3k}$-APE and APE-PIB$_{6k}$-APE mixture in THF with concentration [P]: 6.7 x 10^{-3} M was prepared and subjected to UV irradiation at 365 nm. Figure 4.70 shows that chain extension is taking place; the original polymer peaks denoted as M_p 1 (APE-PS$_{3k}$-APE) and M_p 2 (APE-PIB$_{6k}$-APE) diminish as the high molecular weight peak, denoted as M_p 3, appears and shifts to shorter retention time as the reaction proceeds. As shown in Table 4.12, the amount of increase in the M_p 3 values of the samples taken by two hour intervals suggest that a random coupling in taking place. This would imply that PIB and PS units do not react solely among themselves but with each other as well, forming a heterogeneous chain extension (Figure 4.69). Within 48 h, the M_p value reaches to 35639 and the final M_n is recorded as 13811 (Table 4.12).

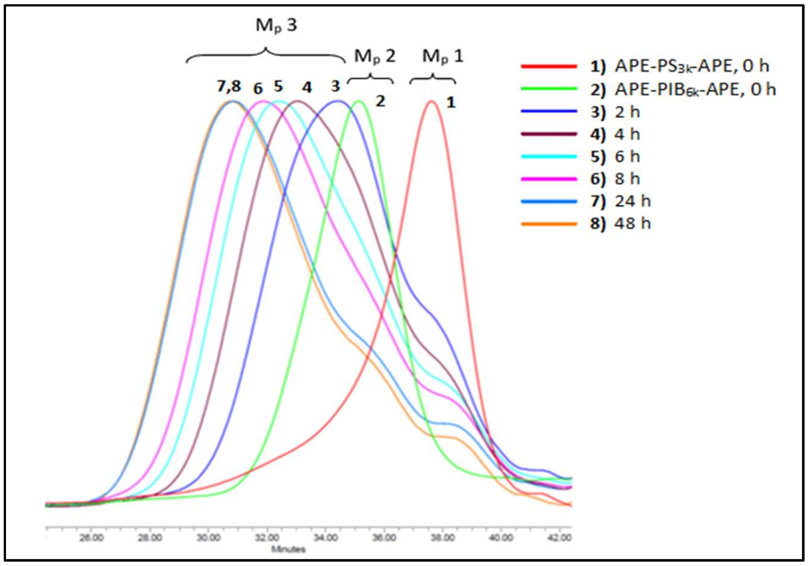

Figure 4.70. SEC RI data of photocycloaddition reaction of APE-PS$_{3k}$-APE and APE-PIB$_{6k}$-APE: APE-PS$_{3k}$-APE before irradiation (1), APE-PIB$_{6k}$-APE before irradiation (2), mixture irradiated at 365 nm for 2 h (3), at 365 nm for 4 h (4), at 365 nm for 6 h (5), at 365 nm for 8 h (6), at 365 nm for 24 h (7), at 365 nm for 48 h (8).

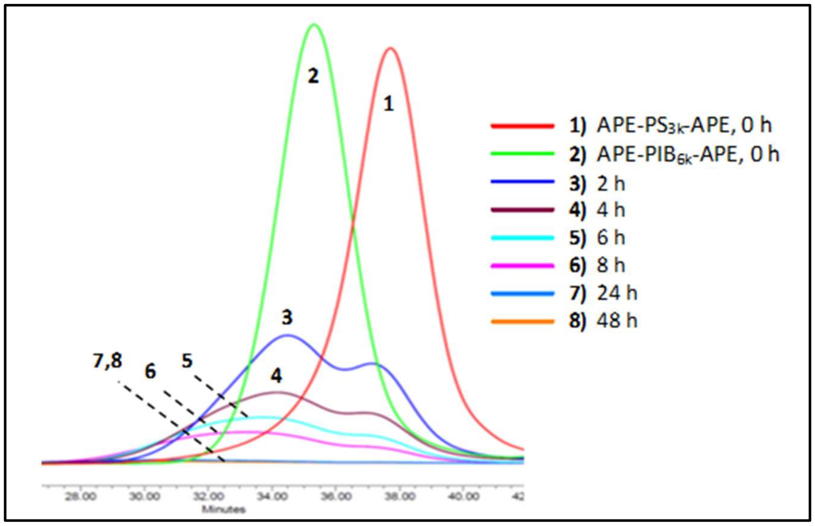

Figure 4.71. SEC UV data of photocycloaddition reaction of APE-PS$_{3k}$-APE and APE-PIB$_{6k}$-APE: APE-PS$_{3k}$-APE before irradiation (1), APE-PIB$_{6k}$-APE before irradiation (2), mixture irradiated at 365 nm for 2 h (3), at 365 nm for 4 h (4), at 365 nm for 6 h (5), at 365 nm for 8 h (6), at 365 nm for 24 h (7), at 365 nm for 48 h (8).

The reaction does not proceed beyond 48 h, the corresponding UV absorbance peaks diminish (Figure 4.71), which suggests that formation of cyclic products are also possible to an extent. The small amount of original polymers left may have formed cyclic products as well; the shift of APE-PS$_{3k}$-APE peak, denoted as M_p 3, to longer retention time can be observed in particular at 24 h and 48 h irradiations (Figure 4.70, Line 7-8), (Table 4.12).

Table 4.12. SEC data of photocycloaddition reaction of APE-PS$_{3k}$-APE and APE-PIB$_{6k}$-APE depicted in Figure 4.70.

	365 nm irradiation time	M_n Final	M_p Max	M_p Initial	M_n Initial
Line 1	0 h	APE-PS$_{3k}$-APE		2994	3223
Line 2	0 h	APE-PIB$_{6k}$-APE		7456	6893
Line 3	2 h	7116	10842		
Line 4	4 h	8651	16933		
Line 5	6 h	10015	20806		
Line 6	8 h	10892	24472	M_p Final (APE-PS$_{3k}$-APE)	
Line 7	24 h	13638	34294	2720	
Line 8	48 h	13811	35639	2666	

Next, the final product of the photocycloaddition experiment (48 h sample) was subjected to UV irradiation at 254 nm (Figure 4.72). For the first sample ([P]: $2\mathrm{x}10^{-4}$ M) irradiation at 254 nm was performed for 24 h, with light intensity of 5.5 mW/cm^2 (Figure 4.72, Line 4). SEC RI data shows the shift to higher retention time, which indicates that the polymer chains are undergoing photoscission. Then, for the second sample the intensity of light is increased to 11 mW/cm^2 and the sample is further diluted to enable mobility ([P]: 10^{-4} M). SEC RI data displays a further shift in the retention time towards low molecular weight region, which implies that these conditions enable the photoscission to proceed further (Figure 4.72, Line 5), (Table 4.13).

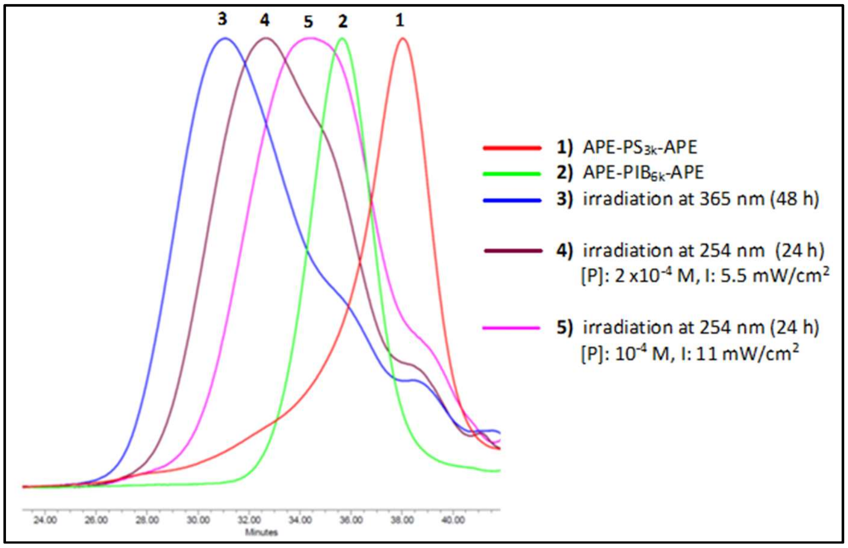

Figure 4.72. SEC data of photoscission reaction of photocoupled APE-PS$_{3k}$-APE and APE-PIB$_{6k}$-APE recorded by RI detector; APE-PS$_{3k}$-APE before irradiation (1), APE-PIB$_{6k}$-APE before irradiation (2) mixture irradiated at 365 nm for 48 h (3), followed by irradiation at 254 nm for 24 h with different precursor polymer concentrations and light intensities: [P]: 2 x10^{-4} M, I: 5.5 mW/cm^2 (4), [P]: 10^{-4} M, I: 11 mW/cm^2 (5).

Table 4.13. SEC RI data of photoscission reaction of photocoupled APE-PS$_{3k}$-APE and APE-PIB$_{6k}$-APE depicted in Figure 4.72.

				M_n Initial	M_p Initial
Line 1	APE-PS$_{3k}$-APE			2994	3223
Line 2	APE-PIB$_{6k}$-APE			7456	6893
		[P] (M)	I (mW/cm^2)	M_n Final	M_p Max
Line 3	365 nm	-	-	13811	35639
Line 4	254 nm	2 x10^{-4}	5.5	9839	19288
Line 5		10^{-4}	11	6413	11002

For both APE-PS$_{3k}$-APE and APE-PIB$_{6k}$-APE, the optimum time for 254 nm irradiation had been designated as 6 h, as discussed in the previous chapters. On the other hand, the irradiation of the mixture was continued for a total 24 h to allow the photoscission to proceed as much as possible. Sampling at different time intervals was performed on a separate experiment, with dilute conditions ([P]: 10^{-4} M) and high light intensity (I: 11 mW/cm^2), in order to compare the efficiency of photoscission at 254 nm. SEC UV data in Figure 4.73 demonstrates that the absorbance value increases with irradiation time due to the regeneration of anthryl moieties via photocleavage under 254 nm UV light. The increase in UV absorbance does not diminish after 6 h but continues up to 24 h of irradiation. When compared to the absorbance values of the nonirradiated initial polymers (Figure 4.73, Line 1-2) and the following decrease to minimum via irradiation at 365 nm (Figure 4.73, Line 3), the sample irradiated at 254 nm exhibits a 34.8 % recovery of anthryl units at 6 h (Figure 4.73, Line 6) and 40.3 % at 24 h (Figure 4.73, Line 7). Up to 3 h of irradiation, the majority of the freed anthryl units belong to photoscissioned APE-PIB$_{6k}$-APE chains, due to the initial increase in absorbance in the corresponding region

(Figure 4.73, Line 2). When irradiation is continued up to 6 h and 24 h, a small increase in absorbance arising from photoscissioned APE-PS$_{3k}$-APE chains can be observed as well under the corresponding region (Figure 4.73, Line 1). Therefore; it is concluded that the overall photoscission process is more efficient when the irradiation time is increased to 24 h.

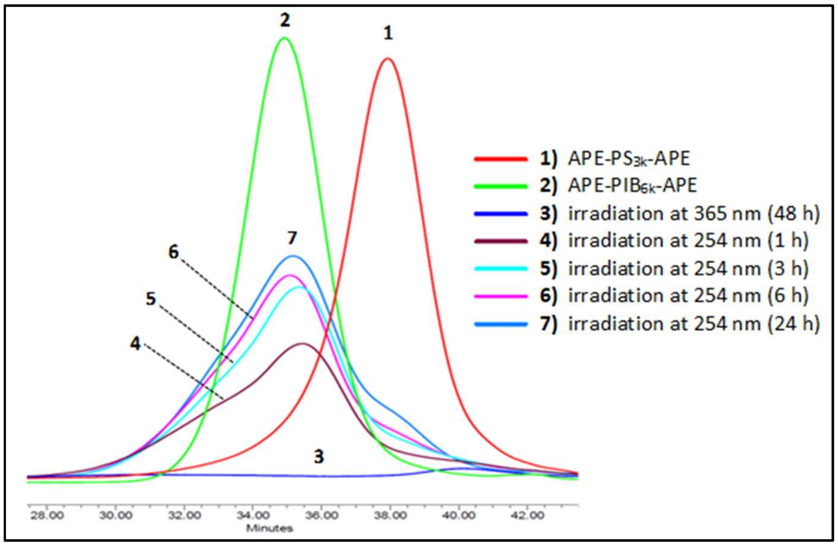

Figure 4.73. SEC data of photocycloaddition reaction of APE-PS$_{3k}$-APE and APE-PIB$_{6k}$-APE recorded by UV absorbance detector: APE-PS$_{3k}$-APE before irradiation (1), APE-PIB$_{6k}$-APE before irradiation (2), mixture irradiated at 365 nm for 48 h (3), followed by irradiation at 254 nm for 1 h (4), irradiation at 254 nm for 3 h (5), irradiation at 254 nm for 6 h (6), irradiation at 254 nm for 24 h (7).

Next, the 6 h and 24 h products of the photoscission experiments were subjected to 365 nm irradiation once again. Table 4.14 shows the specification of these samples and the obtained SEC RI data upon the second 365 nm irradiations. Both samples exhibit an increase in the M_n and M_p values (M_n Final and M_p Max, respectively) after being treated with 365 nm light for 24 h. These data demonstrate that both samples are viable and able to participate in further photocoupling reaction. This progress is up to a lesser extent with respect to the first 365 nm irradiation, which could be expected due to the possible loss of anthryl functionalities during the successive irradiations via side reactions. Nevertheless, the increase in molecular weight is evident for both samples as shown in Figure 4.74 and Figure 4.75 in terms of shift to shorter retention time and also depicted in Table 4.14.

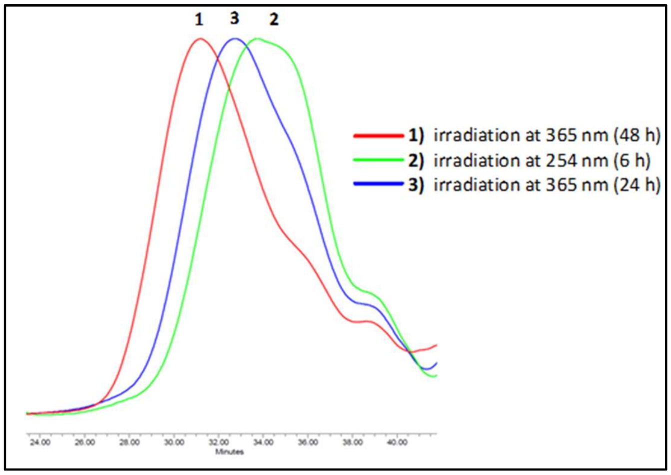

Figure 4.74. SEC RI data of photocycloaddition and photoscission reactions of APE-PS$_{3k}$-APE and APE-PIB$_{6k}$-APE mixture: irradiated at 365 nm for 48 h (1), followed by irradiation at 254 nm for 6 h (2), followed by irradiation at 365 nm for 24 h (3).

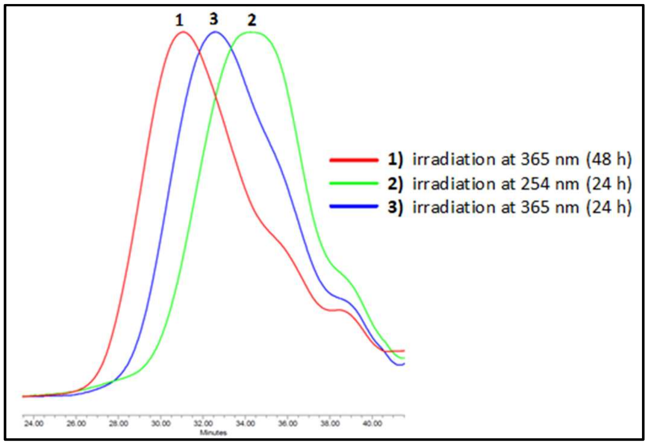

Figure 4.75. SEC RI data of photocycloaddition and photoscission reactions of APE-PS$_{3k}$-APE and APE-PIB$_{6k}$-APE mixture: irradiated at 365 nm for 48 h (1), followed by irradiation at 254 nm for 24 h (2), followed by irradiation at 365 nm for 24 h (3).

Table 4.14. SEC data of photoscission reaction of photocoupled APE-PS$_{3k}$-APE and APE-PIB$_{6k}$-APE mixture.

	[P] (M)	I (mW/cm^2)	Irradiation time	M_{n1} Final	M_{p1} Max		M_{n2} Final	M_{p2} Max
365 nm			48 h	13811	35639			
254 nm	10^{-4}	11	6 h	7567	12398	2nd 365 nm	9347	20664
	10^{-4}	11	24 h	6413	11002		8607	19766

Then this sample was subjected to a second irradiation at 254 nm in order to examine the revival of anthryl units. Samples taken at 1, 2 and 3 hours showed an increase in the UV absorbance at 365 nm (Figure 4.76); indicating that the photocoupled anthracenes are once again undergoing photoscission and being recovered. At 4 h the absorbance value starts to decrease.

Corresponding SEC RI data also shows a shift to longer retention as a result of the photoscissioned chains (Figure 4.77, Line 6). Once again it is observed the second 254 nm irradiation is not as efficient as the initial one, due to the loss of active anthryl units during the prolonged irradiations via aforementioned side reactions. The sample re-irradiated at 254 nm for 3 h exhibited a 14 % recovery of anthryl units. The overall changes in the M_n and M_p values of the polymer samples recorded by SEC RI detector are given in Table 4.15.

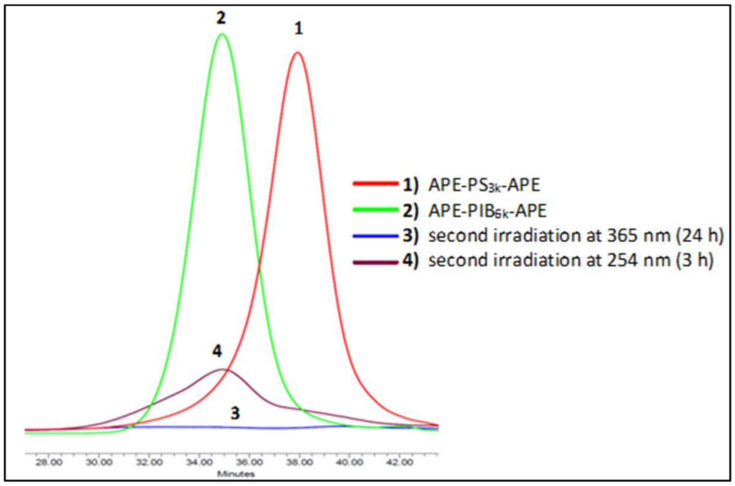

Figure 4.76. Absorbance of APE-PS$_{3k}$-APE and APE-PIB$_{6k}$-APE mixture at 365 nm recorded by SEC UV detector; APE-PS$_{3k}$-APE before irradiation (1), APE-PIB$_{6k}$-APE before irradiation (2), after second irradiation at 365 nm for 24 h (3), followed by second irradiation at 254 nm for 3 h (4).

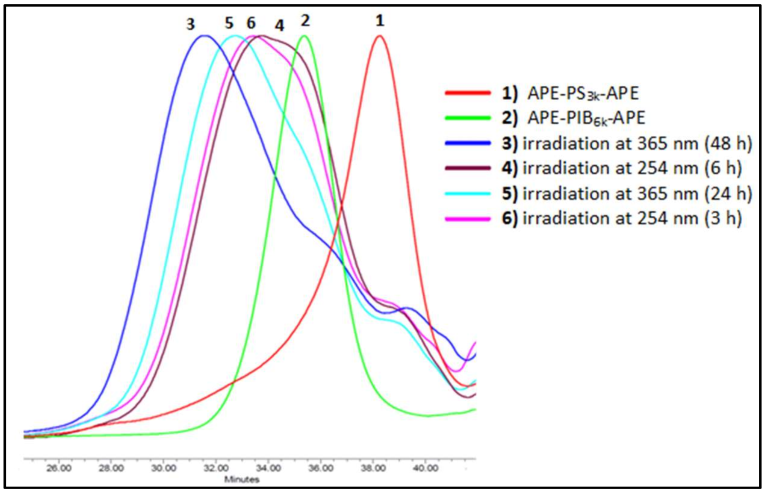

Figure 4.77. SEC RI data of photoscission reaction of photocoupled APE-PS$_{3k}$-APE and APE-PIB$_{6k}$-APE; APE-PS$_{3k}$-APE before irradiation (1), APE-PIB$_{6k}$-APE before irradiation (2) mixture irradiated at 365 nm for 48 h (3), after irradiation at 254 nm for 6 h (4), after second irradiation at 365 nm for 24 h (5), after second irradiation at 254 nm for 3 h (6).

Table 4.15. SEC RI data of APE-PS$_{3k}$-APE and APE-PIB$_{6k}$-APE before and after irradiation reactions depicted in Figure 4.77.

		M_n	M_p Max
Line 1	APE-PS$_{3k}$-APE	3223	2994
Line 2	APE-PIB$_{6k}$-APE	6893	7456
Line 3	365 nm (48 h)	13811	35639
Line 4	254 nm (6 h)	7567	12398
Line 5	365 nm (24 h)	9347	20664
Line 6	254 nm (3 h)	8620	16008

4.5.5.1. APE-PS$_{3k}$-APE and APE-PIB$_{18k}$-APE. APE-PS$_{3k}$-APE and APE-PIB$_{18k}$-APE mixture in THF with concentration [P]: 6.4 x 10^{-3} M was prepared and subjected to UV irradiation at 365 nm for 24 h (Figure 4.78). At first glance the SEC RI data closely resembles that of photocoupled APE-PIB$_{18k}$-APE. However, upon closer inspection it can be observed that the peaks with M_p: 23516 and M_p: 39816 have both shifted to shorter retention time with respect to APE-PIB$_{18k}$-APE (M_p: 20288) and APE-PIB$_{18k}$-APE dimer at 24 h irradiation (M_p: 34157), (Table 4.16). Figure 4.79 also depicts the comparison of the aforementioned SEC RI chromatograms. These data suggest that PS and PIB chains are reacting with each other to form heterogeneous photocoupled chains, but the chain extension is occurring to a lesser degree with respect the lower molecular weight APE-PIB$_{6k}$-APE + APE-PS$_{3k}$-APE mixture. This would also suggest that the anthryl moieties remain embedded in polymer matrix especially in the higher molecular weight samples [27]. Overall, the chain extension proceeds as a molecular weight dependent process.

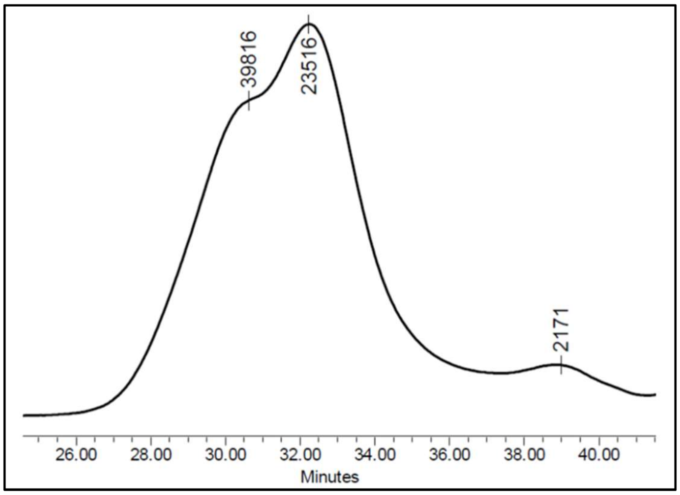

Figure 4.78. SEC data of photocycloaddition reaction of APE-PS$_{3k}$-APE and APE-PIB$_{18k}$-APE recorded by RI detector after irradiation at 365 nm for 24 h.

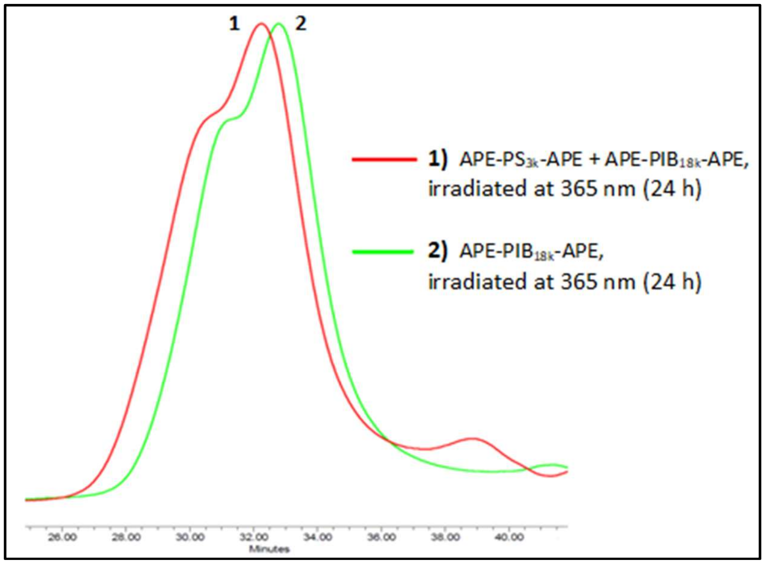

Figure 4.79. SEC RI data of photocycloaddition reactions: APE-PS$_{3k}$-APE and APE-PIB$_{18k}$-APE mixture irradiated at 365 nm for 24 h (1), APE-PIB$_{18k}$-APE irradiated at 365 nm for 24 h (2).

Table 4.16. SEC RI data of APE-PS$_{3k}$-APE and APE-PIB$_{18k}$-APE before and after photocycloaddition reactions.

	M_n	M_p Max
APE-PS$_{3k}$-APE	3223	2994
APE-PIB$_{18k}$-APE	18005	20288
APE-PIB$_{18k}$-APE (365 nm, 24 h)	21276	34157
APE-PS$_{3k}$-APE + APE-PIB$_{18k}$-APE (365 nm, 24 h)	20490	39186

4.5.5.3. APE-PS$_{15k}$-APE and APE-PIB$_{6k}$-APE. APE-PS$_{15k}$-APE and APE-PIB$_{6k}$-APE mixture in THF with concentration [P]: 6.4 x 10^{-3} M was prepared and subjected to UV irradiation at 365 nm for 24 h (Figure 4.80). This mixture yields a product with higher M_p max value than the previous cases. The irradiation of APE-PS$_{15k}$-APE solely had led to an M_p max value of 56304 upon 8 h treatment.

In this case the increased molecular weight (Table 4.17) suggests that the di-anthryl telechelic PIB and PS chains are undergoing photocycloaddition reaction with each other that results in heterogeneous chain extension.

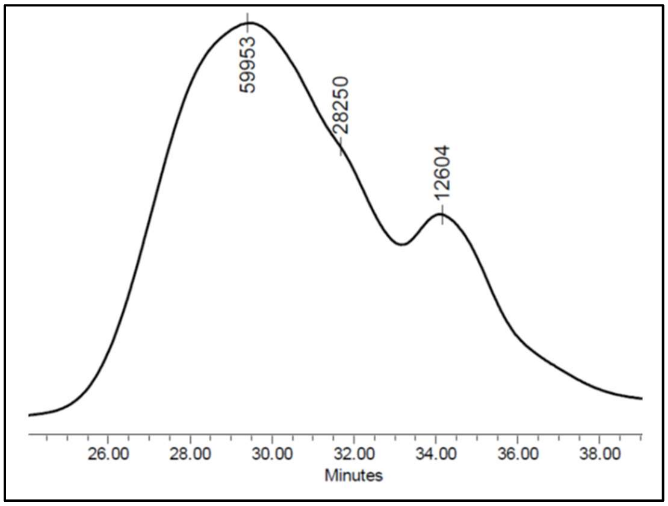

Figure 4.80. SEC data of photocycloaddition reaction of APE-PS$_{15k}$-APE and APE-PIB$_{6k}$-APE recorded by RI detector after irradiation at 365 nm for 24 h.

Table 4.17. SEC RI data of APE-PS$_{15k}$-APE and APE-PIB$_{6k}$-APE before and after photocycloaddition reactions.

	M_n	M_p Max
APE-PS$_{15k}$-APE	15755	14106
APE-PIB$_{6k}$-APE	6893	7456
APE-PS$_{15k}$-APE + APE-PIB$_{6k}$-APE (365 nm, 24 h)	26100	59953

4.5.5.4. APE-PS$_{15k}$-APE and APE-PIB$_{18k}$-APE. APE-PS$_{15k}$-APE and APE-PIB$_{18k}$-APE mixture in THF with concentration [P]: 4.4 x 10^{-3} M was prepared and subjected to UV irradiation at 365 nm for 24 h (Figure 4.81). Once again an increase in the overall M_p value is observed with a final value of 52900 (Table 4.18).

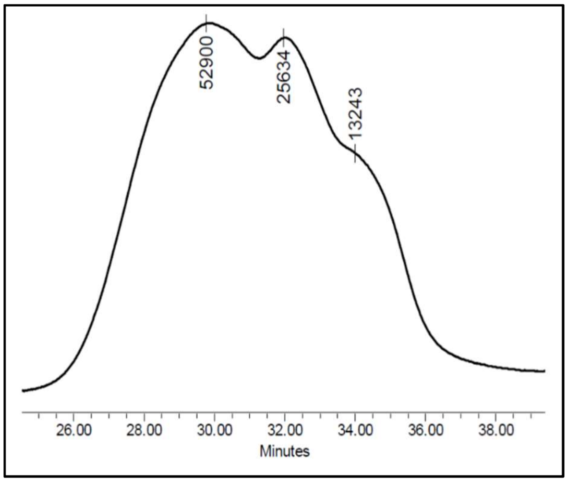

Figure 4.81. SEC data of photocycloaddition reaction of APE-PS$_{15k}$-APE and APE-PIB$_{18k}$-APE recorded by RI detector after irradiation at 365 nm for 24 h.

Table 4.18. SEC RI data of APE-PS$_{15k}$-APE and APE-PIB$_{18k}$-APE before and after photocycloaddition reactions.

	M_n	M_p Max
APE-PS$_{15k}$-APE	15755	14106
APE-PIB$_{18k}$-APE	18005	20288
APE-PS$_{15k}$-APE + APE-PIB$_{18k}$-APE (365 nm, 24 h)	26425	52900

4.5.6. Photocycloaddition Reaction of Anthryl Telechelic Polystyrene with diAnthryl Telechelic Polystyrene and Polyisobutylene

The experiment was conducted in order to examine the coupling of PS_{4k}-APE units with a previously prepared PIB-PS chain extended product. Initially, APE-PS_{3k}-APE and APE-PIB_{6k}-APE mixture in THF with was prepared and subjected to UV irradiation at 365 nm. The irradiation was limited to 8 h and not extended to 24 h for this experiment. This was done to ensure that anthryl moieties at the chain ends of the extended PIB-PS polymer were still viable and able to undergo further photocycloaddition reaction with a second addition of anthryl telechelic PS. After 8 h of irradiation, PS_{4k}-APE in THF was introduced into the vial under N_2 flow and irradiated for a further 16 h ([P]: 7 x 10^{-3} M). PS_{4k}-APE amount was calculated in excess with respect to the chain ends of PIB-PS polymer.

At the end of a total 24 h irradiation at 365 nm, SEC RI data displays unreacted PS_{4k}-APE (M_p: 4441), a larger amount of PS_{4k}-APE dimer formed via homogeneous photocycloaddition (M_p: 8859) and the extended PIB-PS heterogeneous chain (M_p: 22891) (Figure 4.82). In order to perform better characterization on the sample, the large amount of PS_{4k}-APE related compound should be removed from the final product.

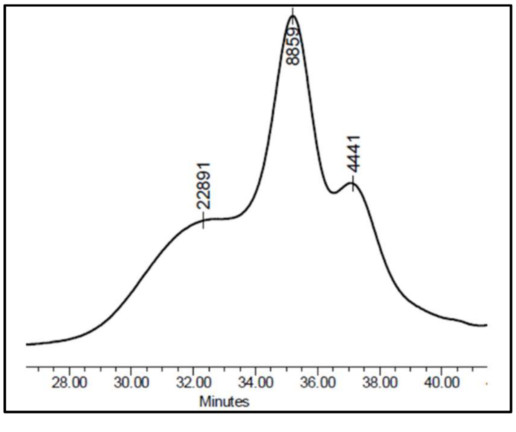

Figure 4.82. SEC RI data of photocycloaddition reaction of [APE-PS_{3k}-APE + APE-PIB_{6k}-APE] and PS_{4k}-APE.

The mixture in THF was precipitated into acetone; which would dissolve the excess polystyrene products. The precipitate could not be obtained by decantation due to colloidal suspension of the polymer in solution. The mixture was then centrifuged with 4000 rpm for 1 h; thus the non-solvent acetone could be separated from the polymers stuck on the flask. Examination of this film-like polymer by SEC analysis showed that PS_{4k}-APE and dimers were successfully removed. Evaporation of acetone in rotary evaporator yielded the polymeric residue of these polystyrenes. Figure 4.83 shows the comparison of SEC RI data of APE-PS_{3k}-APE and APE-PIB_{6k}-APE mixture irradiated for 8 h, and the final purified product after PS_{4k}-APE addition. The shift of final product to short retention time can be observed, the final M_p increased to 24552 from the initial value of 20442 (Table 4.19). This indicates that the extended PIB-PS polymer underwent further photocycloaddition reaction; either with remaining APE-PS_{3k}-APE or the newly added PS_{4k}-APE. SEC RI data shows that the unreacted APE-PS_{3k}-APE units in the 8 h irradiation product were removed from the final product. This might be due to further addition to the extended PIB-PS chains, or due to removal by acetone. In any case; the unreacted and homogeneously chain extended PS units are removed from the final compound and the PIB-PS chains are extended further with the addition of PS units essentially.

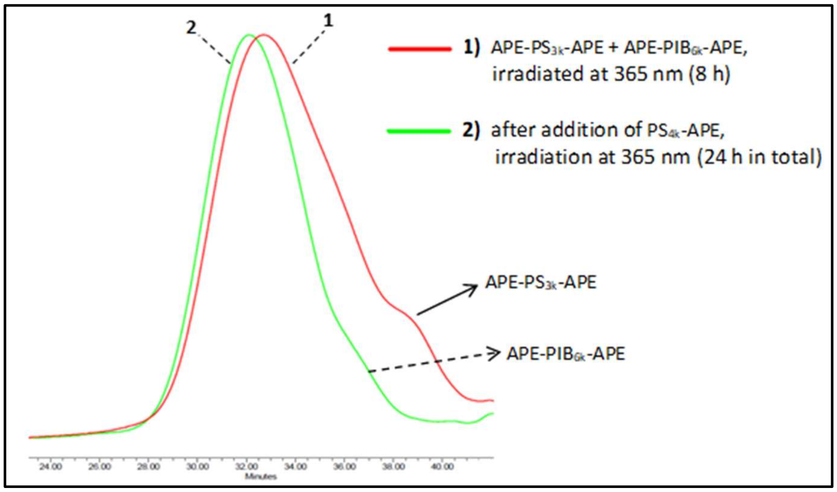

Figure 4.83. SEC RI data of photocycloaddition reactions: APE-PS_{3k}-APE and APE-PIB_{18k}-APE mixture irradiated at 365 nm for 8 h (1), after addition of PS_{4k}-APE with further irradiated at 365 nm to 24 h (2).

Table 4.19. SEC RI data of Photocycloaddition Reaction of Anthryl Telechelic Polystyrene with di-Anthryl Telechelic Polystyrene and Polyisobutylene

	M_n	M_p Max
PS_{4k}-APE	4054	4335
APE-PS_{3k}-APE + APE-PIB_{6k}-APE	9257	20442
[APE-PS_{3k}-APE + APE-PIB_{6k}-APE] + PS_{4k}-APE	16902	24552

4.5.7. Thermal and Mechanical Analysis of Polymer Films

The products obtained by 365 nm irradiations of APE-PS-APE and APE-PIB-APE mixtures were dissolved in small amount of THF, poured into Teflon molds and dried in room temperature and vacuum oven. Examination of the polymer films showed that the two products containing the higher molecular weight APE-PS_{15k}-APE were quite brittle and could not be removed from the mold without breakage (Figure 4.84b and Figure 4.84c). The product [APE-PS_{3k}-APE + APE-PIB_{18k}-APE] displayed stickiness due to the high molecular weight PIB domain and could not be removed wholly from the mold either (Figure 4.84a). However, APE-PIB-APE itself is a honey-like viscous material that can not be molded properly. In spite of the stickiness, the product [APE-PS_{3k}-APE + APE-PIB_{18k}-APE] is a completely different material than pure APE-PIB-APE sample. On the other hand, [APE-PS_{3k}-APE + APE-PIB_{6k}-APE] and [APE-PS_{3k}-APE + APE-PIB_{6k}-APE + PS_{4k}-APE] yielded films with elastic properties (Figure 4.85) most probably due to lower molecular weight of PIB causing higher contribution of rigid PS in the mixture.

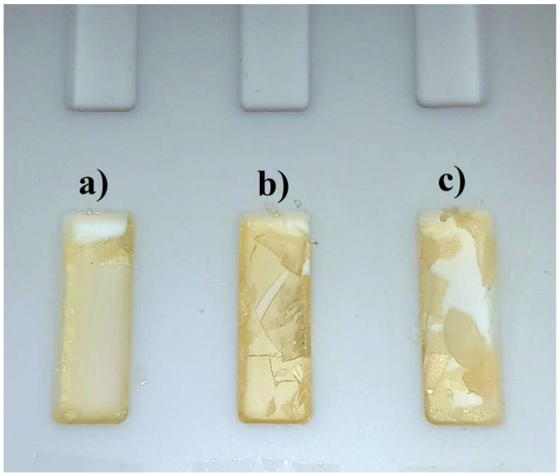

Figure 4.84. a) [APE-PS$_{3k}$-APE + APE-PIB$_{18k}$-APE], b) [APE-PS$_{15k}$-APE + APE-PIB$_{6k}$-APE], c) [APE-PS$_{15k}$-APE + APE-PIB$_{18k}$-APE].

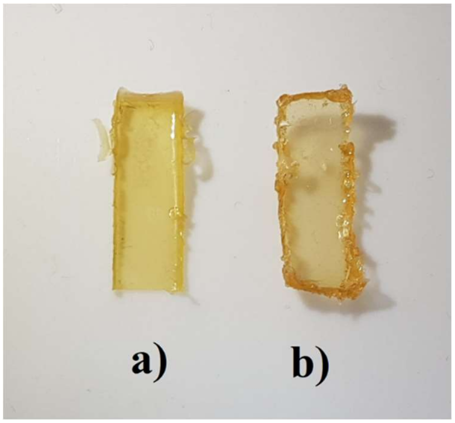

Figure 4.85. a) [APE-PS$_{3k}$-APE + APE-PIB$_{6k}$-APE], b) [APE-PS$_{3k}$-APE + APE-PIB$_{6k}$-APE + PS$_{4k}$-APE].

The tensile properties of [APE-PS$_{3k}$-APE + APE-PIB$_{6k}$-APE] and [APE-PS$_{3k}$-APE + APE-PIB$_{6k}$-APE + PS$_{4k}$-APE] were examined (Figure 4.86). [APE-PS$_{3k}$-APE + APE-PIB$_{6k}$-APE] displays typical weak rubbery behavior, with 115 % elongation at break. The material is quite soft and weak with ultimate tensile strength of 0.42 MPa and exhibits low modulus (0.85 MPa) and toughness values (11.7 Nmm); which could be expected due to higher amount of PIB domain. The mechanical response of [APE-PS$_{3k}$-APE + APE-PIB$_{6k}$-APE + PS$_{4k}$-APE], on the other hand, is quite different than the first sample; with higher modulus value (30 MPa) and high toughness (23.6 Nmm). An initial steep increase in modulus occurs due to the presence of additional rigid PS domains, followed by rubber-like deformation with characteristic high elongation. This states that after the addition of PS_{4k}-APE into the [APE-PS_{3k}-APE + APE-PIB_{6k}-APE] sample, further chain extension occurs by the addition of anthryl telechelic PS to the PIB-PS heteropolymer via photocycloaddition reaction. This results in the decrease of the amount of dangling PIB chain ends, which improves the tensile strength of the product; with ultimate tensile strength value of 1.95 MPa. The sample displays plastic behavior in terms of an earlier breakage at 63 % elongation. Overall, these data show that the secondary addition of PS domain to PIB-PS multiblock copolymer decreases the dangling chain end content. However, significant mechanical improvement can not be obtained which could be expected since the product is a multiblock copolymer rather than a PS-PIB-PS thermoplastic elastomer. The relatively low molecular weight domains of the sample also induce low phase segregation [121] and the film displays a multiphase system behavior.

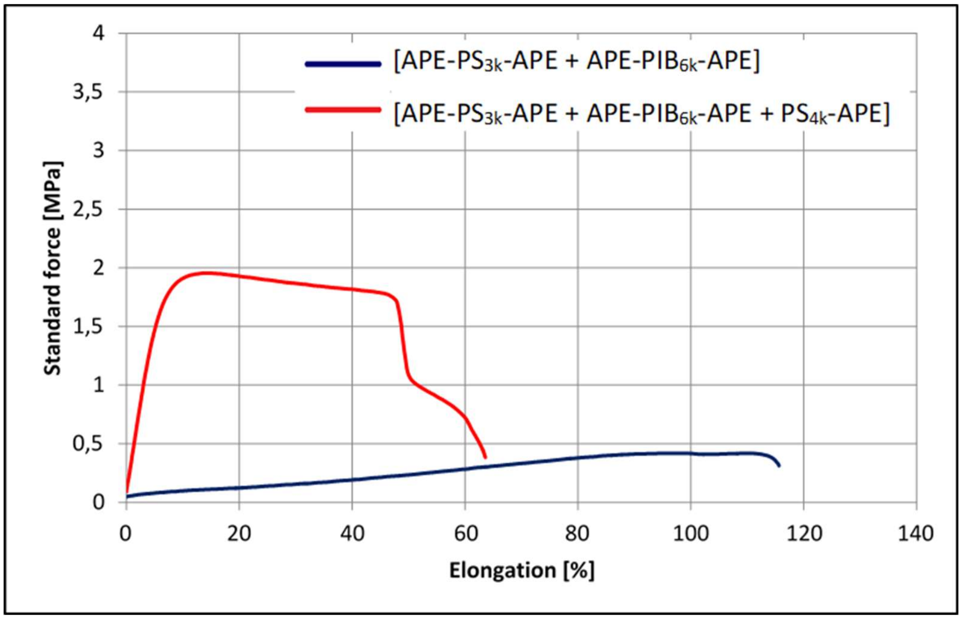

Figure 4.86. Stress-strain traces of [APE-PS_{3k}-APE + APE-PIB_{6k}-APE] and [APE-PS_{3k}-APE + APE-PIB_{6k}-APE + PS_{4k}-APE].

Thermal gravimetric analysis (TGA) of [APE-PS-APE + APE-PIB-APE + PS_{4k}-APE] mixture product and the four [APE-PS-APE + APE-PIB-APE] mixture products were performed (Figure 4.87). Thermogram shows that the PS and PIB segments display thermal degradation together in all samples; as another proof of multiblock character of the resultant product inhibiting phase segregation due to the low molecular weight domains. A small initial loss in weight is observed between 100-200 °C which is estimated to be due to solvent trapped particularly in PIB domains. The major decomposition starts around 300 °C; reaching a maximum rate around 410 °C. All samples exhibit high thermal stability, mainly due to the presence of PIB segments in the mixture chain extension products, as PIB displays thermal decomposition at *ca.* 330-350 [122].

The DSC analysis of [APE-PS-APE + APE-PIB-APE + PS_{4k}-APE] mixture product and the four [APE-PS-APE + APE-PIB-APE] mixture products were performed (Figure 4.88). An initial trial run was done on separate samples up to 250 °C and it was observed that major decompositions and dissociations took place after 150 °C. Therefore in the analysis the first run was done up to 105 °C; in order to avoid the thermal dissociation of anthryl dimer structures and chain scission of the polymers, which could occur at a temperature range of 110-180 °C [11]. The second run of the analysis showed relaxations at *ca.* -68 °C to -64 °C arising from the soft PIB domains in the multiblock copolymers. When [APE-PS_{3k}-APE + APE-PIB_{6k}-APE + PS_{4k}-APE] is compared with [APE-PS_{3k}-APE + APE-PIB_{6k}-APE], it can be observed that the addition of PS segments at the chain ends induce a 2 °C increase in the relaxations, to -62 °C. The two samples with larger PS domains (APE-PS_{15k}-APE) exhibit endothermic heat flow at *ca.* 63 °C and 67 °C. As polystyrene generally exhibits Tg at 100 °C [123]; these data might suggest that the PIB domains in the copolymer structure induce a lowering of the Tg of PS domains. The other samples do not show such a transition; the relatively low molecular weight PS domains of the samples induce low phase segregation and the PIB and PS phases flow together. Mechanical analysis results are in accord with these DSC data.

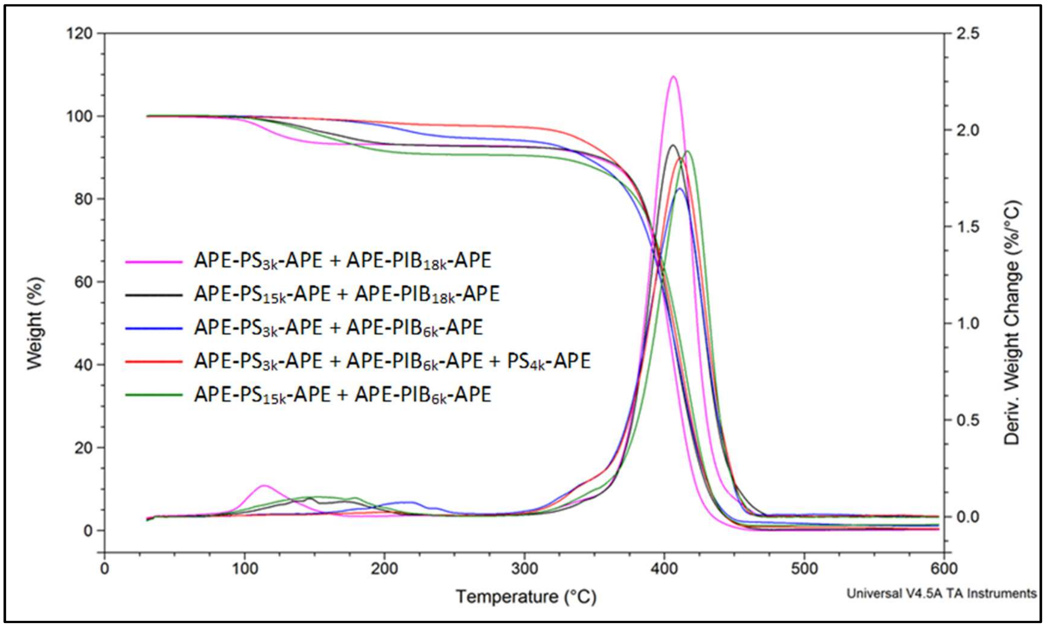

Figure 4.87. TGA thermograms of [APE-PS-APE + APE-PIB-APE] photocycloaddition reaction products.

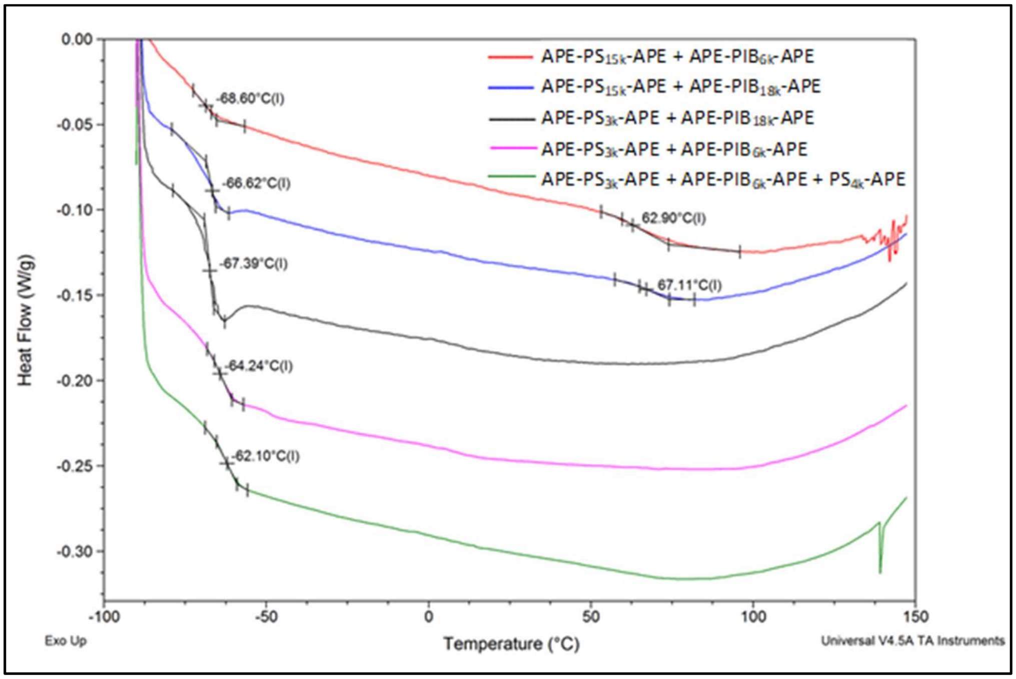

Figure 4.88. DSC traces of [APE-PS-APE + APE-PIB-APE] photocycloaddition reaction products, obtained in the second run of analysis.

5. CONCLUSION

In this project, anthryl telechelic and di-telechelic polymers were synthesized by the utilization of 1-(2-anthryl)-l-phenylethylene (APE), in order to study the reversible photocycloaddition reactions of the anthryl moieties. For this purpose, the three step synthesis and purification of APE was done successfully. The synthesis of novel 1-(2-anthryl)-1-phenylethylene di-telechelic polyisobutylenes were done by the utilization of a difunctional cationic initiator and the in situ addition of the non-homopolymerizable APE monomer to the chain ends. Mono and di-anthryl telechelic polystyrenes and anthryl telechelic poly(methyl methacrylate)s were also synthesized via living anionic polymerization by the incorporation of APE at initiation step or at chain end. Products were characterized by ^{1}H NMR spectroscopy and Size Exclusion Chromatography (SEC).

The APE functionalized polymers were subjected to UV irradiation at 365 nm to study the reversible [$4\pi+4\pi$] photocycloaddition of the anthryl units; and at 254 nm to examine the photoscission process. Irradiations at 365 nm were conducted to obtain chain extension of anthryl and di-anthryl telechelic polymers; initially for homopolymer solutions and then for polymer mixtures. The chain extension of di-anthryl telechelic PIBs through photocoupling at 365 nm produced higher molecular weight products from low molecular weight precursors. The effect of precursor polymer concentration on the degree of chain extension was investigated, and the formation of tetramers was observed in concentrated conditions. Intramolecular interactions leading to formation of cyclic products was also observed in some extent during the chain extension process, especially in the low concentration conditions. The photocoupled products were UV irradiated at 254 nm, which yielded partial reversal of photocycloaddition process; converting anthryl dimers to original structure and consequently cause photoscission of polymers. Mixtures of di-anthryl telechelic polyisobutylenes and polystyrenes were irradiated at 365 nm, cast into films and their thermal and mechanical properties were investigated. Thermal gravimetric analysis data showed high thermal stability for the samples. Mechanical testing and differential scanning calorimetry analysis displayed low phase segregation and multiblock system behavior.

REFERENCES

1. Van Damme, J. and F. Du Prez, “Anthracene-containing polymers towards high-end applications”, *Progress in Polymer Science*, https://doi.org/10.1016/ j.progpolymsci.2018.02.002, 2018.

2. Cardenas-Daw, C., A. Kroeger, W., Schaertl, P. Froimowicz and K. Landfester, “Reversible Photocycloadditions, a Powerful Tool for Tailoring (Nano)Materials”, *Macromolecular Chemistry and Physics,* Vol. 213, pp. 144-156, 2012.

3. Fritzsche J., “Uber die festen Kohlenwasserstoffe des Steinkohlentheers”, *Bulletin de l'Academie Imperiale des Sciences de Saint-Pétersbourg*, Vol. 9, pp. 406-419, 1866.

4. Becker, H. D., “Unimolecular Photochemistry of Anthracenes” *Chemical Reviews*, Vol. 93, pp. 145-172, 1993.

5. Bouas-Laurent, H., A. Castellan, J. P. Desvergne and R. Lapouyade, “Photodimerization of anthracenes in fluid solution: structural aspects”, *Chemical Society Reviews*, Vol. 29, pp. 43-55, 2000.

6. Bouas-Laurent, H., A. Castellan, J. P. Desvergne and R. Lapouyade, “Photodimerization of anthracenes in fluid solutions: (part 2) mechanistic aspects of the photocycloaddition and of the photochemical and thermal cleavage”, *Chemical Society Reviews*, Vol. 30, pp. 248-263, 2001.

7. Bratschkov, C., P. Karpuzova, K. Müllen, M. Klapper and I. Schopov, “Synthesis and photochemical transformations of an anthracene containing methacrylic copolymer”, *Polymer Bulletin*, Vol. 46, 345-349, 2001.

8. Radl, S. V., M. Roth, M. Gassner, A. Wolfberger, A. Lang, B. Hirschmann, G. Trimmel, W. Kern and T. Griesser,” Photo-induced crosslinking and thermal de-crosslinking in polynorbornenes bearing pendant anthracene groups”, *European Polymer Journal,* Vol. 52, pp. 98-104, 2014.

9. Bratschkov, C., “FTIR spectroscopy study of the UV irradiation induced changes in an anthracene containing copolymer”, *European Polymer Journal*, Vol. 37, 1145-1149, 2001.

10. Aubrey, J. M., C. Pierlot, J. Rigaudy and R. Schmidt, “Reversible Binding of Oxygen to Aromatic Compounds”, *Accounts of Chemical Research*, Vol. 36, pp. 668-675, 2003.

11. Van Damme, J., L. Vlaminck, G. Van Assche, B. Van Mele, O. Van Den Berg and F. Du Prez, “Synthesis and evaluation of 9-substituted anthracenes with potential in reversible polymer systems”, *Tetrahedron*, Vol. 72, pp. 4303-4311, 2016.

12. Fox, M. A. and M. D. Wooten, “Characterization, Adsorption, and Photochemistry of Self-Assembled Monolayers of 10-Thiodecyl 2-Anthryl Ether on Gold”, *Langmuir*, Vol. 13, pp. 7099-7105, 1997.

13. Jones, J. R., C. L. Liotta, D. M. Collard and D. A. Shiraldi, “Photochemical cross-linking of poly(ethylene terephthalate-co-2,6-anthracenedicarboxylate)”, *Macromolecules*, Vol. 33, pp. 1640-1645, 2000.

14. Trinh, X. A., J. Fukuda, Y. Adachi, H. Nakanishi, T. Norisuye and Q. Tran-Cong-Miyata, “Effects of elastic deformation on phase separation of a polymer blend driven by a reversible photo-cross-linking reaction”, *Macromolecules*, Vol. 40, pp. 5566-5574, 2007.

15. López-Vilanova, L., I. Martínez, T. Corrales and F. Catalina, “Photochemical crosslinking of poly-(ethylene–butyl-acrylate) copolymers functionalized with anthracene moieties by reactive extrusion”, *European Polymer Journal*, Vol. 56, pp. 69-76, 2014.

16. Van Damme, J., O. Van Den Berg, J. Brancart, L. Vlaminck, C. Huyck, G. Van Assche, B. Van Mele and F. Du Prez, “Anthracene-based thiol−ene networks with thermo-degradable and photo-reversible properties”, *Macromolecules*, Vol. 50, pp. 1930-1938, 2017.

17. Matsui, J. Y., Y. Ochi and K. Tamaki, Photodimerization of Anthryl Moieties in a Poly(methacrylic acid) Derivative as Reversible Cross-linking Step in Molecular Imprinting", *Chemistry Letters*, Vol. 38, pp. 80-81, 2006.

18. Zheng, Y., M. Micic, S. V. Mello, M. Mabrouki, F. M. Andreopoulos, V. Konka, S. M. Pham and R. M. Leblanc, "PEG-Based Hydrogel Synthesis via the Photodimerization of Anthracene Groups", *Macromolecules*, Vol. 35, pp. 5228-5234, 2002.

19. Chujo, Y., K. Sada, R. Nomura, A. Naka and T. Saegusa, "Photogelation and redox properties of anthracene-disulfide-modified polyoxazolines", *Macromolecules,* Vol. 26, pp. 5611-5614, 1993.

20. Wells, L. A., S. Furukawa, and H. Sheardown, "Photoresponsive PEG-Anthracene Grafted Hyaluronan as a Controlled-Delivery Biomaterial", *Biomacromolecules,* Vol. 12, pp. 923-932, 2011.

21. Yu, B., X. Jiang and J. Yin, "Responsive fluorescent core-crosslinked polymer particles based on the anthracene-containing hyperbranched poly(ether amine) (hPEA–AN)", *Soft Matter*, Vol. 7, pp. 6853-6862, 2011.

22. Froimowicz, P., H. Frey and K. Landfester, "Towards the Generation of Self-Healing Materials by Means of a Reversible Photo-induced Approach", *Macromolecular Rapid Communications*, Vol. 32, 468-473, 2011.

23. Radl, S., M. Kreimer, T. Griesser, A. Oesterreicher, A. Moser, W. Kern and S. Schlögl, "New strategies towards reversible and mendable epoxy based materials employing [4πs+4πs] photocycloaddition and thermal cycloreversion of pendant anthracene groups", *Polymer*, Vol. 80, pp. 76-87, 2015.

24. Rameshbabu, K., Y. Kim, T. Kwon, J. Yoo and E. Kim, "Facile one-pot synthesis of a photo patternable anthracene polymer", *Tetrahedron Letters,* Vol. 48, pp. 4755-4760, 2007.

25. Connal, L. A., R. Vestberg, C. J. Hawker, and G. G. Qiao, “Fabrication of Reversibly Crosslinkable, 3-Dimensionally Conformal Polymeric Microstructures”, *Advanced Functional Materials*, Vol. 18, pp. 3315-3322, 2008.

26. Manhart, J., S. Ayalur-Karunakaran, S. Radl, A. Oesterreicher, A. Moser, C. Ganser, C. Teichert, G. Pinter, W. Kern, T. Griesser and S. Schlögl, “Design and application of photo-reversible elastomer networks by using the [4πs+4πs] cycloaddition reaction of pendant anthracene groups”, *Polymer*, Vol. 102, pp. 10-20, 2016.

27. Coursan, M., J. P. Desvergne and A. Deffieux, “Reversible photodimerisation of ω-anthrylpolystyrenes”, *Macromolecular Chemistry and Physics*, Vol. 197, pp. 1599-1608, 1996.

28. Ozguc Onal, C. and T. Nugay, “UV induced reversible chain extension of 1-(2-anthryl)-1-phenylethylene functionalized polyisobutylene”, *Designed Monomers and Polymers*, Vol. 20, pp. 514-523, 2017.

29. Goldbach, J. T., T. P. Russell and J. Penelle, “Synthesis and Thin Film Characterization of Poly(styrene-block-methyl methacrylate) Containing an Anthracene Dimer Photocleavable Junction Point”, *Macromolecules*, Vol. 35, pp. 4271-4276, 2002.

30. Ushiki, H., K. Hirayanagi, Y. Sindo, K. Horie and I. Mita, “Molecular-weight dependence of intramolecular end-to-end photodimerization rate of α,ω-dianthryl-polystyrene in dilute solution”, *Polymer Journal*, Vol. 15, pp. 811-819, 1983.

31. Tung, C. H., L. Z. Wu, Z. Y. Yuan and N. Su, “Zeolites as templates for preparation of large-ring compounds: intramolecular photocycloaddition of diaryl compounds”, *Journal of American Chemical Society*, Vol. 120, pp. 11594-11602, 1998.

32. Okada, M. and A. Harada, “Poly(polyrotaxane): photoreactions of 9-anthracene-capped polyrotaxane”, *Macromolecules*, Vol. 36, pp. 9701-9703, 2003.

33. Wang, H., L. Zhang, B. Liu, B. Han, Z. Duan, C. Qi, D. W. Park and I. Kim, "Synthesis of high molecular weight cyclic poly(ε-caprolactone)s of variable ring size based on a light-induced ring-closure approach", *Macromolecular Rapid Communications,* Vol. 36, pp. 1646-1650, 2015.

34. Yamamoto, T., S. Yagyu and Y. Tezuka, "Light- and heat-triggered reversible linear−cyclic topological conversion of telechelic polymers with anthryl end groups", *Journal of American Chemical Society*, Vol. 138, pp. 3904-3911, 2016.

35. Bagdasar'ian K. S. and A. A. Sinitsyna, "Polymerization Inhibition by Aromatic Compounds", *Journal of Polymer Science,* Vol. 52, pp. 31-38, 1961.

36. Rembaum A. and A. Eisenberg, "Poly-9-Vinylanthracene", *Journal of Polymer Science: Macromolecular Reviews,* Vol. 1, pp. 57-90, 1967.

37. Stolka M., "High Molecular Weight Anthracene Containing Polymer", *Macromolecules*, Vol. 8, pp. 8-9, 1975.

38. Zhao, C. L., Y. Wang, Z. Hruska and M. A. Winnik, "Molecular Aspects of Latex Film Formation: An Energy-Transfer Study", *Macromolecules*, Vol.23, pp. 4082-4087, 1990.

39. Liu, R., M. A. Winnik, F. D. Stefano and J. Vanketessan, "Polymerizable Anthracene Derivatives for Labeling Emulsion Copolymers", *Journal of Polymer Science: Part A: Polymer Chemistry*, Vol. 39, pp. 1495-1504, 2001.

40. Szwarc, M., M. Levy and R. Milkovich, "Polymerization Initiated by Electron Transfer to Monomer. A New Method of Formation of Block Copolymers", *Journal of American Chemical Society*, Vol. 78, pp. 2656-2657, 1956.

41. Szwarc, M., "'Living'Polymers", *Nature*, Vol. 178, pp. 1168-1169, 1956.

42. Müller, A. H. E. and K. Matyjaszewski, *Controlled and Living Polymerizatios: From Mechanisms to Applications*, John Wiley & Sons, Inc., 2009.

43. Winstein, S., E. Clippinger, A. H. Fainberg and G. C. Robinson, “Salt Effects and Ion-Pairs in Solvolysis”, *Journal of American Chemical Society*, Vol. 76, pp. 2597-2598, 1954.

44. Hsieh, H. L. and R. P. Quirk, *Anionic polymerization: principles and practical applications*, New York: Marcel Dekker, 1996.

45. Szwarc, M., *Ions and Ion Pairs in Organic Reactions*, Interscience, New York, 1972.

46. Sadek, H. and R. M. Fuoss, “Electrolyte-Solvent Interaction. VI. Tetrabutylammonium Bromide in Nitrobenzene-Carbon Tetrachloride Mixtures1”, *Journal of American Chemical Society*, Vol. 76, pp. 5905-5909, 1954.

47. Fuoss, R. M., “Ionic Association. III. The Equilibrium between Ion Pairs and Free Ions”, *Journal of American Chemical Society*, Vol. 80, pp. 5059-5061, 1958.

48. Saldivar-Guerra, E. and E. Vivaldo-Lima, *Handbook of Polymer Synthesis, Characterization, and Processing*, John Wiley & Sons, Inc., 2013.

49. Szwarc, M., Mechanisms of electron-transfer initiation of polymerization: a quantitative study. In Bailey, F. E. (Ed), ACS Symposium Series. Vol. 212, p. 419, Washington (DC): American Chemical Society; 1983.

50. Odian, G., *Principles of Polymerization*, John Wiley & Sons, Inc., 4th edition, 2013.

51. Quirk, R. P. and W. C. Chen, “Functionalization of Polymeric Organolithium Compounds. Oxidation”, *Journal of Polymer Science: Polymer Chemistry Edition,* Vol. 22, pp. 2993-3000, 1984.

52. Baskaran, D., “Strategic developments in living anionic polymerization of alkyl (meth)acrylates”, *Progress in Polymer Science*, Vol. 28, pp. 521–581, 2003.

53. Wiles, D. M. and S. Bywater, “Polymerization of Methyl Methacrylate Initiated by 1,1-Diphenylhexul Lithium”, *Transactions of the Faraday Society*. Vol. 61, pp. 150-158, 1965.

54. Hatada, K., T. Kitayama and K. Ute, “Stereoregular Polymerizations of α–Substituted Acrylates”, *Progress in Polymer Science*, Vol. 13, pp. 189-276, 1988.

55. Leemans, L., R. Fayt and Ph. Teyssie, “(9-Anthracenylmethy1) lithium-Initiated Living Anionic Polymerization of Alkyl Methacrylates”, *Macromolecules*, Vol. 23, pp. 1554-1555, 1990.

56. Bartz, T., M. Klapper and K. Müllen, “Anthracene Derivatives as Novel Initiators for Anionic and Cationic Polymerizations”, *Macromolecular Chemistry and Physics*, Vol. 195, pp. 1097-1109, 1994.

57. Quirk, R. P., S. Perry, F. Mendicuti and W. L. Mattice, "New Method for Quantitative Functionalization of the Terminus in Poly(styrene). Naphthalene Functionalization”, *Macromolecules*, Vol. 21, pp. 2294-2295, 1988.

58. Quirk, R. P. and L. F. Zhu, “Anionic synthesis of chain-end functionalized polymers using 1,1-diphenylethylene derivatives. Preparation of 4-hydroxyphenyl-terminated polystyrenes”, *Makromolecular Chemistry*, Vol. 190, pp. 487-493, 1989.

59. Quirk, R. P. and L. E. Schock, “Quantitative Anionic Synthesis of Pyrene-End-Labeled Polystyrene and Polybutadiene”, *Macromolecules*, Vol. 24, pp. 1237-1241, 1991.

60. Caldérara F., Z Hruska, G. Hurtrez, T. Nugay, G. Riess and M. A. Winnik “Synthesis of chromophore-labelled polystyrene/poly(ethylene oxide) diblock copolymers”, *Makromolecular Chemistry*, Vol. 194, pp. 1411-1420, 1993.

61. Caldérara F., Z Hruska, G. Hurtrez, J. P. Lerch, T. Nugay and G. Riess, “Investigation of Polystyrene-Poly(ethy1ene oxide) Block Copolymer Micelle Formation in Organic and Aqueous Solutions by Nonradiative Energy Transfer Experiments”, *Macromolecules*, Vol. 27, pp. 121-1215, 1994.

62. Hruska, Z., B. Vuillemin, G. Riess, A. Katz and M. A. Winnik, “Synthesis of polystyrene-poly(tert-butyl acrylate) diblock copolymers bearing fluorescent groups at the junctions”, *Makromolecular Chemistry*, Vol. 193, pp. 1987-1994, 1992.

63. Stolka, M., J. F. Yanus and J. M. Pearson, “Polymerization of Vinylanthracene Monomers. 2. 2-Vinylanthracene and 2-Propenyl-2-anthracene”, *Macromolecules*, Vol. 9, pp. 710-714, 1976.

64. Stolka, M., J. F. Yanus and J. M. Pearson, “Polymerization of Vinylanthracene Monomers. 3. 1- and 9-Vinylanthracenes”, *Macromolecules*, Vol. 9, pp. 715-719, 1976.

65. Stolka, M., J. F. Yanus and J. M. Pearson, “Polymerization of Vinylanthracene Monomers. 4. A Spectroscopic Study of the Anionic Polymerization of 1-, 2-, and 9-Vinylanthracenes”, *Macromolecules*, Vol. 9, pp. 719-723, 1976.

66. Ni,S., D. Juhué, J. Moselhy,Y. Wang and M. A. Winnik, "Energy-Transfer Studies of Donor-Acceptor-Labeled Polystyrene- block-Poly(methy1 methacrylate) Diblock Copolymers in Solution", *Macromolecules*, Vol. 25, pp. 496-498, 1992.

67. Duhamel, J., A. Yekta, S. Ni, Y. Khaykin and M. A. Winnik, "Characterization of the Core of Polystyrene Block Poly(methyl methacrylate) Polymer Micelles by Energy Transfer", *Macromolecules*, Vol. 26, pp. 6255-6260, 1993.

68. Ni, S., P. Zhang, Y. Wang and M. A. Winnik, "Energy Transfer Studies of the Boundary Layer Interphase in Polystyrene-Poly(methy1 methacrylate) Block Copolymer Films", *Macromolecules*, Vol. 27, pp. 5742-5750, 1994.

69. Tcherkasskaya, O., S. Ni and M. A. Winnik, "Direct Energy Transfer Studies of the Domain-Boundary Interface in Polyisoprene-Poly(methyl methacrylate) Block Copolymer Films", *Macromolecules*, Vol. 29, pp. 610-616, 1996.

70. Schillé, K., A. Yekta, S. Niand M. A. Winnik, "Characterization by Fluorescence Energy Transfer of the Core of Polyisoprene-Poly(Methyl Methacrylate) Diblock Copolymer Micelles. Strong Segregation in Acetonitrile", *Macromolecules*, Vol. 31, pp. 210-212, 1998.

71. Tong, J. D., S. Ni and M. A. Winnik, "Synthesis of Polyisoprene-b-Polystyrene Block Copolymers Bearing a Fluorescent Dye at the Junction by the Combination of Living Anionic Polymerization and Atom Transfer Radical Polymerization", *Macromolecules*, Vol. 33, pp. 1482-1486, 2000.

72. Tong, J. D., C. Zhou, S. Ni and M. A. Winnik, "Synthesis of Meth(acrylate) Diblock Copolymers Bearing a Fluorescent Dye at the Junction Using A Hydroxyl-Protected Initiator and the Combination of Anionic Polymerization and Controlled Radical Polymerization", *Macromolecules*, Vol. 34, pp. 696-705, 2001.

73. Moon, B., T. R. Hoye and C. W. Macosko, "Anionic Synthesis and Detection of Fluorescence-Labeled Polymers with a Terminal Anhydride Group", *Journal of Polymer Science: Part A: Polymer Chemistry*, Vol. 38, pp. 2177-2185, 2000.

74. Kos, T., C. Strissel, Y. Yagci, T. Nugay and O. Nuyken, “The use of DPE radical polymerization method for the synthesis of chromophore-labelled polymers and block copolymers”, *European Polymer Journal*, Vol. 41, pp. 1265-1271, 2005.

75. Goethals, E. J. and F. Du Prez, “Carbocationic polymerizations”, *Progress in Polymer Science*, Vol. 32, pp. 220-246, 2007.

76. Matyjaszewski, K., and P. Sigwalt, "Unified Approach to Living and Non-living Cationic Polymerization of Alkenes", *Polymer International*, Vol. 35, pp. 1-26, 1994.

77. Matyjaszewski, K., *Cationic Polymerizations: Mechanisms, Synthesis, and Applications*, Marcel Dekker, New York, 1996.

78. Ummadisetty, S. and R. F. Storey, "Quantitative synthesis of exo-Olefin-Terminated Polyisobutylene: Ether Quenching and Evaluation of Various Quenching Methods", *Macromolecules*, Vol. 46, pp. 2049-2059, 2013.

79. Kennedy, J. P., "Living Cationic Polymerization of Olefins. How Did the Discovery Come About?", *Journal of Polymer Science Part A: Polymer Chemistry*, Vol. 37, pp. 2285-2293, 1999.

80. Boerzel, P., Bronstert, K. and F. Hovermann, US Patent 4,152,499, 1979.

81. Pinchuk, L., G. J. Wilson, J. J. Barry, R. T. Schoephoerster, J.M. Parel, J.P. Kennedy, "Medical applications of poly(styrene-block-isobutylene-block-styrene)("SIBS"))", *Biomaterials*, Vol. 29, p. 448-460, 2008.

82. Faust, R., and J. P. Kennedy, "Living Carbocationic Polymerization. IV. Living Polymerization of Isobutylene", *Journal of Polymer Science: Part A: Polymer Chemistry,* Vol. 25, pp. 1847-1869, 1987.

83. Matyjaszewski, K. and P. Sigwalt, "Unified Approach to Living and Non-Living Cationic Polymerization of Alkenes", *Polymer International*, Vol. 35, pp. 1-26, 1994.

84. Faust, R., Cationic Polymerization of Nonpolar Vinyl Monomers. In Matyjaszewski, K., Möller, M. (Eds), Polymer Science: A Comprehensive Reference, Vol. 3, pp. 501-525, Elsevier Science, Amsterdam, 2012.

85. Winstein, S., E. Clippinger, A. H. Fainberg, R. Heck and G. C. Robinson, "Salt Effects and Ion Pirs in Solvolysis and Related Reactions. III. Common Ion Rate Depression and Exchange of Anions during Acetolysis", *Journal of the American Chemical Society,* Vol. 78, No.2, pp. 328-335, 1956.

86. Paulo, C., J. E. Puskas and S. Angepat, "Effect of Reaction Conditions on the Kinetics of Living Isobutylene Polymerization at High Initiator/$TiCl_4$ Ratios", *Macromolecules*, Vol. 33, No. 13, pp. 4634-4638, 2000.

87. Matyjaszewski, K., "Effect of initiators, Lewis Acids, Deactivators, Additives and medium on Controlled/"Living" Carbocationic Systems", *Macromolecular Symposia*, Vol. 107, No. 1,pp. 53-63, 1996.

88. Storey, R. F., C. L. Curry and L. K. Hendry, "Mechanistic Role of Lewis Bases and Other Additives in Quasiliving Carbocationic Polymerization of Isobutylene", *Macromolecules*, Vol. 34, pp. 5416-5432, 2001.

89. Sipos, L., P. De and R. Faust, "Effect of Temperature, Solvent Polarity, and Nature of Lewis Acid on the Rate Constants in the Carbocationic Polymerization of isobutylene", *Macromolecules*, Vol. 36, pp. 8282-8290, 2003.

90. Fodor, Z., Y. C. Bae, and R. Faust, "Temperature effects on the Living Cationic Polymerization of Isobutylene: Determination of Spontaneous Chain-Transfer Constants in the Presence of Terminative Chain Transfer", *Macromolecules*, Vol. 31, pp. 4439-4446, 1998.

91. Puskas, I. and S. Meyerson, "Anomalous Carbon Numbers in Cationic Oligomers of Propylene and Butylenes", *Journal of Organic Chemistry*, Vol. 49, pp. 258-262, 1984.

92. Kennedy, J. P. and R. A. Smith, "New Telechelic Polymers and Sequential Copolymers by Polyfunctional Initiator-Transfer Agents (Inifers). II. Synthesis and Characterization of α,ω-Di(tert-Chloro)polyisobutylenes", *Journal of Polymer Science: Polymer Chemistry Edition*, Vol. 18, pp. 1523-1537, 1980.

93. Chang, V. S. C., J. P. Kennedy and B. Iván, "New Telechelic Polymers and Sequential Copolymers by Polyfunctional Initiator-Transfer Agents (Inifers) 8. The Effects of Polymerization Conditions on the Functionality of Telechelic Polyisobutylenes", *Polymer Bulletin,* Vol. 3, pp. 339-346, 1980.

94. Santos, R., A. Fehervari, and J. P. Kennedy, "New Telechelic Polymers and Sequential Copolymers by Polyfunctional Initiator-Transfer Agents (Inifers). XII. Kinetic and Reactivity Studies on Sterically Hindered Inifers", *Journal of Polymer Science: Polymer Chemistry Edition*, Vol. 22, pp. 2685-2697, 1984.

95. Mishra, M. K. and J. P. Kennedy, "Living Carbocationic Polymerization. VII. Living Polymerization of Isobutylene by Tertiary Alkyl (or Aryl) Methyl Ether/Boron Trichloride Complexes", *Journal of Macromolecular Science: Part A - Chemistry: Pure and Applied Chemistry,* Vol. 24, pp. 933-948, 1987.

96. Mishra, M. K., B. Wang and J. P. Kennedy, "Living Carbocationic Polymerization. IX. Three-arm star telechelic polyisobutylenes by $C_6H_3(C(CH_3)OCH_3)_3/BCl_3$ complexes", *Polymer Bulletin*, Vol. 17, pp. 307-314, 1987.

97. Kaszas, G. J. Puskas and J. P. Kennedy, "Living Carbocationic Polymerization. XV. Telechelic polyisobutylenes by the $CH_3O(CH_3)_2C\text{-}pC_6H_4\text{-}C(CH_3)_2OCH_3$. $TiCl_4$ initiating system", *Polymer Bulletin*, Vol. 18, pp. 123-130, 1987.

98. Iván, B. and J. P. Kennedy, “Living Carbocationic Polymerization. XXX. One-Pot Synthesis of Allyl-Terminated Linear and Tri-Arm Star Polyisobutylenes, and Epoxy- and Hydroxy-Telechelics Therefrom”, *Journal of Polymer Science: Part A: Polymer Chemistry,* Vol. 28, pp. 89-104, 1990.

99. Hadjikyriacou, S., Z. Fodor and R. Faust, “Synthetic Applications of Nonpolymerizable Monomers in Living Cationic Polymerization: Functional Polyisobutylenes by End-Quenching”, *Journal of Macromolecular Science: Part A - Chemistry: Pure and Applied Chemistry,* Vol. 32, pp. 1137-1153, 1995.

100. Charleux, B., M. Moreau, J. P. Vairon, S., Hadjikyriacou and R. Faust, “Model kinetic study of TiCl4-induced ionization of polyisobutylene capped with diphenylethylene application to the synthesis of block copolymers”, *Macromolecular Symposia*, Vol. 132, pp. 25-35, 1998.

101. Li, D. and R. Faust, “Polyisobutylene-Based Thermoplastic Elastomers. 3. Synthesis, Characterization, and Properties of Poly(α-methylstyrene-b-isobutylene-b-α-methy1styrene) Triblock Copolymers”, *Macromolecules*, Vol. 28, pp. 4893-4898, 1995.

102. Fodor, Z. and R. Faust, “Polyisobutylene-Based Thermoplastic Elastomers. II. Synthesis and Characterization of Poly(p-Methylstyrene-block-isobutylene-block-p-Methylstyrene) Triblock Copolymers”, *Journal of Macromolecular Science: Part A - Chemistry: Pure and Applied Chemistry,* Vol. 32, pp. 575-591, 1995.

103. Feldthusen, J., B. Iván and A. H. E. Müller, “Stable carbanions by quantitative metalation of cationically obtained diphenylvinyl and diphenylmethoxy compounds: new initiators for living anionic polymerizations”, *Macromolecules*, Vol. 30, pp. 6989-6993, 1997.

104. Feldthusen, J., B. Iván and A. H. E. Müller, “Synthesis of linear and star-shaped block copolymers of isobutylene and methacrylates by combination of living cationic and anionic polymerizations”, *Macromolecules*, Vol. 31, pp. 578-585, 1998.

105. Hadjikyriacou, S. and R. Faust, “Amphiphilic block copolymers by sequential living cationic polymerization: synthesis and characterization of poly(isobutylene-b-methyl vinyl ether)”, *Macromolecules,* Vol. 29, pp. 5261-5267, 1996.

106. Feng, D., T. Higashihara, G. Cheng, J. C. Cho and R. Faust, “Block copolymers by the combination of cationic and anionic polymerizations for biomedical applications. *Macromolecular Symposia*, Vol. 105, pp. 14-2, 2006.

107. Feng, D., T. Higashihara and R. Faust, “Facile synthesis of diphenylethylene end-functional polyisobutylene and its applications for the synthesis of block copolymers containing poly(methacrylate)s”, *Polymer*, Vol. 49, pp. 386-393, 2008.

108. Yang, J., J. Lu and M. A. Winnik, “Synthesis and Spectroscopic Characterization of Symmetrical Isoprene-Methyl Methacrylate Diblock Copolymers Bearing Different Anthracene Derivatives at the Junctions”, *Journal of Polymer Science: Part A: Polymer Chemistry,* Vol. 41, pp. 1225-1236, 2003.

109. Mala’bi, T., S. Pogodin and I. Agranat, “Reversible Friedel-Crafts Acylations of Anthracene: Rearrangements of Acetylanthracenes”, *Letters in Organic Chemistry*, Vol. 6, pp. 237-241, 2009.

110. Wang, B., M. K. Mishra, and J. P. Kennedy, “Living carbocationic polymerization XII. Telechelic polyisobutylenes by a sterically hindered bifunctional initiator”, *Polymer Bulletin*, Vol. 17, No. 3, pp. 205-211, 1987.

111. Kennedy, J. P., Erdodi G., Method for the synthesis of low cost initiators for telechelic polyisobutylenes. US 8,889,926 B2, 2014.

112. Quirk, R. P., S. F. Wang and M. D. Foster, “Synthesis of Cyclic Polystyrenes Using Living Anionic Polymerization and Metathesis Ring-Closure”, *Macromolecules*, Vol. 44, pp. 7538-7545, 2011.

113. Fidder, H., A. Lauer, W. Freyer, B. Koeppe and K. Heyne, “Photochemistry of anthracene -9,10-endoperoxide”, *Journal of Physical Chemistry A*, Vol. 113, pp. 6289-6296, 2009.

114. Hargreaves, J.S. and S. E. Webber, "Photophysics of anthracene polymers: fluorescence, singlet energy migration, and photodegradation" *Macromolecules*, Vol. 17, pp. 235-240, 1984.

115. Kricheldorf, H.R., "Cyclic Polymers: Synthetic Strategies and Physical Properties", *Journal of Polymer Science: Part A: Polymer Chemistry,* Vol. 48, pp. 251-284, 2010.

116. Schulz, M., S. Tanner, H. Barqawi and W. H. Binder, "Macrocyclization of polymers via ring-closing metathesis and azide/alkyne-"Click"-Reactions: an approach to cyclic polyisobutylenes", *Journal of Polymer Science: Part A: Polymer Chemistry,* Vol. 48, pp. 671-680, 2010.

117. Hogen-Esch, T. E., "Synthesis and Characterization of Macrocyclic Vinyl Aromatic Polymers", *Journal of Polymer Science: Part A: Polymer Chemistry*, Vol. 4, pp. 2139-2155, 2006.

118. Trenor, S. R., T. E. Long and B. J. Love, "Photoreversible Chain Extension of Poly(ethylene glycol)", *Macromolecular Chemistry and Physiscs*, Vol. 205, pp. 715-723, 2004.

119. Ling, J., M. Z. Rong and M. Q. Zhang, "Coumarin Imparts Repeated Photochemical Remendability to Polyurethane", *Journal of Material Chemistry*, Vol. 21, pp. 18373-18380, 2011.

120. Kuzina, S. I. and A. I Mikhailov, "The photo-oxidation of polymers –Initiation of polystyrene photo-oxidation", *European Polymer Journal*, Vol. 29, pp. 1589-1594, 1993.

121. Walter, H., D. Brooks, P. Srere and K. Jeon, *Microcompartmentation and Phase Separartion in Cytoplasm*, Academic Press, 1999.

122. Crompton, T. R., *Thermal Stability of Polymer*, Smithers Rapra, 2012.

123. Lynwood, C., *Polystyrene Synthesis, Characteristics and Applications*, Nova Science Publishers Inc., New York, 2014.